Current Trends in Biotechnology and Pharmacy

ASSOCIATION OF BIOTECHNOLOGY AND PHARMACY

KNOWLEDGE IS POWER

www.abap.co.in

Current Trends in Biotechnology and Pharmacy
ISSN 0973-8916

Current Trends in Biotechnology and Pharmacy

(An International Scientific Journal)

www.abap.co.in

Indexed in Chemical Abstracts, EMBASE,ProQuest and Indian Science Abstracts

Association of Biotechnology and Pharmacy
(Regn. No. 28 OF 2007)

The *Association of Biotechnology and Pharmacy (ABAP)* was established for promoting the science of Biotechnology and Pharmacy. The objective of the Association is to advance and disseminate the knowledge and information in the areas of Biotechnology and Pharmacy by organising annual scientific meetings, seminars and symposia.

Members

The persons involved in research, teaching and work can become members of Association by paying membership fees to Association.

The members of the Association are allowed to write the title **MABAP** (Member of the Association of Biotechnology and Pharmacy) with their names.

Fellows

Every year, the Association will award Fellowships to the limited number of members of the Association with a distinguished academic and scientific career to be as Fellows of the Association during annual convention. The fellows can write the title **FABAP** (Fellow of the Association of Biotechnology and Pharmacy) with their names.

Membership details

		India	SAARC	Others
Individuals	– 1 year	Rs.600	Rs1000	$100
	LifeMember	Rs.4000	Rs.6000	$500
(Membership and Journal)				
Institutions	– 1 year	Rs.1500	Rs.2000	$200
	Life member	Rs.10000	Rs.12000	$1200
(Journal only)				

Individuals can pay in two instalments, however the membership certificate will be issued on payment of full amount. All the members and Fellows will receive a copy of the journal free

Association of Biotechnology and Pharmacy
(Regn. No. 28 OF 2007)
#5-69-64; 6/19, Brodipet
Guntur – 522 002, Andhra Pradesh, India

Current Trends in Biotechnology and Pharmacy
ISSN 0973-8916

Volume 3 (2)	CONTENTS	April - 2009

Information to Authors

The *Current Trends in Biotechnology and Pharmacy* is an official international journal of *Association of Biotechnology and Pharmacy*. It is a peer reviewed quarterly journal dedicated to publish high quality original research articles in biotechnology and pharmacy. The journal will accept contributions from all areas of biotechnology and pharmacy including plant, animal, industrial, microbial, medical, pharmaceutical and analytical biotechnologies, immunology, proteomics, genomics, metabolomics, bioinformatics and different areas in pharmacy such as, pharmaceutics, pharmacology, pharmaceutical chemistry, pharma analysis and pharmacognosy. In addition to the original research papers, review articles in the above mentioned fields will also be considered.

Call for papers

The Association is inviting original research or review papers in any of the above mentioned research areas for publication in Current Trends in Biotechnology and Pharmacy. The manuscripts should be concise, typed in double space in a general format containing a title page with a short running title and the names and addresses of the authors for correspondence followed by Abstract (350 words), 3 – 5 key words, Introduction, Materials and Methods, Results and Discussion, Conclusion, References, followed by the tables, figures and graphs on separate sheets. For quoting references in the text one has to follow the numbering of references in parentheses and full references with appropriate numbers at the end of the text in the same order. References have to be cited in the format below.

Mahavadi, S., Rao, R.S.S.K. and Murthy, K.S. (2007). Cross-regulation of VAPC2 receptor internalization by m2 receptors via c-Src-mediated phosphorylation of GRK2. Regulatory Peptides, 139: 109-114.

Lehninger, A.L., Nelson, D.L. and Cox, M.M. (2004). Lehninger Principles of Biochemistry, (4th edition), W.H. Freeman & Co., New York, USA, pp. 73-111.

Authors have to submit the figures, graphs and tables of the related research paper/article in Adobe Photoshop of the latest version for good illumination and allignment.

Authors can submit their papers and articles either to the editor or any of the editorial board members for onward transmission to the editorial office. Members of the editorial board are authorized to accept papers and can recommend for publication after the peer reviewing process. The email address of editorial board members are available in website www.abap.in. For submission of the articles directly, the authors are advised to submit by email to krssrao@abap.in or krssrao@yahoo.com.

Authors are solely responsible for the data, presentation and conclusions made in their articles/ research papers. It is the responsibility of the advertisers for the statements made in the advertisements. No part of the journal can be reproduced without the permission of the editorial office.

Molecular farming of Plant Derived Edible Vaccines

D.K.Das

Post Graduate Department of Biotechnology
T. M.Bhagalpur University, Bhagalpur-812007, India
For correspondence - dilipdas@hotmail.com

Abstract

Vaccines have been one of the most far-reaching and important public health initiatives of the 20th century. Edible vaccine, in particular, might overcome some of the difficult of production, distribution and delivery associated with traditional vaccine. Transgenic potatoes expressing LT-B were found to induce both serum and secretory antibodies when fed to mice, these protective in bacterial toxin assays in vitro. This is the first proof of concept for the edible vaccine. The selection of a plant system for delivery of edible vaccines for human has been addressed. Recognising that it is necessary to express the desired protein in a food that is consumed raw (to avoid denaturation of the candidate vaccine protein), a system to transform banana plant has been developed. The expression of candidate vaccines in banana fruit will be dependant upon identification of suitable specific promoter to drive the desired gene expression. The concept of edible vaccine got impetus after Arntzen and co-workers expressed hepatitis B surface antigen in tobacco. Strategies for expression of foreign genes in high amounts in plants include use of strong and organ specific promoters targeting of the protein into endoplasmic reticulum by incorporating ER-targeting and ER-retention signals, creation of optimized translation start site context as well as alleviation of codons to suit the expression of prokaryotic genes in a plant. Retention of heat labile *E.coli* enterotoxin in ER of potato by using ER-retention signal has been reported to elevate the expression levels of the recombinant protein.

Cholera toxin, which is very similar to *E.coli* LT, has also been expressed in plants generated tobacco plants expressing CT-A or CT-B subunits of the toxin. Hepatitis B surface antigen (HBsAG) has been reported to accumulate to 0.01% of soluble protein level in transgenic tobacco. Edible vaccine offer exciting possibilities for significantly reducing the burden of diseases like hepatitis and diarrhoea, particularly in the developing world storing and administering vaccines are often major problems. NIAID have shown for the first time that an edible vaccine can safely trigger significant immune responses in people. Antibodies raised to the H protein after infection with the wild type measles virus (MV) have MV-neutralizing activity and correlate with immunological proteins. Recent studies have shown that mammalian protein can be expressed to high levels in transgenic rice.

Key words - Edible vaccine, Antibodies, Enterotoxin, Surface antigen, Cholera toxin

Introduction

Vaccines are primary tools in programmes for health intervention for both humans and animals. They would be more widely used especially in developing countries. It would be helpful for human society if cost of production could be reduced and they could be distributed without refrigeration. Vaccines couldn't be very popular because of unavailability of electricity for its storage in remotest area in developing countries. Vaccines and antibodies play a key role in healthcare. However, the cost of production and maintaining a chain for vaccine distribution has

so far hampered realizing their full potential. Expression of antigens as vaccines and of antibodies against antigens of pathogens in transgenic plants is a convenient and inexpensive source for these immunotherapeutic molecules. Research underway is dedicated to solving these limitations by finding way to produce oral (edible) vaccines in transgenic plants. Edible vaccines can be produced by transgenic plants in large amount and cost will be also cheap and no problem of refrigeration and all section of people can afford to buy it for remedy of a large number of diseases Hepatitis B virus (HBV) infection is probably the single most important cause of persistent viremia in humans. The disease is characterized by acute and chronic hepatitis, which can also initiate hepatocellular carcinoma. The prevalence of the disease in developing countries justified initial efforts to express HBV candidate vaccines in plants. Currently two forms of HBV vaccines are available, both of which are injectable and expensive- one purified from the serum of infected individuals and the other a recombinant antigen expressed and purified from yeast. This antigen has already been entered in transgenic plant either through *Agrobacterium* mediated transformation or Particle gun bombardment (Biolistics) (38) and encoding the hepatitis B surface antigen (HBsAg); this is the same antigen used in the commercial yeast-derived vaccine. An antigenic spherical particle was recovered from these plants which is analogous to the recombinant hepatitis surface antigen (HBsAg) derived from yeast. Parenteral immunization of mice with the plant–derived material has demonstrated that it retains both B and T-cell epitopes, as compared to the commercial vaccine.

Diarrhoeal disease causes up to 10 million deaths per year in the developing world, primarily among children. Relatively little research to prevent these diseases is underway, as they represent more of a nuisance than a severe problem in developed countries. Studies supported by the World Health Organization have demonstrated an effective vaccine for cholera, which provides cross protection against enterotoxic *Escherichia coli*. This vaccine is not available, however, in large part due to cost of production of the bacterial toxin protein which is a component of its formulation.

To address this limitation, plants were transformed with the gene encoding the B subunit of the *E.coli* heat labile enterotoxin (LT-B). Transgenic potatoes expressing LT-B were found to induce both serum and secretory antibodies when fed to mice; these protective in bacterial toxin assays in vitro. This is the first "proof of concept" for the edible vaccine.

The selection of a plant system for delivery of edible vaccines for humans has been addressed. Recognizing that it is necessary to express the desired protein in a food that is consumed raw (to avoid denaturation of the candidate vaccine protein), a system to transform banana plants has been developed. The expression of candidate vaccines in banana fruit will be dependent upon identification of suitable specific promoter to drive the desired gene expression. Research to find these genetic regulatory elements are now underway.

Edible vaccine research is currently directed at human diseases, with a special emphasis on the developing world. The technology will also have immediate value for the production of inexpensive vaccines as food additives for agricultural animals. Since various plant tissues are fed to animals, other plants such as alfalfa, maize and wheat could be valuable vehicles to deliver vaccines (and perhaps pharmaceuticals) for the betterment of animal health.

Recent progress in the area of transgenic plants has however, once again attracted attention of the scientists, and plants are being looked upon as potential bio-reactors or bio-factories for the production of immunotherapeutic molecules. In

1989 firstly Hiatt and co-workers attempted to produce antibodies in plants which could serve the purpose of passive immunisation but it was appeared in 1990 in the form of patent application (38), the concept of edible vaccine got impetus after Arntzen and co-workers expressed hepatitis B surface antigen in tobacco in 1992 to produce immunologically active ingredient via genetic engineering of plants. This generated a good deal of excitement among biotechnologists, particularly in light of the potential of edible vaccines and antibodies for immunotherapy for countries like India. Various strategies for expression of foreign genes in high amounts in plants include use of strong and organ specific plant promoters, targeting of the protein into endoplasmic reticulum (ER) by incorporating ER-targeting and ER-retention signals, creation of optimized translation start site context as well as alteration of codons to suit the expression of prokaryotic genes in a plant (19 & 66). Though promoters of genes, like maize ubiquitin and rice actin, have been reported to direct high level of expression in monocots, the 35S promoter of cauliflower mosaic virus remains the promoter of choice for dicots (55). Targeting of the protein to appropriate cellular compartment may be helpful in stabilizing the protein. Retention of heat labile *E.coli* enterotoxin in ER of potato by using ER-retention signal has been reported to elevate the expression levels of the recombinant protein (22). Though signals for membrane targeting , protein folding, oligomerization and N-glycosylation are highly conserved in animals and plants (13), while expressing bacterial proteins targeted to ER, it is important to consider the sequence of a signal peptide for targeting to periplasmic space in bacterium may not be equally efficient in plants. Substitution of signal peptide of bacterial origin with a plant specific ER-targeting sequence was observed to dramatically increase the glycosylation and secretion efficiency of chitinase (34). For production of edible vaccines or antibodies, it is desirable to select a plant whose

products are consumed raw to avoid degradation during cooking. Thus, plants like tomato, banana and cucumbers are generally the plants of choice. While expression of a gene that is stably integrated into the genome allows maintenance of the material in the form of seeds, some virus based vectors can also be used to express the gene transiently to develop the products in a short period. This may have the additional advantage of allowing expression of the product at very high level; not always attainable in transgenic systems. While plant system may have the capability of producing any vaccine in large amounts and in a less expensive manner, purification of the product may require the use of existing or even more cumbersome procedures. Attention therefore has been paid to mainly those antigens that stimulate mucosal immune system to produce secretory IgA (S-IgA) at mucosal surfaces, such as gut and respiratory epithelia. In general, a mucosal response is achieved more effectively by oral instead of parenteral delivery of the antigen. Thus, an antigen produced in the edible part of a plant can serve as a vaccine against several infectious agents which invade epithelial membranes. These include bacteria and viruses transmitted via contaminated food or water, and resulting in diseases like diarrhoea and whooping cough. The first report of the production of edible vaccine (a surface protein Streptococcus) in tobacco, at 0.02% of total leaf protein level appeared in 1990 in the form of a patent application published under the International Patent Cooperation Treaty (37). Subsequently, a number of attempts were made to express various antigens in plants. Hein is one of handful researchers using the tools of bioengineering to transform ordinary fruits and vegetables into botanical cargo vessels that carry life saving vaccines. Edible vaccines promise to be an affordable and safe way for people in even the most poverty stricken parts of the world to protect themselves against disease. Normal vaccines need for refrigeration and purified serum, hypodermic needles, or even trained medical

professional to distribute and oversee vaccinations but these conditions are not required for edible vaccines. The goal is to give people in developing countries the genetically engineered seeds that will sprout edible vaccines. "Every culture on this planet raises food" explains Hein. "This can provide developing countries with a stable vaccine source because it will be genetically coded into the food". Using recombinant DNA technology, researchers can now isolate the genes—called antigens—that mobilize our natural defences. But impregnating plants with these antigens requires an impressive bit of molecular legerdemain. At Scrips Research Institute, for instance, the antigen

is snipped off the deadly cholera pathogen. Then it is inserted into the cells of a bacterium that causes a plant disease called crown gall. The alfalfa plants are infected with these transgenic crown gall organisms, which can penetrate the plant's cell walls. The plant cells containing the foreign genes are then cultured in a Petri dish until they are mature enough to be transplanted. The next step is to test the potency of the antigens in plants raised in the field, outside of the cloistered laboratory. "We've just harvested this crop of alfalfa" says Hein, who's in the midst of measuring its antigen level and feed this transgenic grain to mice (64, 39 & 40, 24, 1,2 & 3, 48, 8, 21, 4). .

Table 1. Antigens produced in transgenic plants

Protein	Plant
Hepatitis B surface antigen	Tobacco
Rabies virus glycoprotein	Tomato
Norwalk virus capsid protein	Tobacco
E.coli heat-labile enterotoxin B subunit	Potato
Cholera toxin B subunit	Potato, tobacco
Mouse glutamate decarboxylase	Potato
VP1 protein of foot and mouth disease virus	Arabidopsis
Insulin	Potato
Glycoprotein swine-transmissible gastroenteritis cornavirus	Arabidopsis

Since acute watery diarrhoea is caused by enteroxigenic *Escherichia coli* and *Vibrio cholerae* that colonize the small intestine and produce one or more enterotoxin (LT-B) in tobacco and potato (22). The enterotoxin (LT) from *E.coli* is a multimeric protein, quite similar to cholera toxin (CT) structurally, functionally and antigenically. LT has one A subunit (27 kDa) and a pentamer of B subunits (11.6 kDa). Binding of the non-toxic LT-B pentamer to GM1 gangliosides, present on epithelial cell surfaces, allows entry of the toxin LT-A subunits into the cells. LT-B and CT-B are both potent oral immunogens. An oral vaccine composed of the cholera toxin–B subunit (CT-B) with killed *Vibrio cholera* cells

has been reported to give significant level of protection against cholera (59). But the cost of production of CT-B by conventional methods is too high to allow distribution of this vaccine. The recombinant LT-B (rLT-B) produced in tobacco and potato showed partial pentamerization after the engineering of subunit gene in a way that allowed retention of the protein in microsomal vesicles. On testing immunogenicity of rLT-B by feeding potato tubers to mice, both humoral and mucosal immune responses were reported to be stimulated. This vaccine has gone through pre-clinical trials in humans. The antigenic protein retained its immunogenicity after purification from the transgenic potato expressing it (60). Fourteen

healthy individuals, who ate 50-100 g raw potatoes, were screened for gut-derived antibody secreting cells, which were detectable 7-10 days after immunization. Presence of both anti-LT IgA-secreting cells and anti-LT IgG-secreting cells was detected in the peripheral blood.

Cholera toxin, which is very similar to *E.coli* LT, has also been expressed in plants (24), generated tobacco plants expressing CT-A or CT-B subunits of the toxin. CT-A produced in plant was not cleaved into A1 and A2 subunits, which happens in epithelial cells. Plants expressing CT-B showed the presence of a protein that migrated to the same position in denaturing gel as the CT-B derived from *V.cholerae*, and was recognised by mouse anti-CT-B antibody. Cholera toxin-B subunit, when expressed in potato, was processed in a natural way; the pentameric form (the naturally occurring form) being the abundant form. Antigenically it was found to be similar to the bacterial protein. Even after boiling transgenic potato tubers till they became soft, approximately 50% of the CT-B was present in the pentameric GM1 ganglioside binding form (1, 2).

Similarly, a rabies virus coat glycoprotein gene has been expressed in tomato plants (48). The protein that was expressed had molecular mass of 62 kDa. Since the orally administered protein elicited protected immunity in animals, it was expected that continued efforts would lead to development of an edible oral vaccine against rabies which could be used as a preventive strategy.

The Hepatitis B surface antigen (HBsAG) has been reported to accumulate to 0.01% of soluble protein level in transgenic tobacco (37). The antigens, delivered in a macromolecular form, are known to survive the gut atmosphere and perform better. (8) Carrillo et al 1998 expressed structural protein, VP1, of foot and mouth disease virus in Arabidopsis. The mouse that was immunized intra-peritoneally with a leaf extract elicited immune response to synthetic peptides carrying various epitopes of VP1, or to complete VP1. Furthermore, all the mice immunized with the leaf extract were protected against challenge with virulent foot and mouth disease virus.

One of the alternative strategies of producing a plant-based vaccine is to infect the plants with recombinant viruses carrying the desired antigen that is to infect the plants with recombinant viruses carrying the desired antigen that is fused to viral coat protein. The infected plants have been reported to produce the desired fusion protein in large amounts in a short time. The technique involved either placing the gene downstream a subgenomic promoter or fusing the gene with capsid protein that coats the virus (Table-2). The latter strategy is perhaps the strategy of choice since fusion proteins in particulate form are highly immunogenic. Edible vaccines offer exciting possibilities for significantly reducing the burden of diseases like hepatitis and diarrhoea, particularly in the developing world where storing and administering vaccines are often major problems. Baltimore, Maryland, April 28, 1998 opening a new era in vaccine delivery, researchers supported by the National Institute of Allergy and Infectious diseases (NIAID) have shown for the first time that an edible vaccine can safely trigger significant immune responses in people.

Table 2. Transient production of antigens in plants after infection with plant viruses expressing a recombinant gene

Protein	Plant	Carrier
Influenza antigen	Tobacco	TMV
Murine zona pellucida antigen	Tobacco	TMV
Rabies antigen	Spinach	AFMV
HIV-1 antigen	Tobacco	AFMV
Mink enteritis virus antigen	Black eyed bean	CPMV
Colon cancer antigen	Tobacco	TMV

AFMV, alfalfa mosaic virus; TMV, tobacco mosaic virus; CPMV, cowpea mosaic virus

The Phase 1 proof of concept trial began last fall at the University of Maryland, School of Medicine's Centre for Vaccine development under the direction of Carol O. (60). The goal of the study was to demonstrate that an edible vaccine could stimulate an immune response in humans. Volunteers ate bite sized pieces of raw potato that had been genetically engineered to produce part of the toxin secreted by the Escherichia coli bacterium, which causes diarrhoea. It also showed that transgenic potatoes containing this segment of the toxin stimulated strong immune responses in animals. The trial enrolled 14 healthy adults; 11 were chosen at random to receive the genetically engineered potatoes and three received pieces of ordinary potatoes.

The investigators periodically collected blood and stool samples from the volunteers to evaluate the vaccine stimulate both systemic and intestinal immune responses. Ten of the 11 volunteers (91%) who ingested transgenic potatoes had fourfold rises in serum antibodies at some point after immunization, and six of five (the 91%) developed fourfold rises in intestinal antibodies. The potatoes were well tolerated and no one example for serious adverse side effects. Encouraged by the results of this study, NIAID-supported scientists are exploring the use of this technique administering other antigens. Edible vaccines for other intestinal pathogens are already in the pipeline- for potatoes and bananas that might protect against Norwalk virus, a common cause of diarrhoea, and potatoes and tomatoes that might protect against Hepatitis B. This first trial is a map road to creating inexpensive vaccines that might be particularly useful in immunizing people in developing countries where high cost and logistic issues, such as transportation and the need for certain vaccines to be refrigerated thwart effective vaccination programmes. The study nurse at the University of Maryland peeled the potatoes just before they were eaten, because potatoes sometimes contains a compound that imparts a bitter taste and can cause nausea and stomach upset. The potatoes then cut into small, uniform pieces and weighed into 50-gram and 100-gram doses. Each person received either 50grams or 100 grams of potato over a three-week period, 0, 7 and 21 days. The dosage size varies evaluate any side effects from eating raw potatoes. NIAID is a component of the National Institutes of Health (NIH). NIAID conducts and supports research to prevent, diagnose and treat illnesses such as AIDS and other serious transmitted diseases, malaria, tuberculosis, asthma and allergies; NIH is an agency of the U.S. Department and Human Services. At least 350 genetically engineered pharmaceutical products are currently developed in the United States and Canada. This is a welcome step towards the new world of molecular farming. Plant based biopharmaceuticals have also been produced and expressed (20, 36). Edible vaccine could show multiple T cell epitopes for oral tolerance against antigens (25)

In Canada, a genetically engineered tobacco plant made to produce Interleukin 10 will be tested to treat viral disease, an intestinal disorder. Molecular farming uses the science of genetic engineering to turn ordinary factories for the production of inexpensive drugs and vaccines. Researchers at the London Health Science centre, London, Ontario, Canada are growing potatoes that have been genetically altered to produce a special diabetic protein. When the potatoes are fed to diabetic mice, scientists find that most don't develop Type I diabetic as juvenile-onset diabetes. Scientists believe that the low cost production of this protein may help the people worldwide affected by diabetes. In the lab, the new transgenic potatoes produce large amounts of protein that suppresses the destructive immune response and prevents diabetes from developing.

Molecular biologist (42) of the London Health Sciences Centre developed edible vaccines to combat autoimmune diseases such

as multiple sclerosis, rheumatoid arthritis, lupus and even rejection (8). His team contemplated that plants are ideal because they can synthesize and assemble proteins to provide huge quantities proteins at relatively low cost.

Edible vaccines were first tested on humans in 1997, when scientists asked volunteers to eat anti-diarrhoea potatoes produced by the Boyce Thompson Institute at Cornell University, Ithaca, NY, USA. After consuming the potatoes volunteers produced antigens in their bodies just as if they had received a traditional anti-diarrhoeal vaccine and they experienced no adverse side effects. Roswell Park Cancer Institute in Buffalo, New York also developed edible vaccines in raw potatoes and foreign proteins (HBsIgA) can help to cure human being from Hepatitis B virus. Edible vaccines are currently being developed for a number of human and animal diseases, including measles, cholera, foot and mouth disease, and hepatitis B & C. Many of these diseases are likely to require booster vaccinations or multiple antigens to induce and maintain protective immunity. Plants have the capacity to express more than one transgene, allowing delivery of multiple antigens for repeated inoculations (14). Globally, measles causes over 800,000 deaths every year (Centres for Disease Control and Prevention, 1998). Many other affected people either become deaf or are weakened by pneumonia or encephalitis. The vaccine currently available for measles has been used effectively and safely since the 1960s and results in 95% seroconversion in individuals who are over the age of 18 months at the time of vaccination (15). However, the measles live-attenuated vaccine (LAV) has no oral efficacy and is destroyed by heat, so that its distribution and storage are dependent on maintenance of a "cold-chain" of refrigeration. Finally, the effectiveness of the LAV is reduced by the presence of maternal antibodies (51). These limitations present a serious challenge to the goal of measles eradication.

Development of an edible measles vaccine: The first stage in the development of an edible vaccine is selecting which antigen to express. Measles is an enveloped virus with two major surface proteins- the hemagglutinin (H) and fusion proteins. Antibodies raised to the H protein after infection with the wild type measles virus (MV) have MV-neutralising activity and correlate with immunological protection (12). The H protein subunit from the attenuated Edmonston vaccine strain was therefore selected as the basis for an edible measles vaccine.

Transgenic plants may be produced by a number of methods. The most common uses *Agrobacterium tumefaciens*, a naturally occurring soil bacterium, to transfer a small segment of DNA into the plant genome in a process known as transformation (Fig 1). Whole plants can then be regenerated from individual plant cells that have been successfully transformed. Production of transgenic plants is species-dependent and can take three to nine months. By this method MV-H gene been successfully expressed in the experimental model plant tobacco (29). When given orally to mice, the transgenic plant extract containing the MV-H antigen induced serum antibodies that were able to neutralise wild type MV in vitro, showing that plant-derived MV-H protein retains its immunogenic. Secretary IgA is indicative of a mucosal immune response, which is important for protection against diseases that establish infection through mucosal surfaces such as the respiratory tract. Plant can produce a large amount of recombinant proteins for remedy of different disease and act as factories (49). Needle free vaccination programme could be initiated after the development of rice based mucosal vaccine (50).Vaccines have been developed in fruit which can be used during dinner (53 and 4) and allergic and other immunotherapy could also be possible (57, 28 and 46).

From model system to practical vaccine-The next challenge will be to translate this

technology from a model system into a practical vaccine. While tobacco is a good model system for evaluating the production recombinant proteins, it produces toxic compounds which make it unsuitable for vaccine delivery. Clinical trials have shown the induction of immune responses with antigen expressed in potato and lettuce (61 & 30). Lettuce is a fast growing species suitable for direct consumption and experimental studies. Another practical alternative may be rice, which is commonly used in baby food because of its low allergenicity. Recent studies have shown that mammalian proteins can be expressed to high levels in transgenic rice (58). Furthermore, rice is easy to store and transport, and protein expressed in rice grains is stable at room temperature (58). Rice flour can also be mixed with baby food, clean water or breast milk for delivery to infants.
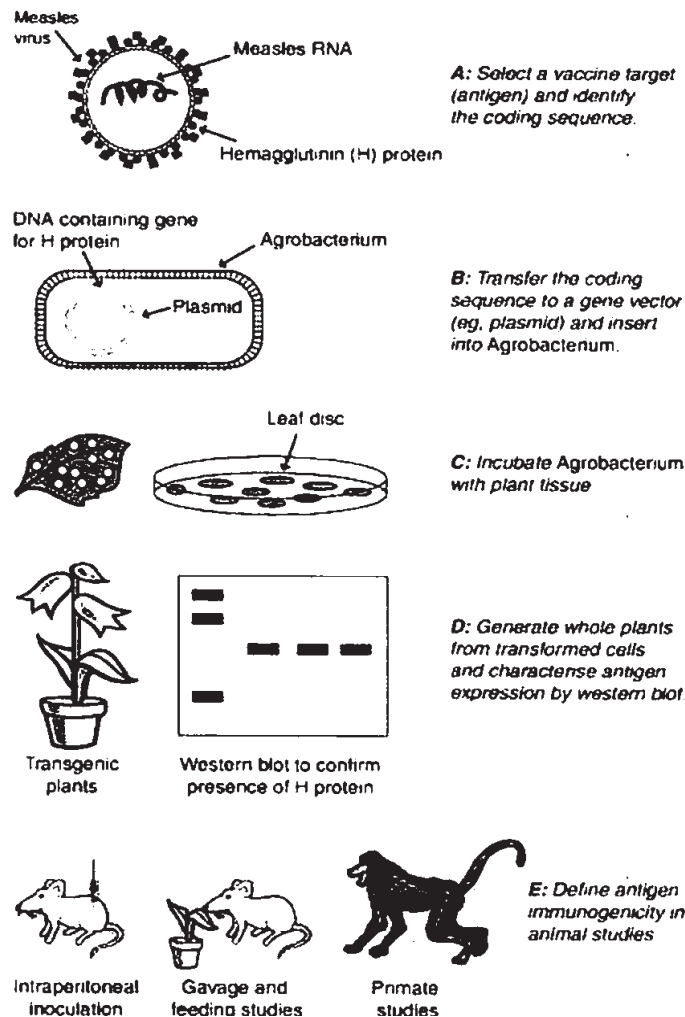

Fig-1 Strategy for the development of plant edible vaccine

Modulation of immune response to acquire immune tolerance

One of the utilities of producing antigens in plants in large amount is in treatment of autoimmune diseases like diabetes mellitus which involve production of antibodies against glutamic acid decarboxylase (GAD) and insulin, leading to destruction of insulin-producing pancreatic cells (17, 65). The antigens targeted for autoimmune response can be fed to the animals to induce immune tolerance. However, since the use of antigens for inducing oral tolerance requires production in large amounts of the human antigens that are generally difficult to produce by conventional means, attempts have been made to produce such antigens in plants. Insulin (2) and GAD (45) have been produced in potato and tobacco, respectively. To detect the delivery of plant-synthesized insulin to the gut associated lymphoid tissue, insulin was linked to cholera-toxin B subunit. Non-obese diabetic mice which were fed with the transformed potato tuber tissue containing microgram level of the recombinant insulin delayed the progression of clinical diabetes. Similarly, GAD-producing tobacco plants, given as a dietary supplement, inhibited the development of diabetes in the non-obese diabetic mouse.

Expression and assembly of antibodies in plants

Transgenic plants are also being looked upon as a source for producing large-scale antibodies which can serve the purpose of passive immunization by direct application, in addition to providing a tool for drug targeting or interactive inactivation of undesirable molecules (41, 27). Gene technology has provided great impetus to the utility of antibodies, since antibody genes can be altered to order. Thus not only genes coding for both the light and heavy chains have been expressed, but modified genes capable of expressing only Fab fragments (assembled light chains and shortened heavy chains) or ScFV (single peptide chains where variable domains of heavy and light chains are covalently linked by a short flexible peptide) have also been expressed in bacteria and mammalian cells (19, 7, 10, 52, 63, 18, 67, 53 & 54, 5, 6, 56, 33, 68) (Table-3). Murine antibodies have humanized by changing the constant and framework domains. In addition, recent technology involving PCR (Polymerase chain reaction) and phage display allow cloning and screening of antibodies with suitable avidity easily.

Table 3. Antibodies and antibody fragments produced in transgenic plants

Antibody	Antigen	Plant
IgG (k)	Transition stage analog	Tobacco
IgM (ë)	NP(4-hydroxy-3-nitrophenyl) acetyl hapten	Tobacco
Single domain (dAb)	Substance P	Tobacco
Single chain Fv	Phytochrome	Tobacco
Single chain Fv	Artichoke mottled virus coat protein	Tobacco
Fab; IgG (k)	Human creatin kinase	Arabidopsis
IgG (k)	Fungal cutinase	Tobacco
IgG (k) and SIgG/A hybrid	S. mutagens adhesin	Tobacco
Single chain Fv	Abscisic acid	Tobacco
Single chain Fv	Nematode antigen	Tobacco
Single chain Fv	â-glucuronidase â-1,4 endoglucanase	Tobacco
Single chain antibody fragment	Atrazin, Paraquat	Tobacco
IgG	Glycoprotein B of Herpes simplex virus	Soybean

Transgenic plants not only provide the means to express antibodies but also enable the glycosylation and entry into secretory pathway which allow assembly of complete antibodies and Fab fragments. Variable fragments (Fv) can be produced in cytosol, directed to different compartments and fused with proteins such as protein A and phosphatase to improve the detection and purification of single chain Fv (scFv). In plants, antibody production (1-5% of total plant protein) has been achieved by cross-pollination of individually transformed plants expressing light or heavy chains (29). Other approaches involve double transformation or transformation by constructs having genes for both light and heavy chains on the same vector. Despite the fact that production of antibodies in plants takes longer, the low cost of production and capability of increasing production simply by increased propagation make plant antibodies an attractive proposition.

Aiming at therapeutic treatment (14) , have succeeded in producing multimeric secretory IgA (SIgA) molecules in plants which represent the predominant form of immunoglobulin in mucosal secretions. SIgA not only contains heavy and light chains but it is also dimerized by a J chain, and protected from proteolysis by a fourth polypeptide, the SC. Production of such antibodies in mammalian cells is very complex because of the requirement of B cell as well as gut epithelial cells for the formation of the SIgA. Thus, four transgenic tobacco plants were produced by genetic engineering which produced a murine monoclonal antibody light k chain, the hybrid IgA-G antibody heavy chain, murine J chain and rabbit secretory component. A series of sexual crosses was carried out to allow expression of all the four proteins simultaneously. The progeny produced a functional secretory immunoglobulin very efficiently. This demonstrated the potential of plants in assembly of antibodies, and the flexibility of system. Recently, a humanized monoclonal antibody against glycoprotein B of herpes simplex virus 2 (HSV-2) has been expressed in soybean. This antibody was found to possess the same efficacy for prevention of vaginal HSV-2 infection in mice and similar stability in human semen as the antibody expressed in human cell culture (52) and also plant cell cultures (23).

Topical application of antibodies has already been shown to control infection by way of passive immunization. A hybrid monoclonal antibody (IgA/G), having constant regions of IgG and IgA fused, has been used successfully against human dental caries caused by the bacterium *Streptococcus mutans* (33). Ma et al. (1998) compared the secretory antibody produced in transgenic tobacco (SIgA/G) and the original mouse IgG. Though both had similar binding affinity to surface adhesion protein of *S.mutans*, SIgA/G survived for three days in the oral cavity, whereas IgG could survive for just one day. The plant antibody provided protection against the colonization of the *S. mutans* for at least four months. These results show that this strategy could be useful for many other mucosal infections in humans and animals. Medical molecular farming has been done for the production of antibodies, biopharmaceuticals and edible vaccines in plants for immunotherapy (16, 31 and 32). Co-expression of soybean glycinias A1 aB 1b and A3B4 enhances their accumulation levels in transgenic rice seeds (62).

Scope for future study

Vaccines have been one of the most far-reaching and important public health initiatives of the 20th century. Advancing technology, such as oral DNA vaccines, intranasal delivery and edible plant derived vaccines, may lead to a future of safer and more effective immunization. Edible vaccines, in particular, might overcome some of the difficulties of production, distribution and delivery associated with traditional vaccines. Significant challenges are still to be overcome before vaccine crops can become a reality.

However, while access to essential healthcare remains limited in much of the world and the scientific community is struggling with complex diseases such as HIV and malaria, plant derived vaccines represent an appetising prospect. The potential advantages of plant based vaccines are edible means of administration, reduced need for medical personnel and sterile injection conditions, economical to mass produce and transport, reduced dependence on foreign supply, storage near the site of use, heat stable, eliminating the need for refrigeration, antigen protection through bioencapsulation, subunit vaccine (not attenuated pathogens) means improved safety, seroconversion in the presence of maternal antibodies, generation of systemic and mucosal immunity, enhanced compliance (especially in children), delivery of multiple antigens, and integration with other vaccine approaches.

References

1. Arakawa, T., Chong, D.K.X., and Langridge, W.H.R. (1997). Expression of Choleratoxin B subunit oligomers in transgenic potato plants, Transgenic Res, 6: 403-413

2. Arakawa, T., Chong, D.K.X. and Langridge, W.H.R. (1998). Transgenic plants for the production of edible vaccine and antibodies for immunotherapy, Nature Biotechnol, 16: 292-297

3. Arakawa, T., Yu, J. and Chong, D.K.X. (1998). A plant based cholera toxin B subunit insulin fusion protein protects against the development of autoimmune diabetes, Nat. Biotechnol., 16: 934-938

4. Arntzen, C.J. (1998). Pharmaceutical foodstuffs-oral immunization with transgenic plants, Nature Medicine (supplement), 4: 502-03

5. Artsaenko, O., Peisker, M., Zurniedan, U., Fielder, U., Weiler, E.W., Muntz, K., Conrad, U. (1995). Expression of a single chain FV antibody against abscisic acid creats a wilty phenotypes in transgenic tobacco, Plant J., 8: 745-750

6. Baum, T.J., Hiatt, A., Parrott, W.A., Pratt, L.H., Hussey, R. S. (1996). Expression in tobacco of a monoclonal antibody specific to secretion of the root knot nematode, Mol. Plant Microbe Interact., 9: 382-387

7. Benvenuto, E., Ordas, R.J., Tavazza, R., Ancora, G., Biocca, S., Cattaneo, A. and Galeffi, P. (1991). Phytoantibodies: A general vector for the expression of immunoglobular domains in transgenic plants, Plant Mol. Biol., 17: 865-874

8. Carter, J.E.III and Langridge, W.H.R. (2004). Plant based vaccine for protection against infectious and autoimmune diseases, Crit. Rev. Plant Sci., 21: 93-109

9. Carrillo, C., Wigdorovitz, A., Oliveros, J.C., Zamorano, P.I., Sadir, A.M., Gomez, N., Salinas, J., Escribano, J.M. and Borca, M.V. (1998). Expression of immunogenic S1 Glycoprotein of infectious Bronchitis virus in transgenic potatoes, J.Virol., 72: 1688-1690

10. Carrillo, C.A., Wigdorovitz, K., Trono, M.J., Dus Santos, S., Castanon, A.M., Sadir, R., Ordas, J.M., Escribano, J.M., Borca, M.V. (2001). Induction of a virus-specific antibody response to foot and mouth disease virus using the strain VP1 expressed in transgenic potato plants, Viral Immunol., 14:49-57

11. Centers for Disease Control and Prevention Global measles control and regional elimination, 1998-1999, MMWR Morb Mortal Wkly Rep. 1999, 48: 1124-1130

12. Chen, R. T., Markowitz, L.E., Albrecht, P. (1999). Measles antibody re-evaluation of protective titres , J. Infect Dis, 162 ; 1036-1042

13. Chrispeels, M.J. and Tague, B.W. (1991). Protein sorting in the secretory system of plant cells, Int. Rev. Cytol.,125: 1-45

14. Conrad, U.; Fiedler, U. (1994). Expression of engineered antibodies in plant cells, Plant Mol. Biol., 26:1023-1030

15. Cutts, F., Henao-Restrepo, A.M., Olive, J. (1999). Measles elimination: progress and challenges, Vaccine, 17: S47-S52

16. Daniell, H., Streatfield, S.J. and Wycoff, K. (2001). Medical molecular farming production of antibodies, biopharmaceuticals and edible vaccines in plants, Trends Plant Sci., 6: 219-226

17. DeAizpura, H.J., Wilson, Y.M. and Harrison, L.C. (1992). Transgenic plants for the production of edible vaccine and antibodies for immunotherapy, Proc. Natl. Acad. Sci. USA, 89: 9841-9845

18. De Neve, M., De Loose, M., Jacobs, A., Van Houdt, H., Kaluza, B., Weidle, U. and Depicker, A. (1993). Silencing of antibody genes in plants with single copy transgene inserts as a result of gene dosage effects, Plant Mol.Biol., 2: 227-237

19. During, K., Hippe, S., Kreuzaler, F. and Schell, J. (1990). Transgenic plants expressing a function single-class FV antibody are specifically protected from virus attach, Transgenic Res., 15: 281-293

20. Fischer, R., Stoger, E., Schillberg, S., Christou, P. And Twyman, R.M. (2004). Plant-based production of biopharmaceuticals, Curr. Opin. Plant Biol., 7: 152-158

21. Gomez, N., Carrillo, G.N., Salinas, J., Parra, F., Borca, M.V.and Escribano, J.M.(1998). Expression of immunogenic glycoproteins 3 polypeptides from trans Virology, 249: 352-358

22. Haq, T.A., Mason, H.S., Clements, J.D.and Arntzen, C.J.(1995). Oral immunization with a recombinant bacterial antigen produced in transgenic plants, Science, 268:714-716

23. Hellwig, S., Drossard, J., Twyman, R.M. and Fischer, R. (2004). Plant cell cultures for the production of recombinant proteins, Nature Biotechnol,22: 1415-14

24. Hein, M.B., Yeo, T.C., Wang, F. and Sturtevant, A. (1996). Expression of cholera toxin subunits in plants, Ann. NY Acad. Sci., 792 : 51-56

25. Hidenori, T., Takachika H., Lijun, Y., Yoshifumi, T., Yoshikazu, Y., Karoru, T., Ryotaro, I., Hideyuki, K., Hiroshi, K. And Fumio, T. (2005). A rice-based edible vaccine expressing multiple T cell epitopes induces oral tolerance for inhibition of Th2-mediated IgE responses, Proc. Natl. Acad. Sci. U.S.A., 102: 17255-17530

26. Hiatt, A., Cafferkey, R and Bowdish, K (1989). Production of antibodies in transgenic plants, Nature, 342: 76-78

27. Hiatt, A. and Mostov, K. (1993). In Transgenic Plants: Fundamentals and Applications (ed. Hiatt. A), Marcel Dekker, Inc, New York, pp. 221-237

28. Hidenoi, T. (2009). Oral edible vaccine for allergy vaccines, National Kidney Foundation 2009 Spring Symposium, UK

125

29. Huang, Z., Dry, I., Webster, D. (2001). Plant derived measles virus hemagglutinin protein induces neutralizing antibodies in rice, Vaccine, 19: 2163-217

30. Kapusta, J., Modelska, A., Figlerowicz, M. (1999). A plant derived edible vaccine against hepatitis B virus, FASEB J., 13: 1796-1799

31. Kawakatsu, T., Yamamoto, M.P., Hirose, S., Yano, M., Takaiwa, F. (2008). Characterization of a new rice gluteilin gene GluD-1 expressed in the starchy endosperm, J.Exp. Bot., 1: 261-265

32. Kong, Q., Richter, L., Yang, Y.F., Arntzen, C.J., Mason, H.S. and Thanawala, Y. (2001). Oral immunization with hepatitis B surface antigen expressed in transgenic plants, Proc. Natl. Acad. Sci., USA, 98: 11539-11544

33. Longstaff, M., Newell, C.A., Boonstra, B., Strachan, G., Learmonth, D., Harris, W.J., Porter, A.J. and Hamilton, W.D. (1998). Expression and characterization of single chain antibody fragments produced in transgenic plants against the organic herbicides atrazine and panaquate, Biochem. Biophys. Acta, 1381: 147-160

34. Lund, P. and Dunsmuir, P. (1992). A plant signal sequence enhances the secretion of bacterial ChiA in transgenic tobacco, Plant Mol. Biol., 18: 47-53

35. Ma, S.W., Zhao, D.L., Yin, Z.Q., Mukherjee, R., Singh, B, Quin, H.Y., Stiller, C.R. and Jevnikar, A.M. (1997). Transgenic plants expressing autoantigens fed to mice to induce oral immune tolerance, Nature Med., 3: 793-796

36. Ma, J.K-C., Drake, P.M.W., Christou, P. (2003). The production of recombinant pharmaceutical proteins in plants, Nature Reviews/Genetics, 4: 794-805

37. Mason, H.S. and Arntzen, C.J. (1995). Transgene plants as vaccine production systems, Trends Biotechnol., 13: 388-392

38. Mason, H.S., Lam, D.M. and Arntzen, C.J. (1992). Expression of hepatitis B surface antigen in transgenic potato, Proc.Natl. Acad Sci. USA, 89: 11745-11749

39. Mason, H.S., Ball, J.M., Shi. J.J., Jiang, X., Estes, M.K. and Arntzen, C.J. (1996). Expression of Norwalk viral protein in transgenic potato and protein and its immunogenicity in mice, Proc. Natl. Acad. Sci. USA, 93: 5335-5340

40. Mason, H.S., Haq, T.A., Clements, J.D. and Arntzen, C.J. (1998). Edible vaccine protects mice against E.coli heat labile toxin (LT): potatoes expressing a synthetic LT-B gene, Vaccine, 16: 1336-1343

41. Ma, J.K. and Hein, M.B. (1995). Antibody production in plants, Trends Biotechnol., 13: 522-527

42. Ma, J.K.C., Lehner, T., Stabilla, P., Fux, C. I. and Hiatt, A. (1994). Assembly of monoclonal antibody with IgG L and IgA heavy chain domains in transgenic tobacco, Eur. J.Immunol., 24: 131-138

43. Ma, J.K.C., Hiatt, A., Hein, M.B., Vine, N., Wang, F., Stabila, P., Van Dolleweered, C., Mostov, K. and Lehner, T. (1995). Generation and assembly of secretory antibodies in plants, Science, 268: 716-719

44. Ma, J.K.C., Hikmat, B.Y., Wycoff, K., Vine, N.D., Changelegue, D., Yu, L., Hein, M.B. and Lehner, T. (1998). Characterization of a recombinant plant monoclonal secretory antibody and preventive immunotherapy, Nature Med., 4: 601-606

45. Ma, S.W., Zhao, D.L, Yin, Z.Q., Mukherjee, R., Singh, B., Quin, H.Y., Stiller, C.R. and Jevnikar, A.M. (1997). Transgenic plants expressing auto antigens fed to mice to induce oral immune tolerance, Nature Med., 3: 793-796

46. Maand, S., Jevnikar, A.M. (2005). Transgenic rice for immunotherapy, Proc. Nattl. Acad. Sci. U.S.A., 102: 17255-17256

47. McElroy, D. and Bretell, R.I.S. (1994). Foreign gene expression in transgene plants, Trends Biotechnol., 12: 62-68

48. McGarvey, P.B., Hammond, J., Dienelt, M.M., Hooper, D.C., Fu, Z.F., Dietzschold, B., Koprowski, H and Michaels, F.H. (1995). Expression of the Rabies Virus glycoprotein in Transgenic tomatoes, BioTechnology, 13: 1484-1487

49. Nikolov, Z. and Hammes, D. (2002). Production of recombinant proteins from transgenic crops In: Hood E-E Howard J.A. (edv) Plants as factories for protein production, Kluwer, Durdrecht 159-174

50. Nochi, T., Takagi, H., Yuki, Y., Yang, L., Masumura, T., Mejima, M., Nakanishi, L., Matsumura, A., Uozumi, A., Hiroi, T., Morita, S., Tanaka, K., Taaiwa, F. And Kiyono, H. (2007). Rice-basal mucosal vaccine as a global strategy for cold-chain and needle free vaccination, Proc. Natl. Acad. Sci. U.S.A., 104: 10986-10991

51. Osterhaus, A., Van Amerongen, G., Van Binnendijk, R. (1998). Vaccine strategies to overcome maternal antibody mediated inhibition of measles vaccine, Vaccine, 16: 1479-1481

52. Owen, M., Gandecha, A., Cockburn, B. and Whitelam, G. (1992). Synthesis of a functional anti-Phytochrome single chain FV protein in transgenic tobacco, Biotechnology, 10: 790-794

53. Pascual, D.W.(2007). Vaccines are for dinner, Proc. Natl. Acad. Sci. U.S.A., 104:10757-10758

54. Ruf, S., Hermann, I.J., Berger, I.J., Carner, H. And Bock, I.(2001). Stable genetic transformation of tomato plastids and expression of a foreign protein in fruit, Nat. Biotechnol., 19; 870-875

55. Schledzewski, K and Mendal, R.R. (1994). Quantitative transient gene expression : comparison of the promoters for maize polyubiquitin L, rice actin L, maize derived Emu and CaMV 35 S in cells of barley, maize and tobacco, Transgenic Res., 3: 249-255

56. Schouten, A., Roosien, J., de Boer, J. M., Wilmink, A., Rosso, M.N., Bosch, D., Stieckema, W.J., Gommers, F.J., Bakker, J. and Schots, A. (1997). Improving ScFv antibody expression levels in the plant cytosol, FEBS Lett., 415: 235-241

57. Shengwu, M., and Anthony, M.J. (2005). Transgenic rice for allergy immunotherapy, Proc. Natl. Acad. Sci. U.S.A., 102: 17255-17256

58. Stoger, E., Vaquero, C., Torres, E. (2000). Cereal crops as viable production and storage systems for pharmaceuticals ScFv antibodies, Plant Mol. Biol., 42: 583-590

59. Svennerholm, A.M., Jetborn, M., Gothefors, L., Karim, A.M.M.M., Sack, D.A. and Holmgren, J. (1984). Mucosal anti toxic and antibacterial immunity after cholera disease and after immunisation with a combined â –subunit whole cell vaccine, J.Infect.Dis., 149: 884-893

60. Tacket, C.O., Mason, H.S., Losonsky, G., Clements, J.D., Levine, M.M. and Arntzen, C.J. (1998). Immunogenicity in humans of a recombinant bacterial antigen delivered in transgenic potato, Nature Med., 4: 607-609

61. Tacket, C.O., Mason, H.S., Losonsky, G., Estes, M.K., Levine, M.M. and Arntzen, C.J.(2000). Human immunization a most Norwalk virus vaccine delivered in transgenic potatoes, J.Infect.Dis., 182:302-305

62. Takaiwa, F., Sakuta, C., Choi, S-K., Tada, Y., Motoyama, T. And Utsumi, S. (2008). Co-expression of soybean glycinias A1 aB 1b and A3B4 enhances their accumulation levels in transgenic rice seed, Plant Cell Physiol., 49: 1589-1599

63. Tavladoraki, P., Benvenuto, E., Trinca, S., De Martinis, D., Cattaneo, A. and Galeffi, P. (1993). Transgenic plants expressing a functional single-chain Fv antibody are specifically protected from virus attack, Nature, 366: 469-472

64. Thanavala, Y., Yang, Y.F., Lyons, P., Mason, H.S., Arntgen, C.J.(1995). Immunogenicity of transgenic potatoes for hepatitis B surface antigen, Proc.Natl. Acad. Sci. USA, 92:3358-3361

65. Tisch, R. and McDevitt, H. (1996). Insulin dependent diabetes mellitus (IDDM) is a multifactorial auto immune disease for which susceptibility is determined by environmental and genetic factors. Inheritance is polygenic, with the genotype of the major, Cell, 85: 291-297

66. Tyagi, A.K., Bajaj, S., Mohanty, A., Choudhary, A. and Maheshwari, S.C. (1999). Transgenic rice: A valuable monocot system for crop improvement and gene research, Crit. Rev. Biotechnol., 19: 41-79

67. Van Engelen, F.A., Schouten, A., Molthoff, J.W., Roosien, J., Salinas,J., Dirkse, W.G., Schots, A., Bakkar, J., Gommers, F.J., Jongsma, M.A., Bosch, D.and Stiekema, W.J.(1994). Co-ordinate expression of antibody subunit genes yielded high levels of monoclonal antibodies in roots of transgenic tobacco, Plant Mol.Biol., 26: 1701-1710

68. Zeitlin, L., Olmsted, S.S., Moench, T.R., Co, M.S., Martinell, B.J., Paradkar, V.M., Russell, D.R., Queen, C., Cone, R.A. and Whaley, K.J.(1998). A Rumanised monoclonal antibody produced in transgenic plants for immunoprotection of the vagina against genital Herpes, Nat ure Biotechnol., 16:1361-1364

Regulation of CIP/KIP cell cycle inhibitors and their biological implications

Jinhwa Lee

Dept. of Clinical Lab Science, Dongseo University, Busan 617-716, Korea

For correspondence: jinhwa2000@gdsu.dongseo.ac.kr

Abstract

The cell cycle regulation is a key homeostatic device upon the cellular decision during the multi processes like proliferation, differentiation, survival and death. Human cancers can arise from the result of functional failure in cell cycle regulators. Therefore, activity of the major cell cycle regulator, cyclin-dependent kinase (CDK), is tightly regulated by cyclin dependent kinase inhibitors (CKIs) such as the p21CIP1 and p27KIP1. These CKIs, mainly functioning as a cyclinE/CDK2 complex inhibitor during the G_1 cell cycle, have been reported to play disparate roles including the assembly of cyclinD/CDK4,6 and others that apparently assist cell growth if not help carcinogenesis. While their genetic disruptions are rarely found in human cancers, low expression levels or cytoplasmic mislocalizations of the p21CIP1 and p27KIP1 often correlate with human malignancies. Recent studies show that signalling kinases can directly phosphorylate these proteins as a substrate and change their activities in the role of a cell cycle inhibitor by switching interacting partner proteins after the phosphorylation-driven structural modifications. This report will discuss the complex regulatory mechanisms of p21CIP1 and p27KIP1 proteins on the cue of extracellular signals and their indications of functional importance to carcinogenesis.

Keywords: Cell cycle; Proliferation; CDK, p21CIP1, p27KIP1

Introduction

The mammalian cell cycle operates with four distinct phases, G_1, S, G_2 and M in a tightly regulated manner, each of which should be completed before the next begins (1). Progression of cell cycle transitions is mediated by sequential activation of the cyclin/CDK complexes. Since timely regulation is absolutely important in normal cell cycle progression, cyclin/CDK complexes are integrators of the multiple signals. Those signals include extracellular signals such as cytokines, hormones, or physical interactions with extracellular matrix or other cells. In mammalian tissues, several cyclin/CDK complexes play a role in the G_1-to-S transition (2). In early G_1, D-type cyclins are elevated from mitogenic signals and activate CDK4 or CDK6 (3). The three D-type cyclins (D1, D2 and D3) are expressed differentially when CDK4 and CDK6 are co-expressed in many cell types (4). In late G_1, cyclin E/CDK2 activity is elevated due to the initial cyclin D/CDK4,6 activation, not by mitogenic stimulation. The increased cyclin E/CDK2 activity phosphorylates pRb and releases E2F transcription factors from an inactive or repressive pRb–E2F complex, which initiates a whole new synthesis of proteins involved in DNA replication (5). The E2F genes also involve some protooncogenes and some cell-cycle regulatory proteins, as well as cyclin E that forms a feedback loop to expedite and commit to enter S phase. Activity of cyclin/CDK complexes is regulated

in multiple ways by the accumulation of the cyclin, at the level of assembly into the cyclin/CDK complexes, and by specific phosphorylation and dephosphorylation of the components. One additional and important regulatory mechanism of these G_1 cyclin/CDK complexes is their association with CKIs. The CKIs either physically bind and block the cyclin/CDK complexes or inhibit substrate/ATP access. Early investigators postulated that some of these CKIs have additional functions (6). CKIs are grouped to two gene families: the smaller INK4 (inhibitors of CDK4) and the larger CIP/KIP (CDK interacting protein/ kinase inhibitory protein).

The INK4 family is composed of p16INK4A, p15INK4B, p18INK4C, p19INK4D (7). The common structural feature among them is the ankyrin repeats and all of them can inhibit CDK4. They compete with D-type cyclins for binding to the CDK subunit (8). The INK4 family proteins are characterized by specific binding to CDK4 and CDK6. Tissue-specific functions of this family of cell cycle inhibitors have been suggested recently because of the diversity in the pattern of expression of INK4 genes (9). The INK4 proteins are commonly lost or inactivated by mutations in many different cancer types. In addition to their role in arresting cells in the G_1-phase of the cell cycle, it also increases interests of researchers that they have been shown to participate in different cellular processes other than cell cycle regulation. The discoveries of involvement of INK4 proteins include their functions in senescence, apoptosis, DNA repair, and multistep oncogenesis. The p16INK4A is a tumor suppressor that inhibits the cyclin D-associated kinase complexes. Loss of function in p16INK4A results in the same effect of loss of function in Rb (10). It has been reported that p14ARF protein is closely related to p16INK4A. The ARF protein, a spliced variant of the INK4A gene, is known to have a function of stabilizing p53 by preventing degradation (11). The second

INK4 family protein, p15INK4B, regulates the cell cycle clock by inhibiting cyclinD/CDK4- or cyclinD/CDK6-mediated phosphorylation of Rb. Induction of p15INK4B-triggered G_1-phase arrest occurs in response to TGF-â (12). Loss of p15INK4B gene is associated with lympho-proliferative disorders and tumor formation (13). The p15INK4B mediated pathways that control G_1/S transition are frequently deregulated in human cancers such as prostate cancer, melanoma, pituitary adenoma, acute myeloid leukemia, gastric cancer. The p18INK4C seems to play an important role in growth control and its expression is found in many different tissue types. It has been suggested that loss of p18INK4C function results in shortening the G_1 phase and thus facilitates the cell cycle progression. Interestingly, functional synergism between p18INK4C and p27KIP1 has been implicated in pituitary tumors (14, 15). A recent study of the gene encoding p19INK4D is induced by vitamin D3 derivatives and by retinoids. Therefore, the chemopreventive effects of vitamin D3 may be associated with this induction of p19INK4D expression. Recent studies reported that the knockdown of p19INK4D renders cells sensitive to autophagic cell death (16)

The second group of cell cycle inhibitors is CIP/KIP family proteins: p21CIP1, p27KIP1 and p57KIP2. The structural feature of these proteins shows an ability to bind a whole cyclin/ CDK complex, different from INK4 family proteins' ability to bind CDK protein alone by competing for cyclin's binding. They can function throughout the all cell cycle phases by interacting with different kinds of cyclin D, E, A/CDK complexes. Although initially identified as cell cycle inhibitors, these CIP/KIP family proteins have emerged to display roles in different cellular functions ranging from apoptosis to cell migration and have appeared to add their lists on other important cellular functions. These functions are essential for the maintenance of normal cell

homeostasis. The first identified inhibitor in this family is p21CIP1 that is also named SDI1 (senescent cell-derived inhibitor 1) or WAF1 (wild-type p53-activated fragment 1). The existence of p27KIP1 is discovered by TGF-β induced G_1 arrest and its function as a G_1 arrest controller diversifies into cases such as contact inhibition mediated G_1 arrest. p57KIP2 that is discovered during the search for homologues of p21CIP1 and p27KIP1 also participates in the control of cell cycle regulation as well as differentiation and apoptosis in particular tissues (17). Recent studies demonstrate that p57KIP2 functions in many different cellular processes beyond cell cycle control. In Schwann cells, the myelinating glial cells of the peripheral nervous system, small hairpin RNA dependent suppression of p57KIP2 results in cell cycle exit and the initiation of the cellular differentiation program via p57KIP2/LIMK-1 interactions (18). While function and regulation of p57KIP2 are under active investigations, this manuscript will focus on the p21CIP1 and p27KIP1 proteins that have recently been demonstrated extensively for their regulatory mechanisms with relation to cellular transformation into cancer.

Upon the exposure of cells to growth inhibitory signals, p21CIP1 and p27KIP1 bind to cyclin/CDK complexes to inhibit cyclin/CDK catalytic activity and result in cell cycle arrest. It becomes evident that p21CIP1 and p27KIP1 might have new activities that are unrelated to their function as CDK inhibitors. From the help of copious publications, the importance of cytoplasmic localization and the identification of new targets have revealed novel functions for these p21CIP1 and p27KIP1 proteins beyond cell cycle controls. A complex signaling and phosphorylation network modifies these proteins and changes their degradation, subcellular localization, and protein-protein interactions. This article will focus on reviewing the cellular functions and recent advances of the p21CIP1 and p27KIP1 proteins.

A CIP/KIP protein interacts with cyclin/CDK complexes

G_1 cell cycle progression relies on the sequential activation of G_1 cyclin/CDK complexes to enter the S phase. Tight regulation of G_1 cyclin/CDK complexes therefore is essential when cells decide to divide because the commitment site, restriction point, for cell division lies at late G_1. INK4 family proteins bind and inhibit CDK4 and CDK6 specifically and CIP/KIP proteins interact with the cyclin E/CDK2 complex, inhibiting cell cycle transition from G_1 to the S phase (19). Different from the INK4 family proteins, CIP/KIP proteins do not dissociate cyclin/CDK complexes (20). The first á-helical loop of a CIP/KIP protein interacts with the cyclin, and the second helix binds to the catalytic cleft of the CDK subunit, thereby blocking ATP loading (21, 22). Many cyclinD/CDK4,6 complexes have been found to contain p21CIP1or p27KIP1 and surprisingly maintain the active state of the cyclin D/CDK4,6 complex. With the help of data from animals of the knockout p21CIP1 and p27KIP1 genes, p21CIP1and p27KIP1 proteins are now believed to facilitate assembly of the two subunits of cyclin D1 and the CDK4 or CDK6 (5). Then these contradictory dual functions of p21CIP1 and p27KIP1 comprise inhibition of the nuclear CDK2 and assembly, thus activation, of cytosolic CDK4 or CDK6 with cyclin D. Therefore, the p21CIP1 and p27KIP1 proteins might have totally irrelevant functions in different intracellular locations and their structural modifications or interacting proteins might also be differentiated according to the localization.

In addition to the assembly, cytoplasmic CIP/KIP proteins also promote the nuclear accumulation of D-type cyclins. p27KIP1 protein can bind to the nuclear pore-associated protein mNPAP60, and interact with the nuclear export

protein CRM1 (23, 24). p21CIP1 blocks the interaction between cyclin D1 and the CRM1, leading to increased cyclin D levels in the nucleus. Since nuclear export is mediated by CRM1, CRM1 interaction with p21CIP1 and p27KIP1 causes trans-localization into the cytoplasm. It can also be interpreted that the interaction displaces cyclin D1 from CRM1 to increase the cyclin level in the nucleus. The binding ability of the CIP/KIP proteins to cyclin D/CDK4,6 complexes can be viewed cyclin D/CDK4,6 complexes as a sequestering station for the CIP/KIP cell cycle inhibitors, thus freeing and activating the cyclin E/CDK2 complex. p16INK4A null mouse shows a high incident of tumor development and p16INK4 null phenotype is similar to the null phenotype of pRb. The INK4-free cyclin D/ CDK4 complexes can sequester the CIP/KIP proteins, freeing cyclinE/CDK2 and resulting in hyperphosphorylation of Rb from the inhibitor-free cyclinE/CDK2 activity. Different from the p16INK4 null mouse phenotype, p27KIP1 null mice do not show an increased tumor frequency. However, null mice of multiple cell cycle inhibitors display severe developmental defects although null phenotypes show clear discrepancies between INK and CIP/KIP family proteins, suggesting the existence of redundant roles.

The CIP/KIP family proteins are best known as cell cycle inhibitors but they also play a role in cell differentiation, senescence and apoptosis. p21CIP1 is involved in p53-dependent DNA damage-induced G_1 arrest. The main role of p21CIP1 of course is G_1 arrest through inhibiting the activity of cyclinE/CDK2. Cytokines such as TGF-beta, TNF, or IL6 induce p53-independent expression of p21CIP1 which can suppress apoptosis and at the same time cell cycle inhibition (25). Since p21CIP1 functions in a variety of different cellular processes, the consequences of changes in p21CIP1 regulation after DNA damage are complex. Previous reports indicate that p21CIP1 plays both anti- and proapoptotic roles. Cytoplasmic p21CIP1 can interact with ASK1 and procaspase 3 to suppress apoptosis. On the other hand, overexpression of p21CIP1 and retinoic acid-induced p21CIP1 promote apoptosis. In many cell types, p27KIP1 plays a key role in the decision to the G_1-S entry. First identified as a CDK2-inhibitor in contact inhibition or TGF-beta arrested cells, 27KIP1 is also induced by other anti-mitogenic signals such as cAMP and rapamycin or lovastatin treatment. Decreased expression of p27KIP1 in breast cancer cells correlates with poor prognosis.

CIP/KIP protein phosphorylation by mitogenic, antimitogenic and other signaling pathways

CIP/KIP proteins are able to respond to diverse extracellular demands and help cells become fit to the new environment through proper cell cycle regulation. On performing the critical actions, p21CIP1 and p27KIP1 proteins share common cell cycle effects as they have conserved sequences in their inhibitory domains and both proteins can form a ternary complex with cyclin/ CDK in response to extracellular signals. Both p21CIP1 and p27KIP1 proteins are short-lived: activity of these proteins largely depends on the protein levels that are regulated mainly through proteasome-dependent degradation and/or transcriptional control. Still under active uncovering of mechanisms involved, these proteins possess seemingly contradictory actions of facilitating cell motility and interacting with proteins involved in functions aside from cell cycle regulations when they are localized in the cytoplasm. Fibroblasts are the model system that is mainly used to study the activities of p21CIP1 and p27KIP1 and their role on cell cycle control. In other cell types, p21CIP1 and p27KIP1 are unusually controlled by different regulatory curcuits that are sometimes contrasting in functions between these two proteins. As p21CIP1 and p27KIP1 knock-out mice display different phenotypes, it is not unusual that

p21CIP1 and p27KIP1 demonstrate nonoverlapping and distinctive functions (26). Significance of multiple biological functions such as apoptosis and differentiation of these two p21CIP1 and p27KIP1 proteins are gradually acknowledged. The onset of environmental cues delivers these cell cycle inhibitors to a new biological role following posttranslational modifications like phosphorylation or ubiquitination (27). Extensive studies have informed us that p21CIP1 and p27KIP1 proteins remodel themselves predominantly through phosphorylation and consequent alteration of their interacting protein partners, resulting in the changes in cellular functions and localization as well as their protein levels.

It is well known that induced phosphorylation by growth factors activates cytoplasmic protein kinases such as Raf, MEK, ERK, JNK, p38 MAPK or SAPK, JAK, AKT and other kinases. Nonetheless, it is interesting to know that some of them directly phosphorylate CKI as exampled above in the case of p21CIP1 and p27KIP1 by using the cell cycle inhibitors as their own substrates. It is more important to know the condition, function and the precise phosphorylation sites of the substrate in order to understand how individual signaling network can communicate with these cell cycle regulators. Protein kinases which interact and phosphorylate directly p21CIP1 and p27KIP1 proteins have been studied intensively during recent years using in vivo or in vitro studies (28). Glycogen Synthase Kinase 3 beta phosphorylates p21CIP1 and enhances proteasomal degradation after UV irradiation. PIM-1 Kinase phosphorylation of p21CIP1 promotes stability of p21CIP1 in H1299 cells. AKT phosphorylation of p21CIP1 functions in increasing protein stability of p21CIP1 and cell survival (29). Other studies regarding AKT-induced phosphorylation at threonine 145 of p21CIP1 present the function for subcellular localizations in HER2 overexpressing breast cancer cells. Protein phosphorylation has an essential function in all kinds of cells but the delicate regulation pattern tells us that the same kinase-substrate interaction does not always aim for the same functional outcome; these examples are found more frequently when other cell types or different conditions even with the same cell types are used. When a kinase phosphorylates the substrate on multiple sites, one site can be more phosphorylated than others in a certain condition probably because of the presence of the third protein or small molecules that affect interaction between the kinase-substrate. Phosphorylation and functional changes like cytoplasmic localization of p21CIP1 with HER2 overexpression in breast cancer cells impose clinical values (30). The very kinase critical for transformation therefore becomes an important question to answer; however, there might be more than one kinase for the final target of CIP/KIP proteins because both p21CIP1 and p27KIP1 proteins possess multiple phosphorylation sites. Cytokines inducing differentiation also end up on phosphorylating the same targets as antimitogen signals. Myoblast cell survival has been reported to be promoted by p21CIP1 protein through the MAPK cascade activation (31). It would be biologically meaningful to discover the phosphorylation sites and the kinases for the p21CIP1 protein during this myocyte differentiation. In K562 human leukemia cells, both p21CIP1 and p27KIP1 are involved in the regulation of cell cycle progression and differentiation. Interestingly, there is a difference in the biological effects as p21CIP1 directs cells toward megakaryocytic differentiation and p27KIP1 provokes an erythroid differentiation response.

Important roles of p27KIP1 on guarding cells against breast cancer have advanced our understanding in relationship between the phosphorylation and regulation of the inhibitor protein. Phosphorylation on serine/threonine of

p27KIP1 by ERK1 is a signal for ubiquitination and phosphorylation on more than one threonine sites by different kinases involves cytoplasmic localization. CyclinE/CDK2 phosphorylates p27KIP1 on Thr187 and leads to ubiquitin-dependent phosphorylation. p27KIP1 protein phosphorylated by AKT at Thr157 and Thr198 becomes better assembler of cyclin D/CDK4 complex formation (32, 33). Since p27KIP1 binding to cyclin D/CDK4 facilitates activation of cyclinE/CDK2 through sequestration of the inhibitory protein, the differential binding of p27KIP1 to the distinct CDKs during G_1 cell cycle can be attributed to the phosphorylation status of p27KIP1. Altered p27KIP1 phosphorylation would then switch p27KIP1 cyclin/complexes. As p27KIP1 phosphorylation is cell cycle dependent, the cyclinE/CDK2 inhibitory activity of p27KIP1 is maximal in G_0 and falls as cells move through G_1 into S phase. At the same time, the cyclin D/CDK4 bound p27KIP1 is maximal during early G_1. Anti-mitogenic signaling dissociates p27KIP1 from CDK4/6 complexes and accumulates in cyclinE/CDK2. As with Thr145 phosphorylation of p21CIP1 by PIM1, PIM kinases promote cell cycle progression by phosphorylating and down-regulating p27KIP1

Phosphorylation affects degradation and localization of p21CIP1 and p27KIP1 proteins

Mitogenic signalings often cause down-regulation through accelerated proteolysis and mislocalization out of nucleus into cytoplasm of p21CIP1 and p27KIP1 proteins. The fact that mutation or deletion of p21CIP1 and p27KIP1 genes is uncommon in human cancers suggests that post-transcriptional regulatory mechanisms may be more important in the process of cancer development. These proteins are short lived and their expression is tightly regulated by proteasome-mediated protein degradation. The ubiquitination-dependent degradation pathway involves E3-ubiquitin ligases, such as SCFSKP2 (34). While less often than accelerated proteolysis in human cancers, cytoplasmic localization of p27KIP1 – that of p21CIP1 in cancers is less understood- has been observed in some advanced cancers. Many tumor suppressor proteins including p53, FOXO family gene products, p21CIP1 and p27KIP1 proteins function when they are present in the cell to prevent cancer initiation or progression. Inhibition of FOXO family proteins that compose p21CIP1 and p27KIP1 gene transcription factors can result in the negative transcriptional regulation of p21CIP1 and p27KIP1 proteins. Therefore, mislocalization of those nuclear proteins including FOXO family proteins into the cytoplasm can disable them as a tumor suppressor. In the cytoplasm, FOXO family proteins can no longer exercise a transcription factor, nor do the p21CIP1 and p27KIP1 proteins the cyclinE/CDK2 inhibitor. Export of nuclear proteins generally involves modification in the leucine-rich nuclear export signal sequences which allows binding to the CRM1/RanGTP proteins and then the nuclear proteins are ready for the journey out of nucleus to the cytoplasm. SCFSKP2 and CRM1 proteins are notably recognized in the study of cancer development for this very reason that they help nuclear tumor suppressive proteins evacuate from the functional site, nucleus.

The p21CIP1 protein level is mainly controlled at the transcriptional level. Nonetheless, the fact that a half-life of p21CIP1 is less than 30 min dictates p21CIP1 stability as a considerable control site. Cytoplasmic localization of this nuclear CDK inhibitor of the p21CIP1 protein can be added as another regulatory site. Modification of p21CIP1 by phosphorylation that changes interaction with other cellular proteins is one mechanism to control the protein level in general by qualifying the protein for ubiquitin-dependent proteosomal degradation and by mislocalization into cytoplasm. Degradation of p21CIP1 protein

involves ubiquitination-dependent and - independent proteasomal targeting. This occurs through binding of its COOH terminus with the C8 subunit of the 20S core of the proteasome. Mitogenic signaling induced phosphorylation of p21CIP1 is precedent in this process. CDK2, AKT, p38MAPK or SAPK, JNK, GSK-3ß, PKA, and PKC have been shown to phosphorylate p21CIP1. PKC can phosphorylate Ser146 in the COOH terminus of p21CIP1 and facilitate degradation. Phosphorylation of p21CIP1 affects interaction with its binding partners, regulating the stability of the protein and its subcellular localization. AKT phosphorylates p21CIP1 at Thr145 and Ser146 within the binding site of PCNA which is known to promote the ubiquitination and degradation of p21CIP1. Phosphorylation at Ser146 by AKT significantly increases the p21CIP1 protein level and Thr145 phosphorylation by AKT prevents PCNA binding and promotes the nuclear export of p21. A link between intracellular localization and proteolysis is better identified for the p27KIP1. Antimitogenic signaling induced phosphorylation of p21CIP1, as predicted, inhibits p21CIP1 degradation. p38MAPK or SAPK and JNK1 activated by TGFß -1 phosphorylates p21CIP1 at Ser130 and increases p21CIP1 stability.

Activity of the target protein CDK2 can affect p21CIP1 stability. While it is intriguing to understand how CDK inhibitors can put the CDK activity to use for their degradation, a novel idea has been recently reported with an introduction of a model of high affinity binding motif, cy1, and low affinity binding motif, cy2, for CDK on p21CIP1 (35, 36). In the model, CDK2 may promote p21CIP1 degradation in a sequential pathway. CDK2-dependent phosphorylation of p21CIP1 at Ser130 would be recognized by a SKP2-containing SCF complex, and ubiquitinated and degraded by the proteasome. Direct phosphorylation on the Thr145 of p21CIP1 by PIM-1 stabilizes it and results in a shift in the subcellular localization of p21CIP1 in H1299 cells (29). The finding that p21CIP1 phosphorylation at Ser114 by GSK-3ß is critical for p21CIP1 protein degradation by UV shows an example of proteosomal degradation of p21CIP1 protein without ubiquitination.

While clinical importance of a cytoplasmic mislocalization of p21CIP1 in tumors is not understood as well as that of p27KIP1, p21CIP1 protein might be more involved in apoptosis compared to p27KIP1 protein. For p27KIP1, cytoplasmic localization is closely linked to poor prognosis in human breast, colon, ovarian, thyroid and esophageal cancers and low protein levels have been identified and associated with tumor progression and poor prognosis in many different cancers including colon, breast, prostate, ovarian, and brain cancer. At G_0, p27KIP1 stabilization is a result of Ser10 and Thr198. Ser10 phosphorylation in quiescent cells is attributed to MIRK/DYRK1B. Ser10 phosphorylation interferes with the binding of p27KIP1 to cyclin/CDKcomplexes which may reduce p27KIP1 stability. At mitogenic signal, KIS is responsible for Ser10 phosphorylation and becomes an important regulator of p27KIP1 (37). Phosphorylation at Ser10 triggers the export of p27KIP1 from the nucleus into the cytoplasm by a CRM1-mediated export pathway. Therefore, Ser10 phosphorylation results in nuclear export on the mitogenic cues which might expose the protein to the cytoplasmic proteosome and therefore indirectly decrease the stability of p27KIP1 (38). Thr157 located within the nuclear localization sequence of p27KIP1 can be phosphorylated by AKT. It is found that phosphorylation at Thr157 and Thr198 cooperates to enhance cytoplasmic localization of p27KIP1. In addition to the threonine/serine phosphorylation sites, p27KIP1 possesses three tyrosine residues, Tyr74, Tyr78, and Tyr79, all of which are phosphorylated by SRC family kinases. These

phosphorylation sites are in the CDK binding region of p27KIP1 and the phosphorylation of these tyrosines makes p27KIP1 unstable. The protein unstability is because p27KIP1 is a poor inhibitor of CDK2 and thus partially restore the kinase activity after tyrosine phosphorylation. Phosphorylation at Thr187 of p27KIP1 by cyclinE /CDK2 complexes provides a binding site for the SCFSKP2 E3 ubiquitin ligase (39). Therefore, p27KIP1 protein levels significantly decrease when cyclinE/CDK2 is activated.

Conclusion

Understanding the p21CIP1 and p27KIP1 protein regulation provides a better insight on the cell cycle regulation mechanisms in human cancer. As their primary function as a CKI is to bind and inhibit a cyclin/CDK complex, these two p21CIP1 and p27KIP1 proteins function throughout the all cell cycle phases by interacting with different kinds of cyclin D, E, A/CDK complexes. These cell cycle inhibitors have emerged to display roles in other cellular functions such as apoptosis and cell migration. Their functions are differentiated through exchanging partner proteins. Therefore a competent structure of these proteins for punctual or scrupulous partner proteins may be critical for the maintenance of normal cell homeostasis. After de novo synthesis, p21CIP1 and p27KIP1 proteins are extensively modified by post-translational modifications of phosphorylation. Phosphorylation of these proteins has been recently reported to be the result of direct substrate-kinase interactions of major signalling molecules such as MAPK or AKT as a final molecular event of extracellular signaling pathways. Mitogen- or antimitogen-induced phosphorylation causes alteration in expression levels and the intracellular location of p21CIP1 and p27KIP1 proteins. The mechanisms involved in cytoplasmic localization as well as degradation of these proteins are important in understanding many human carcinogenesis.

References

1. Collins, I. and Garrett, M.D. (2005). Targeting the cell division cycle in cancer: CDK and cell cycle checkpoint kinase inhibitors. Curr. Opin. Pharmacol., 5: 366–373.

2. Vermeulen, K., Van Bockstaele, D.R. and Berneman, Z.N. (2003). The cell cycle: a review of regulation, deregulation and therapeutic targets in cancer. Cell Prolif., 36: 131–149.

3. Park, M.T. and Lee, S.J. (2003). Celll cycle and cancer. J. Biochem. Mol. Biol., 23: 60–65.

4. Schwartz, G.K. and Shah, M.A. (2005). Targeting the cell cycle: a new approach to cancer therapy. J. Clin. Oncol., 23: 9408–9421.

5. Coqueret, O. (2003). New targets for viral cyclins. Cell Cycle, 2: 293–295.

6. Sherr, C.J. (2001). The INK4a/ARF network in tumour suppression. Nat. Rev. Mol. Cell. Biol., 2: 731–737.

7. Carnero, A. and Hannon, G.J. (1998). The INK4 family of CDK inhibitors. Curr. Top. Microbiol. Immunol., 227: 43–55.

8. Jeffrey, P.D., Tong, L. and Pavletich, N.P. (2000). Structural basis of inhibition of CDK-cyclin complexes by INK4 inhibitors. Genes Dev., 14: 3115–3125.

9. Grant, S. and Roberts, J.D. (2003). The use of cyclin-dependent kinase inhibitors alone or in combination with established cytotoxic drugs in cancer chemotherapy. Drug Resist. Updates, 6: 15–26.

Jinhwa

10. Guan, K.L., Jenkins, C.W., Li, Y., Nichols, M.A., Wu, X., O'Keefe, C.L., Matera, A.G. and Xiong, Y. (1994). Growth suppression by p18, a p16INK4/MTSer1- and p14INK4B/MTS2-related CDK6 inhibitor, correlates with wild-type pRb function. Genes Dev., 8: 2939–2952.

11. James, M.C. and Peters, G. (2000). Alternative product of the p16/CKDN2A locus connects the Rb and p53 tumor suppressors. Prog. Cell Cycle Res., 4: 71–81.

12. Hannon, G.J. and Beach, D. (1994). p15 INK 4B is a potential effector of TGF-beta-induced cell cycle arrest. Nature, 371: 257–261.

13. Latres, E., Malumbres, M., Sotillo, R., Martin, J., Ortega, S., Martin-Caballero, J., Flores, J.M., Cordon-Cardo, C. and Barbacid, M. (2000). Limited overlapping roles of P15 (INK4b) and P18 (INK4c) cell cycle inhibitors in proliferation and tumorigenesis. EMBO J., 19: 3496–3506.

14. Franklin, D.S., Godfrey, V.L., Lee, H., Kovalev, G.I., Schoonhoven, R., Chen-Kiang, S., Su, L. and Xiong, Y. (1998). CDK inhibitors p18 (INK4c) and p27 (KIP1) mediate two separate pathways to collaboratively suppress pituitary tumorigenesis. Genes Dev., 12: 2899–2911.

15. Hirai, H., Roussel, M.F., Kato, J.Y., Ashmun, R.A. and Sherr, C.J. (1995). Novel INK4 proteins, p19 and p18, are specific inhibitors of the cyclin D-dependent kinases CDK4 and CDK6. Mol. Cell Biol., 15: 2672–2681.

16. Tavera-Mendoza, L.E, Wang, T.T., White, J.H. (2006) p19INK4D and cell death. Cell Cycle, 5: 596–598.

17. Yan, Y., Frisen, J., Lee, M.H., Massague, J. and Barbacid, M. (1997). Ablation of the CDK inhibitor p57KIP2 results in increased apoptosis and delayed differentiation during mouse development. Genes Dev., 11: 973–983.

18. Heinen, A., Kremer, D., Gottle, P., Kruse, F., Hasse, B., Lehmann, H., Hartung, H.P., and Kury, P. (2008). The cyclin-dependent kinase inhibitor p57kip2 is a negative regulator of Schwann cell differentiation and in vitro myelination. PNAS, 105: 8748–8753.

19. Sherr, C.J. and Roberts, J.M. (1999). CDK inhibitors: Positive and negative regulators of G_1-phase progression. Genes & Dev., 13: 1501–1512.

20. Murray, A.W. (2004). Recycling the cell cycle: Cyclins revisited. Cell, 116: 221–234.

21. Polyak, K., Kato, J.Y., Solomon, M.J., Sherr, C.J., Massague, J., Roberts, J.M., and Koff, A. (1994). p27KIP1, a cyclin–Cdk inhibitor, links transforming growth factor-â and contact inhibition to cell cycle arrest. Genes & Dev., 8: 9–22.

22. Lee, M.H., Reynisdottir, I., and Massague, J. (1995). Cloning of p57KIP2, a cyclin-dependent kinase inhibitor with unique domain structure and tissue distribution. Genes & Dev., 9: 639–649.

23. Ishida, N., Kitagawa, M., Hatakeyama, S., and Nakayama, K. (2000). Phosphorylation at serine 10, a major phosphorylation site of p27 (KIP1). increases its protein stability. J. Biol. Chem., 275: 25146–25154.

24. Nakayama, K., Ishida, N., Shirane, M., Inomata, A., Inoue, T., Shishido, N., Horii, I., and Loh, D.Y. (1996). Mice lacking p27 (KIP1) display increased body size, multiple organ hyperplasia, retinal dysplasia, and pituitary tumors. Cell, 85: 707–720.

25. Toyoshima, H. and Hunter, T. (1994). p27, a novel inhibitor of G_1 cyclin–Cdk protein kinase activity, is related to p21. Cell, 78: 67–74.

26. Kiyokawa, H., Kineman, R.D., Manova-Todorova, K.O., Soares, V.C., Hoffman, E.S., Ono, M., Khanam, D., Hayday, A.C., Frohman, L.A., and Koff, A. (1996). Enhanced growth of mice lacking the cyclin-dependent kinase inhibitor function of p27 (KIP1). Cell, 85: 721–732.

27. Pagano, M., Tam, S.W., Theodoras, A.M., Beer-Romero, P., Del Sal, G., Chau, V., Yew, P.R., Draetta, G.F., and Rolfe, M. (1995). Role of the ubiquitin–proteasome pathway in regulating abundance of the cyclin-dependent kinase inhibitor p27. Science, 269: 682–685.

28. Alessandrini, A., Chiaur, D.S., and Pagano, M. (1997). Regulation of the cyclin-dependent kinase inhibitor p27KIP1 by degradation and phosphorylation. Leukemia 11: 342–345.

29. Zhang, Y., Wang, Z. and Magnuson, N.S. (2007). PIM-1 Kinase-Dependent Phosphorylation of p21Cip1/WAF1 Regulates Its Stability and Cellular Localization in H1299 Cells. Mol Cancer Res., 5: 909–922.

30. Lee, S. and Helfman, D.M. (2004). Cytoplasmic p21Cip1 is involved in Ras-induced inhibition of the ROCK/LIMK/cofilin pathway. J. Biol. Chem., 279: 1885–1891.

31. Hauck, L., Harms, C., Grothe, D., An, J., Gertz, K., Kronenberg, G., Dietz, R., Endres, M. and von Harsdorf, R. (2007). Critical Role for FoxO3a-Dependent Regulation of p21CIP1/WAF1 in Response to Statin Signaling in cardiac myocytes. Circ. Res., 100: 50–60.

32. Viglietto, G., Motti, M.L., Bruni, P., Melillo, R.M., D'Alessio, A., Califano, D., Vinci, F., Chiappetta, G., Tsichlis, P., Bellacosa, A., Fusco, A. and Santoro, M. (2002). Cytoplasmic relocalization and inhibition of the cyclin-dependent kinase inhibitor p27kip1 by PKB/AKT-mediated phosphorylation in breast cancer. Nat. Med., 8: 1136–1144.

33. Liang, J., Zubovitz, J., Petrocelli, T., Kotchetkov, R., Connor, M.K., Han, K., Lee, J.H., Ciarallo, S., Catzavelos, C., Beniston, R., Franssen, E. and Slingerland, J.M. (2002). PKB/AKT phosphorylates p27, impairs nuclear import of p27KIP1 and opposes p27-mediated G_1 arrest. Nat. Med., 8: 1153–1160.

34. Carrano, A.C., Eytan, E., Hershko, A., and Pagano, M. (1999). SKP2 is required for ubiquitin-mediated degradation of the CDK inhibitor p27. Nat. Cell Biol., 1: 193–199.

35. Zhu, H., Nie, L., Maki, C.G. (2005). Cdk2-dependent Inhibition of p21CIP1 stability via a C-terminal cyclin-binding motif. J Biol Chem., 280: 29282–29288.

36. Fukuchi, K., Nakamura, K., Ichimura, S., Tatsumi, K. and Gomi, K. (2003). The association of cyclin A and cyclin kinase inhibitor p21CIP1 in response to gamma-irradiation requires the CDK2 binding region, but not the Cy motif. Biochim Biophys Acta., 1642: 163-171.

37. Zeng, Y., Hirano, K., Hirano, M., Nishimura, J., and Kanaide, H. (2000). A cyclin-dependent kinase inhibitor. Minimal requirements for the nuclear localization of p27 (KIP1). Biochem. Biophys. Res. Commun., 274: 37–42.

38. Boehm, M., Yoshimoto, T., Crook, M.F., Nallamshetty, S., True, A., Nabel, G.J. and Nabel, E.G. (2002). A growth factor-dependent nuclear kinase phosphorylates p27 (KIP1) and regulates cell cycle progression. EMBO J., 21: 3390–3401.

39. Tsvetkov, L.M., Yeh, K.H., Lee, S.J., Sun, H. and Zhang, H. (1999). p27 (KIP1) ubiquitination and degradation is regulated by the SCF (SKP2) complex through phosphorylated Thr187 in p27. Curr. Biol., 9: 661–664.

Withaferin A suppresses the expression of vascular endothelial growth factor in Ehrlich ascites tumor cells via Sp1 transcription factor

Prasanna Kumar S., Shilpa P. and Bharathi P. Salimath*

Department of Studies in Biotechnology,
University of Mysore, Manasagangotri, Mysore-570006, India.
For Correspondent : Salimathuom@rediffmail.com

Abstract

In the ayurvedic system of medicine, the medicinal plant, *Withania somnifera* Dunal (Solanaceae) finds application for numerous ailments including cancer. This herbal plant yields a host of steroidal lactones called withanolides, some of which have shown growth inhibition of human tumor cell lines. Withaferin A amongst these withanolides reportedly is very active in impairing antitumor activity. However; the underlying molecular mechanisms of this activity remains still unclear. In the present study, we have shown that withaferin A inhibited vascular endothelial cell growth factor (VEGF) -induced tube formation by human umbilical vein endothelial cells (HUVECs) and angiogenesis in chick chorioallantoic membrane (CAM) assay. In Ehrlich ascites tumor (EAT) model, the animals treated with withaferin A suppressed in vivo, the peritoneal angiogenesis and microvessel density. When compared to the untreated animals, the withaferin A treated tumor bearing mice showed a decrease in the volume of ascites and tumor cell number. Quantitation of VEGF levels in ascites from withaferin A untreated or treated tumor bearing mice indicated decreased secretion of VEGF in ascites from treated mice, as measured by ELISA. Studies at molecular level revealed that withaferin A inhibits binding of Sp1 transcription factor to VEGF-gene promoter, in order to exert its antiangiogenic activity. These results clearly indicate the antiangiogenic potential of withaferin A in modulating antitumor activity.

Keywords: Ehrlich ascites tumor; Withaferin A; Angiogenesis; Sp1, VEGF.

Introduction

Several natural compounds are recognized as cancer chemo preventive agents. Withanalides are especially well known to suppress tumor cell growth via cell-cycle arrest and by the induction of apoptosis in several tumor cell lines (1-3). Moreover, withaferin A inhibits endothelial cell proliferation and angiogenesis *in vitro* (4). Angiogenesis is essential for the growth, progression and metastasis of solid tumors (5). Withaferin A, a member of the withanalides family that is present at high levels in roots and leaves of *Withania somnifera* plant has been found to possess antioxidant and antitumor activity (6-9). However, the mechanism by which withaferin A suppresses angiogenesis has not been fully elucidated.

Vascular endothelial growth factor (VEGF) is a major angiogenic factor that facilitates tumor growth and metastasis. Hypoxia is known to induce the expression of VEGF gene (10, 11). VEGF promoter analysis has revealed several potential transcription factor-binding sites, such as hypoxia-inducible factor-1(HIF-1), activator

Sp1 transcription factor

protein (AP)-1, AP-2, early growth response-1(Egr-1) and Sp1 (12).

The GC box-binding protein, Sp1 is a ubiquitous transcription factor that belongs to the Sp family of transcription factors, consisting of Sp1, Sp2, Sp3, and Sp4 (13). Sp1 has been implicated in the transcription of large number of genes, including housekeeping genes, tissue-specific genes and genes involved in growth regulation (13-15). Sp1 activities are regulated by a variety of stimuli. Most of these regulations occur through either post-translational modification or alteration of Sp1 protein abundance.

The principal known post-translational modifications are phosphorylation and glycosylation through the *O*-linkage of the monosaccharide, *N*-acetylglucosamine (*O*-GlcNAc) (16).

Expression level of the VEGF mRNA is tightly regulated by both transcriptional and post-transcriptional mechanisms. Recent studies have demonstrated that intracellular signaling pathways and genetic elements are involved in controlling its expression. VEGF promoter activity is preceded by the activation of transcription factor Sp1 (17). Therefore it is clear that a constitutive Sp1 activation is essential for the differential over expression of VEGF, which in turn plays an important role in angiogenesis and the progression of cancer. It has also been shown that Sp1 in particular, plays an important role in tumor angiogenesis and contributes to the aggressive nature of human pancreatic adenocarcinoma (18).

In this study, we tested the hypothesis that the antiangiogenic effect of withaferin A on EAT cells involves a reduction in secretion of ascites fluid and expression of VEGF, which is regulated by Sp1 transcription factor. Moreover, we investigated the molecular mechanism by which withaferin A inhibits angiogenesis *in vivo*.

Materials and methods

Materials

Ehrlich ascites tumor (EAT) cells were routinely maintained in Swiss albino mice in the animal house, University of Mysore, Mysore, India. Endothelial growth medium (EGM-2) was procured from Cambrex Biosciences, Walkersville, USA. Dulbecco's modified Eagle's medium (DMEM), fetal bovine serum (FBS), penicillin-streptomycin and trypsin-EDTA were purchased from Invitrogen, USA.T4 polynucleotide kinase kit was obtained from Amersham biosciences. The Sp1 oligonucleotides (5'-d (ATTCGA TCG GGG CGG GGCGAG C)-3') for gel shift assays were obtained from Promega. Radioacive ã-[^{32}P] ATP was obtained from Bhabha Atomic Research Centre (BARC), Mumbai, India. RNA isolation kit was procured from Qiagen, USA. Secondary antibodies conjugated to alkaline phosphatase and proteinase inhibitors were obtained from Bangalore Genei, Bangalore, India. The rest of the chemicals were of analytical grade of purity and were procured locally.

Methods

Isolation of withaferin A from *Withania somnifera* roots

Withania somnifera roots were collected locally from Mysore, India. The plant specimens were identified and authenticated at the herbarium of the Department of Botany, University of Mysore, Mysore, India. The roots were washed, shade dried and powdered. One hundred grams of the root powder was extracted in 500ml of methanol overnight. Withaferin A was isolated from the methanol extract of *Withania somnifera* roots as previously described (4). The compound Withaferin A (10mg) was dissolved in 100ìl of DMSO and diluted 100 times with sterile distilled water to make final concentration 1ìg/ìl and used for subsequent experiments.

Human Umbilical Vein Endothelial Cells (HUVECs) culture

HUVECs were purchased from Cambrex Biosciences, Walkersville, USA. The cells were cultured in 25 cm^3 tissue culture flask (NUNC, Genetix Biotech Asia, Bangalore, India) and grown using EGM-2 medium and endothelial cell basal medium according to the manufacturer's protocol. Incubation was carried out in a humidified atmosphere of 5% CO_2 in air at 37^{0}C. When cells reached confluency, they were passaged after trypsinization. HUVECs of passages 2-5 were used for the experiments.

Animals and *in vivo* tumor generation

Six to eight weeks old mice were acclimated for one week while caged in groups of five. Mice were housed and fed a diet of animal chow and water ad libitum throughout the experiment. All experiments were conducted according to the guidelines of the Committee for the Purpose of Control and Supervision of Experiments on Animals (CPCSEA), Government of India. EAT cells (5×10^6cells/ mouse) injected intraperitoneally grow in mice peritoneum forming an ascites tumor with massive abdominal swelling. The animals show a dramatic increase in body weight over the growth period and the animals succumb to the tumor burden 15-16 days after implantation. The number of cells increased over the 14 days of growth with formation of 7-8 ml of ascites fluid with extensive neovascularization in the inner lining of peritoneal wall. EAT cells from fully grown tumor bearing mice were harvested from the peritoneal cavity of mice (19). The ascites fluid was collected in isotonic saline solution containing 3.8% sodium citrate. The cells were pelleted by centrifugation (3000 rpm for 10 min at 4^{0}C). Contaminating red blood corpuscles if any were lysed with 0.8% ammonium chloride. Cells were resuspended in 0.9% saline. These cells or their aliquots were used either for transplantation or for further experiments.

Tube formation assay

Tube formation of HUVECs was conducted for the assay of *in vitro* angiogenesis. The assay was performed as described in earlier report (20). Briefly, a 96-well plate was coated with 50µl of Matrigel (Becton Dickinson Labware, Bedford, MA), which was allowed to solidify at 37^{0}C for 1 hour. HUVECs (5x 10^3 cells per well) were seeded on the Matrigel and cultured in EGM medium containing withaferin A (3.5-14µg) for 8 hours. After incubation at 37^{0}C and 5% CO2, the enclosed networks of complete tubes from five randomly chosen fields were counted and photographed under an Olympus inverted microscope (CKX40; Olympus, New York, NY) connected to a digital camera at 40X magnification.

Chick chorioallantoic membrane (CAM) assay

CAM assay was carried out according to the detailed procedure as described by Gururaj, A.E. *et al.* (21, 22). In brief, fertilized chicken eggs were incubated at 37^{0}C in a humidified incubator. On the 11th day of development, a rectangular window was made in the egg shell and glass cover slips (6-mm diameter) saturated with 25ng/ml vascular endothelial growth factor (VEGF) and VEGF + withaferin A (7ìg) was placed on the CAM and the window was closed using sterile wrap. The windows were opened after 48h of incubation and were inspected for changes in the microvessel density in the area below the cover slip and photographed using a Nikon digital camera.

In vivo withaferin A treatment inhibits EAT growth

To determine whether withaferin A inhibits tumor growth and angiogenesis in EAT cells *in vivo,* withaferin A (7mg/kg/day/mouse) and vehicle control (0.1% of DMSO) was injected into the EAT bearing mice every alternate day

Sp1 transcription factor

after 6th day of tumor transplantation and growth of the tumor was monitored by taking the body weight of the animals. Animals were sacrificed on the 14th day and the EAT cells along with ascites fluid were harvested into the beaker and centrifuged at 3000 rpm for 10 min at 4^0C. The pelleted cells were counted by Trypan blue dye exclusion method using a haemocytometer. A measure of the supernatant gave the volume of ascites fluid.

Peritoneal angiogenesis and micro vessel density

After harvesting the EAT cells from control and withaferin A-treated animals, the peritoneum was cut open and the inner lining of the peritoneal cavity was examined for extent of neovasculature and photographed. Formaldehyde fixed and paraffin embedded tissues of peritoneum from EAT bearing mice either treated or untreated with withaferin A were taken and 5ìm sections were prepared using automatic microtome (SLEE Cryostat) and stained with hematoxylin and eosin. The images were photographed using Leitz-DIAPLAN microscope with CCD camera and the blood vessels were counted.

Quantitation of VEGF

EAT bearing mice were treated with or without withaferin A (7mg/kg/day) for 5 doses on 6th, 8th, 10th and 12th day of tumor transplantation. The animals were sacrificed and ascites fluid was collected after 24h of each dose. VEGF-ELISA was carried out using the ascites fluid (21, 23, 24). In brief, 100µl of ascites from tumor bearing mice either with or without withaferin A treatment, was coated using coating buffer (50 mM carbonate buffer pH 9.6) at 4^0C overnight. Subsequently, wells were incubated with anti-VEGF$_{165}$ antibodies, followed by incubation with secondary antibodies tagged to alkaline phosphatase and detection using p-nitro-phenyl phosphate (pNPP) as a substrate.

Preparation of nuclear extracts

Nuclear extracts were prepared according to the method previously described (25). Briefly, cells ($5X10^6$) treated either with or without withaferin A in complete HBSS for different time intervals were washed with cold phosphate buffered saline and suspended in 0.5 ml of lysis buffer (20mM HEPES, pH 7.9, 350 mM NaCl, 20% Glycerol, 1% NP-40, 1 mM MgCl$_2$, 0.5 mM EGTA, 0.5 mM DTT, 1 mM Pefablock, 1µg/ml Aprotinin, 1µg/ ml Leupeptin). The cells were allowed to swell on ice for 10 min; the tubes were then vigorously mixed on a vortex mixer for 1 min and centrifuged at 10,000 rpm for 10 min at 4^0C. The supernatant was immediately stored at -20^{0}C.

Electrophoretic Mobility Shift Assay (EMSA)

Nuclear proteins were extracted from EAT cells treated either with or without withaferin A for 60,120 and 180 min respectively. The EMSA was performed as described in earlier report (26, 27). The double stranded Sp1 consensus oligonucleotide probes [5'-d (ATT CGA TCG GGG CGG GGC GAG C)-3'] were end-labeled with ã-[^{32}P] ATP. Nuclear proteins (40ìg) were incubated with 40fmoles of ã-[^{32}P]-labeled Sp1 consensus oligonucleotides for 30min in binding buffer containing 100mM HEPES (pH 7.9),10mM MgCl$_2$ 125 mM KCl, 0.5mM EDTA, 4% glycerol,0.5% NP-40,1ìg of poly [dI-dC] and 1mg/ml BSA. The samples were electrophoresed in 4% non denaturing polyacrylamide gel in 0.5% TBE at room temperature for 2 hr at 200V. The gel was dried, transferred to imaging plate (IP) and the image was scanned by image analyzer Fujifilm (FLA-5000).

Results

Withaferin A inhibits tube formation of HUVECs induced by VEGF

In order to verify if withaferin A interferes directly with the formation of blood vessels by HUVECs, we performed tube formation assay

in vitro. The HUVECs were plated on the Matrigel. The HUVECs in the basal medium could not form tubes and VEGF was used to induce the tube formation. In the positive control group stimulated with VEGF (10ng), HUVECs rapidly aligned with one another and formed tube-like structures resembling a capillary plexus within 8 hours, after VEGF treatment. However, treatment with withaferin A prevented VEGF - stimulated tube formation of HUVECs in a concentration (3.5-14μg) - dependent manner (Fig. 1). Meanwhile, no cytotoxicity was observed under this concentration range of withaferin A used in the assay. Withaferin A was shown to interfere with the ability of HUVECs to form the *in vitro* vessel-like tubes, one of the important traits of the endothelial cells.
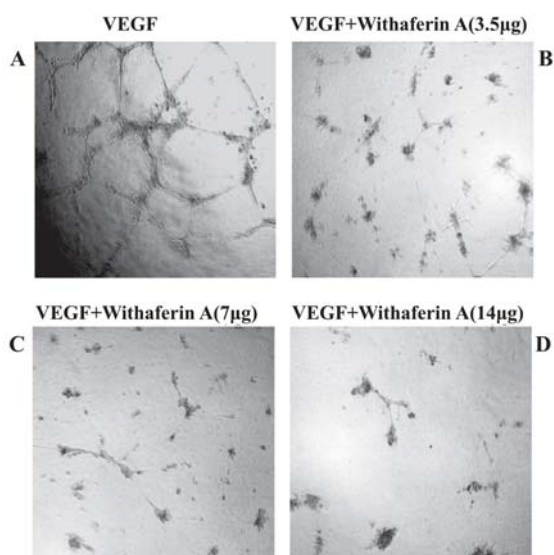

Fig. 1: Effect of withaferin A on VEGF induced HUVECs tube formation

HUVECs (5×10^3 cells) cultured in EGM medium with 3.5μg, 7μg and 14 μg withaferin A was added to the Matrigel coated 96 wells plate. After incubation for 8 hours at 37^0C, capillary networks were photographed and quantified (Magnification: X40). Concentration dependent inhibition of tube formation by withaferin A was recorded. All datas are presented as mean from three different experiments with triplicates and means of ± S.E.M. P<0.05 vs control.

Withaferin A inhibits VEGF induced neovascularization on chick chorioallantoic membrane

CAM assay is one of the widely used validation assays for formation of new blood vessels. In order to further verify if withaferin A is an inhibitor of new blood vessel formation, withaferin A was applied on chorioallantoic membrane of chick embryo to test its *in vivo* antiangiogenic activity. In the CAM assay model withaferin A induced avasculature zone formation in the developing embryos. Notably newly formed microvessels were regressed around the area of withaferin A treated CAM (Fig. 2).
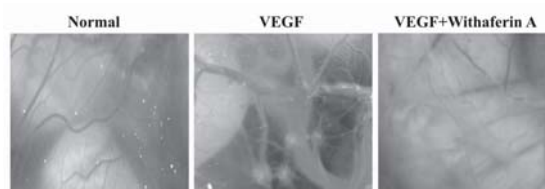
Fig. 2: Effect of withaferin A on neovascularization in the chick CAM

Withaferin A was applied on CAM of 11-day-old chicken embryo. After 48h of incubation, the applied area was inspected for changes in neovascularization. The arrows indicate the applied area. The data shown represents the result of an experiment, which was done using maximum six eggs in each group. All photographs were taken at same magnification.

Withaferin A inhibits growth of EAT cells and secretion of ascites *in vivo*

Initially, proliferation of tumor cells in mice was monitored by measuring the weight of the animals every day. A decrease in body weight in withaferin A treated animals was observed when compared to the increased body weight of the untreated tumor bearing mice. It was also observed that withaferin A lessened the tumor burden considerably in a dose dependent manner showing the optimum activity at 7mg/kg/dose. Cell number was counted after each dose of withaferin A treatment. In control group, which is tumor bearing mice not treated with withaferin A, the number of EAT cells increased exponentially. In

contrast, in the withaferin A treated group, the number of cells were drastically decreased (Fig. 3A). This implied that withaferin A inhibit tumor cell growth *in vivo*. The volume of ascites was also measured using ascites from EAT bearing as well as withaferin A treated EAT bearing animals. The results indicated that withaferin A treatment reduces the secretion of ascites fluid (Fig. 3B). It is indicative from this data that withaferin A is probably capable of inhibiting the proliferation of tumor cell growth *in vivo*.

Fig. 3: Effect of withaferin A on EAT cell number and ascites volume *in vivo*
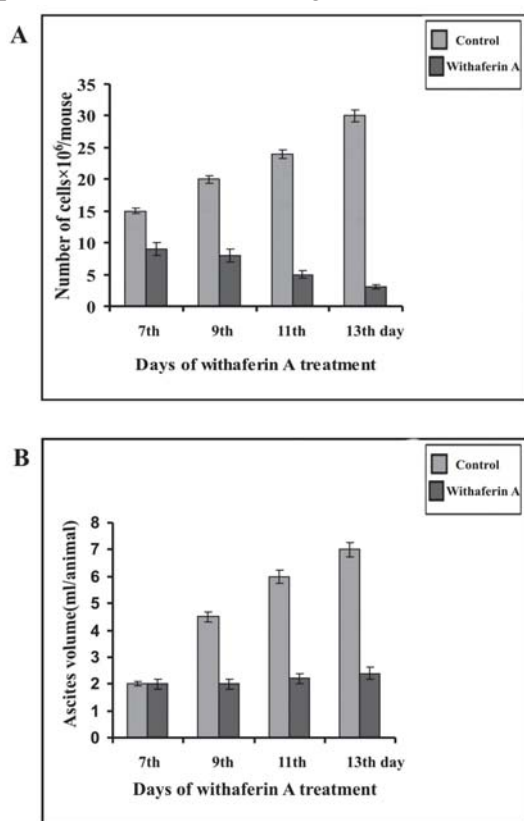
EAT cells (5×10^6 cells/animal, i.p.) were injected into mice. After 6 days of tumor transplantation, withaferin A (7mg/kg/animal) was injected on days 7th, 9th, 11th and 13th. The animals were sacrificed on days 8th, 10th, 12th and 14th. EAT cells were collected along with ascites fluid. Cells were counted in haemocytometer (A) and ascites volume was measured (B). At least five mice were used in each group and the results obtained are an average of three individual experiments and means of ± S.E.M.

Withaferin A inhibits angiogenesis *in vivo*

Sprouting of new blood vessels is evident in the inner peritoneal lining of EAT bearing mice. The peritoneal lining of EAT bearing animals and withaferin A treated mice was inspected for the effect on tumor-induced peritoneal neovascularization. EAT bearing mice treated with withaferin A showed decreased peritoneal angiogenesis when compared to the extent of peritoneal angiogenesis in untreated EAT bearing mice (Fig. 4A). Histopathological staining of peritoneum sections from the EAT bearing group appeared well vascularized. In contrast withaferin A treated peritoneum sections were characterized by a pronounced decrease in micro vessel density and the caliber of detectable vascular channels. While tumor bearing peritoneum sections showed 17 ± 1.2 blood vessels, withaferin A treated peritoneum showed 6.8 ± 1.3 blood vessels (Fig. 4B).
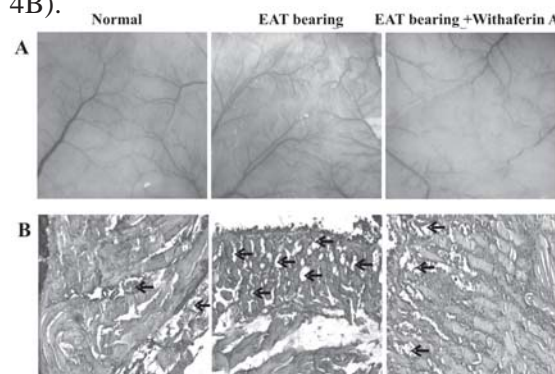
Fig. 4: Withaferin A inhibits angiogenesis and microvessel density

A) Inhibition of peritoneal angiogenesis.
EAT bearing mice were treated with and without withaferin A for four doses (7mg/kg/animal). The mice were sacrificed and the peritoneal lining was observed for extent of neovascularization. We presented representative photograph of peritoneum.

B) Reduction in microvessel density (MVD)
The peritoneum of control as well as withaferin A treated EAT bearing mice was embedded in paraffin and 5ìm sections were taken using microtome. The sections were stained with hematoxyline and eosine and observed for microvessel density. Arrows indicate the microvessels.

Withaferin A inhibits VEGF secretion in ascites fluid of EAT bearing mice

In order to verify whether withaferin A induced inhibition of neovascularization and microvessel density is due to decreased secretion of VEGF by EAT cells, we have quantified the secreted VEGF in ascites fluid of control and different doses of withaferin A treated animals by ELISA. It is evident in Fig. 5 that withaferin A inhibits production of VEGF in EAT cells. In EAT bearing mice, 1280ng of VEGF was detected in ascites. However in case of withaferin A treated animal ascites 220ng of VEGF was detected per mouse.
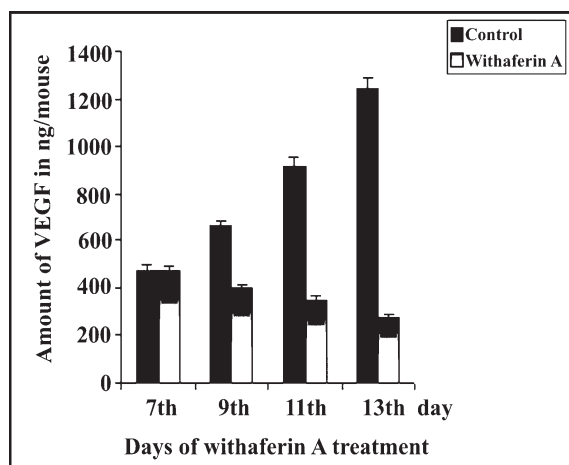
Fig. 5: Effect of withaferin A on *in vivo* production and expression of VEGF

EAT bearing mice were injected with withaferin A (7mg/kg/animal) for four doses and ascites fluid was collected after sacrificing the animal every alternate day after each dose of treatment. ELISA was carried out to quantitate VEGF in ascites fluid using anti-VEGF$_{165}$ antibodies. Animals bearing EAT cells not treated with withaferin A was used as control.

Withaferin A inhibits Sp1 DNA binding activity in EAT cells

To verify for the involvement of transcription factor Sp1 in withaferin A induced inhibition of VEGF gene expression, an electrophoretic mobility shift assay was performed. The results indicated that withaferin A inhibits binding of Sp1 transcription factor to the proximal promoter region of the VEGF gene. In contrast, there was prominent band showing the binding of Sp1 to the proximal promoter region (Fig. 6) when nuclear extract from tumor bearing mice was used.
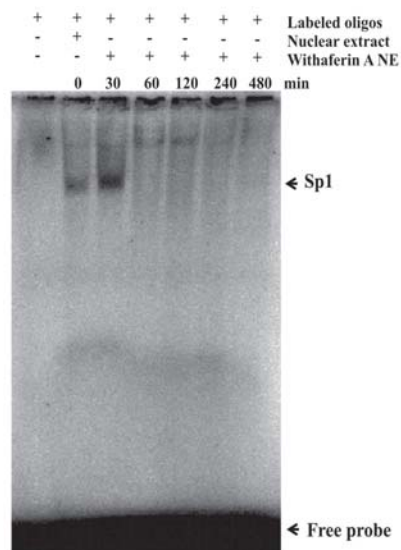
Fig. 6: Effect of withaferin A on Sp1-DNA binding activity

Nuclear extracts were prepared from EAT cells untreated and treated with withaferin A. Sp1-DNA binding activity was assayed by EMSA using Sp1 oligonucleotides.

Discussion

Plant and dietary products contribute to about one-third of potential anticancer drugs and the preventive effects of plant-based diets on tumorigenesis and other chronic diseases have been well documented (28). *Withania somnifera* (L.) Duna1 commonly known as Ashwagandha (family Solanaceae) is extensively used in many indigenous preparations. *W. somnifera* is reported to have anti-inflammatory (29), anti-arthritic (30) and anti-tumor (31) activities. Withaferin A, a withanolide was isolated and reported to be antiangiogenic and anti-tumor active

principle from *Withania somnifera*. A recent study demonstrated that the anti-angiogenic effect of withaferin A was due to the inhibition of endothelial cell proliferation (4). However, the detailed molecular mechanisms involved in the anti-angiogenic effect of withaferin A were not clearly understood. In this study we investigated the anti-angiogenic effects of withaferin A both *in vitro* and *in vivo* model. Withaferin A suppressed human endothelial cell- tube formation which is one of the hallmarks of angiogenesis indicating that withaferin A inhibits endothelial cell proliferation. This may be due to the induction of HUVECs apoptosis by withaferin A (4). Further, in Ehrlich ascites tumor bearing mice and also by using several *ex-vivo* and cell based validation assays, we observed that withaferin A besides inhibiting the growth of the tumor suppressed peritoneal angiogenesis and microvessel density by down regulating VEGF gene expression and VEGF secretion into the ascites of tumor bearing mice. It also inhibited neoangiogenesis induced by VEGF in CAM assay indicating that withaferin A targets both tumor and endothelial cell to exert its anti proliferative and antiangiogenic activities.

Increased VEGF expression is closely associated with an increase in microvessel density (32). VEGF being a permeability factor plays fundamental role in the fluid accumulation and tumor growth in ascites tumor. By secreting VEGF, ascites tumor enhances the permeability of preexisting microvessel lining of peritoneal cavity to stimulate ascites formation thereby tumor progression. Inhibition of fluid accumulation, tumor growth and microvessel density by neutralization of VEGF has been demonstrated underlying the importance of VEGF in malignant ascites formation (33-35). Our results indicated that there was decrease in the VEGF secretion in withaferin A treated animals. Inhibition of VEGF secretion could be due to inhibition of activity of transcription factors NF-êB, AP-1 or Sp1 which are involved in the regulation of VEGF gene

expression. Withaferin A is already reported as a potent inhibitor of NF-êB and AP-1 DNA binding activity (4, 36, 37).

Recent studies indicated that Sp1 transcription factor plays an important role in VEGF expression and tumor angiogenesis. A region between nucleotide-109 and -61 of the VEGF promoter and its intact Sp1-binding sites were required for the inhibition of VEGF promoter activity. In this study, we found that withaferin A treatment reduced Sp1 DNA binding activity to the proximal promoter region of VEGF gene in a time dependent manner. It was shown recently that celecoxib inhibits VEGF expression and reduces angiogenesis and metastasis of human pancreatic cancer via suppression of Sp1 (38). Sp1 suppression was closely correlated with reduced VEGF level. Withaferin A has been reported as potent inhibitor of PKC and TNF dependent IêB kinase β, which subsequently blocks NF-êB nuclear translocation (3, 37). PKC isoforms are also involved in the activation of Sp1, NF-êB and AP-1 in B16F1 murine melanoma cells (39, 40).

In summary, our experiments have shown that inhibition of VEGF secretion and tumor microvessel formation is one of the potential mechanisms by which withaferin A suppresses the growth of Ehrlich ascites tumor. Additionally, the suppression of VEGF secretion appears to be as a consequence of altered Sp1 transactivation and inhibition of VEGF gene expression. The data clearly indicates a novel mechanism for the antiangiogenic activity of withaferin A and also substantiate the important role of Sp1 in tumor biology and the biological basis for the development of new Sp1-targeting agents for cancer treatment.

Acknowledgements

References

1. Srinivasan, S., Ranga, R.S., Burikihanov, R., Han, S.S. and Chendil, D. (2007). Par-4-Dependent Apoptosis by the Dietary Compound Withaferin A in Prostate Cancer Cells. Cancer Research, 67: 246-53.

2. Malik, F., Kumar, A., Bhushan, S., Khan, S., Bhatia, A., Suri, K.A., Qazi, G.N. and Singh, J. (2007). Reactive oxygen species generation and mitochondrial dysfunction in the apoptotic cell death of human myeloid leukemia HL-60 cells by a dietary compound withaferin A with concomitant protection by *N*-acetyl cysteine. Apoptosis, 12:2115-2133.

3. Sen, N., Banerjee, B., Das, B.B., Ganguly, A., Sen, T., Pramanik, S., Mukhopadhyay, S. and Majumder, H.K. (2007). Apoptosis is induced in leishmanial cells by a novel protein kinase inhibitor withaferin A and is facilitated by apoptotic topoisomerase I-DNA complex. Cell Death and Differentiation, 14: 358-367.

4. Mohan, R., Hammers, H.J., Mohan, P.B., Zhan, X.H., Herbstritt, C.J., Ruiz, A., Zhang, L., Hanson, A.D., Conner, B.P., Rougas, J. and Pribluda, V.S. (2004). Withaferin A is a potent inhibitor of angiogenesis. Angiogenesis, 7: 115-122.

5. Liotta, L.A., Steeg, P.S. and Stetler-Stevenson, W.G. (1991). Cancer metastasis and angiogenesis: an imbalance of positive and negative regulation. Cell, 64: 327-336.

6. Bhattacharya, S.K., Satyan, K.S. and Ghosal, S. (1997). Antioxidant activity of glycowithanolides from W somnifera in rat brain frontal cortex and striatum. Indian Journal of Experimental Biology, 35: 236-239.

7. Bhattacharya, A., Ghosal, S. and Bhattacharya, S.K. (2001). Anti-oxidant effect of Withania somnifera glycowithanolides in chronic footshock stress-induced perturbations of oxidative free radical scavenging enzymes and lipid peroxidation in rat frontal cortex and striatum. Journal of Ethnopharmacology, 74: 1-6.

8. Mishra, L.C., Singh, B.B. and Dagenais, S. (2000). Scientific basis for the therapeutic use of Withania somnifera (Ashwagandha): a review. Alternative Medicine Review, 5: 334-346.

9. Upton, R. (2000). American Herbal Pharmacopoeia and Therapeutic Compendium: Ashwagandha Root (*Withania somnifera)* - Standards of Analysis, Quality Control, and Therapeutics. Santa Cruz, California.

10. Forsythe, J.A., Jiang, B.H., Iyer, N.V., Agani, F., Leung, S.W., Koos, R.D. and Semenza, G.L. (1996). Activation of vascular endothelial growth factor gene transcription by hypoxia-inducible factor 1. Molecular and Cellular Biology, 16: 4604-4613.

11. Feldser, D., Agani, F., Iyer, N.V., Pak, B., Ferreira, G. and Semenza, G.L. (1999). Reciprocal positive regulation of hypoxia-inducible factor 1alpha and insulin-like growth factor 2. Cancer Research, 59: 3915-3918.

12. Tischer, E., Mitchell, R., Hartman, T., Silva, M., Gospodarowicz, D., Fiddes, J.C. and Abraham, J.A. (1991). The human gene for vascular endothelial growth factor. Multiple protein forms are encoded through alternative exon splicing. Journal of Biological Chemistry, 266: 11947-11954.

Sp1 transcription factor

13. Suske, G. (1999). The Sp-family of transcription factors. Gene, 238: 291-300.

14. Kadonaga, J.T., Jones, K.A., and Tjian, R. (1986). Promoter-specific activation of RNA polymerase II transcription by Sp1. Trends in Biochemical Sciences, 11: 20-23.

15. Cook, T., Gebelein, B. and Urrutia, R. (1999). Biochemical and functional predictions for a growing family of zinc finger transcription factors. Annals of the New York Academy of Sciences, 880: 94-102.

16. Wells, L., Vosseller, K. and Hart, G.W. (2001). Glycosylation of Nucleocytoplasmic Proteins: Signal Transduction and O-GlcNAc. Science, 291: 2376-2823.

17. Shi, Q., Le, X., Abbruzzese, J.L., Peng, Z., Qian, C.N., Tang, H., Xiong, Q., Wang, B., Li, X.C., Xie, K. (2001). Constitutive Sp1 activity is essential for differential constitutive expression of vascular endothelial growth factor in human pancreatic adenocarcinoma. Cancer Res, 61: 4143-54.

18. Yao,J.C., Wang, L., Wei, D., Gong, W., Hassan, M., Wu, T. T., Mansfield, P., Ajani, J., Xie, K.(2004) Association between Expression of Transcription Factor Sp1 and Increased Vascular Endothelial Growth Factor Expression, Advanced Stage, and Poor Survival in Patients with Resected Gastric Cancer. Clinical Cancer Research, 10: 4109-4117.

19. Gururaj, A.E., Belakavadi M., Venkatesh D.A., Marme D. and Salimath, B.P., (2002). Molecular mechanisms of anti-angiogenic effect of curcumin. Biochemical and Biophysical Research Communications, 297: 934-942.

20. Ilan, N., Mahooti, S. and Madri, J. (1998). Distinct signal transduction pathways are utilized during the tube formation and survival phases of in vitro angiogenesis. Journal of Cell Science, 111: 3621-3631.

21. Gururaj, A.E., Belakavadi, M. and Salimath, B.P. (2003). Antiangiogenic effects of butyric acid involve inhibition of VEGF/ KDR gene expression and endothelial cell proliferation. Molecular and Cellular Biochemistry, 243: 107-112.

22. Thippeswamy, G., Sheela, M.L. and Salimath. B.P. (2008). Octacosanol isolated from Tinospora cordifolia downregulates VEGF gene expression by inhibiting nuclear translocation of NF-êB and its DNA binding activity. European Journal of Pharmacology, 588: 141-50.

23. Belakavadi, M. and Salimath, B.P. (2005). Mechanism of inhibition of ascites tumor growth in mice by curcumin is mediated by NF-êB and caspase activated DNase. Molecular and Cellular Biochemistry, 273: 57-67.

24. Belakavadi, M., Prabhakar, B.T. and Salimath, B.P. (2005). Butyrate-induced proapoptotic and antiangiogenic pathways in EAT cells require activation of CAD and down regulation of VEGF, Biochemical and Biophysical Research Communications, 335: 993-1001.

25. Salimath, B.P., Marme, D. and Finkenzeller, G. (2000). Expression of the vascular endothelial growth factor gene is inhibited by p73. Oncogene, 19: 3470-3476.

26. Jayaraman, T., Ondriasova, E., Ondrias, K., Harnick, D.J. and Marks, A.R. (1995). The inositol 1, 4, 5-trisphosphate receptor is essential for T-cell receptor signaling. Proceedings of the National Academy of Sciences, 92: 6007-6011.

27. Prasanna Kumar, S., Thippeswamy, G., Sheela, M.L., Prabhakar, B.T. and Salimath,

B.P. (2008). Butyrate-induced phosphatase regulates VEGF and angiogenesis via Sp1. Archives of Biochemistry and Biophysics, 478: 85-95.

28. Fotsis, T., Pepper, M.S., Aktas, E., Breit, S., Rasku, S., Adlercreutz, H., Wahala, K., Montesano, R. and Schweigerer, L. (1997). Flavonoids, dietary-derived inhibitors of cell proliferation and in vitro angiogenesis. Cancer Research, 57: 2916-2921.

29. Budhi-raja, R.D. and Sudhir, S. (1998). Review of biological activity of withanolides. Journal of Scientific and Industrial Research, 46: 488-491.

30. Sethi, P.D., Thiagarajan, A.R. and Subrahamanian, S.S. (1990). Studies on the anti-inflammatory and anti-arthritic activity of withaferin-A. Indian Journal of Pharmacology, 12: 165-172.

31. Uma Devi, P., Sharada, A.C. and Solomon, F.E. (1995). In vivo growth inhibitory and radiosensitizing effects of withaferin A on mouse Ehrlich ascites carcinoma. Cancer Letters, 95:189-193.

32. Sadick, H., Naim, R., Gossler, U., Hormann, K. and Riedel, F. (2005). Angiogenesis in hereditary hemorrhagic telangiectasia: VEGF165 plasma concentration in correlation to the VEGF expression and microvessel density. International Journal of Molecular Medicine, 15:15-19.

33. Mesiano, S., Ferrara, N. and Jaffe, R.B. (1998). Role of Vascular Endothelial Growth Factor in Ovarian Cancer Inhibition of Ascites Formation by Immunoneutralization. American Journal of Pathology, 153: 1249-1256.

34. Kim, K.J., Li, B., Winer, J., Armanini, M., Gillett, N., Phillips, H.S. and Ferrara, N. (1993). Inhibition of vascular endothelial growth factor induced angiogenesis suppresses tumor growth *in-vivo*. Nature, 362: 841-844.

35. Prabhakar, B.T., Khanum, S.A., Shashikanth, S. and Salimath, B.P. (2006). Antiangiogenic effect of 2-benzoyl-phenoxy acetamide in EAT cell is mediated by HIF-1 á and down regulation of VEGF *in vivo*. Investigation of New Drugs, 24: 471-478.

36. Oh, J.H., Lee, T.J., Kim, S.H., Choi, Y.H., Lee, S.H., Lee, J.M., Kim, Y.H., Park, J.W. and Kwon, T.K. (2008). Induction of apoptosis by withaferin A in human leukemia U937 cells through down-regulation of Akt phosphorylation. Apoptosis, 13:1494-504.

37. Oh, J.H., Lee, T.J., Park, J.W. and Kwon, T.K. (2008). Withaferin A inhibits iNOS expression and nitric oxide production by Akt inactivation and down-regulating LPS-induced activity of NF-kappaB in RAW 264.7 cells. European Journal of Pharmacology, 599:11-7.

38. Divya, S., Amita, A., Rakesh, M. and Sita, N. (2007). *Withania somnifera* inhibits NF-êB and AP-1 transcription factors in human peripheral blood and synovial fluid mononuclear cells. Phytotherapy Research, 21: 905-913.

39. Kaileh, M., Vanden, B.W., Heyerick, A., Horion, J., Piette, J., Libert, C., De Keukeleire, D., Essawi, T. and Haegeman, G. (2007). Withaferin A strongly elicits IêB Kinase beta hyperphosphorylation concomitant with potent inhibition of its kinase activity. Journal of Biological Chemistry, 282: 4253-4264.

40. Wei, D., Wang, L., He, Y., Henry James, Q.X., Abbruzzese, L. and Xie, K. (2004). Celecoxib Inhibits Vascular Endothelial Growth Factor Expression in and Reduces Angiogenesis and Metastasis of Human Pancreatic Cancer via Suppression of Sp1 Transcription Factor Activity. Cancer Research, 64:2030-2038.

Prediction of HIV-1 Protease Inhibitory Activity of (4-Hydroxy-6-Phenyl-2-Oxo-2H-Pyran-3-yl) Thiomethanes: QSAR Study

V. Ravichandran[a+], Abhishek K. Jain[a], V.K. Mourya[b] and R. K. Agrawal[a*]

Department of Pharmaceutical Sciences, Dr. H. S. Gour University, Sagar (M.P.), India
[b] Govt. College of Pharmacy, Osmanpura, Aurangabad, Maharashtra, India
+Present Addres : Faculty of Pharmacy, AIMST University, Semeling - 08100, Kedah, Malaysia
* For Correspondence - dragrawal2001@yahoo.co.in - phravi75@rediffmail.com

Abstract

In pursuit of better HIV-1 protease inhibitory agents, QSAR studies were performed on a series of (4-hydroxy-6-phenyl-2-oxo-2h-pyran-3-yl) thiomethanes using WIN CAChe 6.1. Stepwise multiple linear regression analysis was performed to derive QSAR models which were further evaluated for statistical significance and predictive power by internal and external validation. The best QSAR model was selected, having correlation coefficient (R) = 0.923 and cross-validated squared correlation coefficient $(q^2) = 0.743$. The developed best QSAR model indicates that the hydrophobicity and ionization potential play an important role in the HIV-1 protease inhibitory activities.

Keywords: QSAR; HIV-1 protease inhibitory activity; multiple linear regressions; thiomethane.

Introduction

HIV- 1 (Human Immunodeficiency Virus Type-1) is the pathogenic retrovirus and causative agent of AIDS or AIDS- related complex (ARC) (1). When viral RNA is translated into a polypeptide sequence, it is assembled in a long polypeptide chain, which includes several individual proteins namely, reverse transcriptase, protease, integrase, etc. Before these enzymes become functional, they must be cut from the longer polypeptide chain.

Acquired immune deficiency syndrome (AIDS) is a formidable pandemic that is still wreaking havoc world wide. The catastrophic potential of this virally caused disease may not have been fully realized. The causative moiety of the disease is human immunodeficiency virus (HIV), which is a retrovirus of the lentivirus family (2). The three viral enzymes; reverse transcriptase, protease and integrase encoded by the group specific antigen and group specific antigen-polyprotein genes of HIV play an important role in the virus replication cycle. Among them, viral protease catalyzes the formation of viral functional enzymes and proteins necessary for its survival. The viral particles at this stage are called virions. The virus particles after the protease action have all the necessary constituents of mature virus and are capable of invading other T4 cells and repeating the life cycle of proviral DNA from viral RNA, the key stage in viral replication. Its central role in virus maturation makes protease is a prime target for anti-HIV-therapy.

Computational chemistry has developed into an important contributor to rational drug design. Quantitative structure activity relationship (QSAR) modeling results in a quantitative correlation between chemical structure and biological activity. QSAR analyses of HIV-1 reverse transcriptase inhibitors (3), HIV-1

protease inhibitors (4,5) and HIV-1 integrase inhibitors (6,7) and gp 120 envelope glycoprotein (8) were reported. Leonard et al. has developed a few QSAR models for anti-HIV activities of different group of compounds (9,10). The present group of authors has developed a few quantitative structure-activity relationship models to predict anti-HIV activity of different group of compounds (11-20). In continuation of such efforts, in this article, we have performed QSAR analysis to explore the correlation between physicochemical and biological activity of thiomethane derivatives using modeling software WIN CAChe 6.1 (molecular modeling software, a product of Fujitsu private limited, Japan) and statistical software STATISTICA version 6 (StatSoft, Inc., Tulsa, USA).

Materials and Methods

In the present work we have taken 16 thiomethane compounds (Table 1) and their HIV-1 protease inhibitory activity from the reported work (21). Many of these compounds inhibited wild type HIV-1 protease with IC_{50} values between 0.058 μM and 7.82 μM. There is high structural diversity and a sufficient range of the biological activity in the selected series of thiomethane derivatives. It insists as to select these series of compounds for our QSAR studies. All the HIV-1 protease inhibitory activities used in the present study were expressed as $pIC_{50} = -\log_{10} IC_{50}$. Where IC_{50} is the micro molar concentration of the compounds producing 50% reduction in the HIV-1 protease activity is stated as the means of at least two experiments. The compounds which did not show confirmed HIV-1 protease inhibitory activity and the compounds having particular functional groups at a particular position once in the above cited literature have not been taken for our study. We carried out QSAR analysis and established a QSAR model to guide further structural optimization and predict the potency and physiochemical properties of clinical drug candidates.

All the sixteen compounds (13 compounds in training set and three in test set, training and test set selection has been done manually) were built on workspace of molecular modeling software WIN CAChe 6.1, which is a product of Fujitsu private limited, Japan. The energy minimization was done by geometry optimization of molecules using MM2 (Molecular Mechanics) followed by semi empirical PM3 method available in MOPAC module until the root mean square gradient value becomes smaller than 0.001 kcal/mol Å. The physicochemical properties were calculated on project leader file of the software. These properties were fed manually into statistical software named STATISTICA version 6 (StatSoft, Inc., Tulsa, USA) and a correlation matrix was made to select the parameters having very less inter-correlation and maximum correlation with activity. This was followed by multiple linear regression analysis to achieve best model.

Internal validation was carried out by Leave one out (LOO) method using statistical software STATISTICA. The cross-validated correlation coefficient, q^2, was calculated using the following equation:

$$q^2 = 1 - PRESS / \sum_{i=1}^{N} (y_i - y_m)^2$$

$$PRESS = \sum_{i=1}^{N} (y_{pred,i} - y_i)^2$$

Where y_i is the activity for training set compounds, y_m is the mean observed value, corresponding to the mean of the values for each cross-validation group, and $y_{pred,i}$ is the predicted activity for y_i. The LOO predicted values are shown in table 1.

In present study the calculated descriptors were conformational minimum energies (CME), Zero-order connectivity index

Table 1: Structure, selected parameters and their HIV-1 protease inhibitory activity of thiomethane analogues
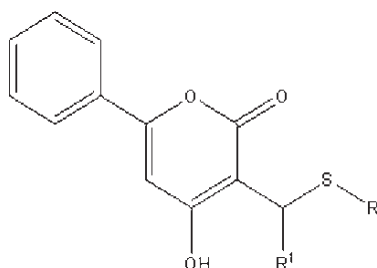
Comp. No.	R	R^1	logP	IP	pIC_{50} $(\mu M)^b$	Cal. Act.	Pred. Act. (LOO)
1	C_6H_5	C_6H_5	4.112	9.027	0.108	0.293	0.321
2	C_6H_5	2-naphthyl	5.114	8.815	-0.893	-0.767	-0.618
3	C_6H_5	cyclohexyl	4.234	8.656	-0.387	-0.206	0.008
4	C_6H_5	isobutyl	3.873	8.804	0.387	0.253	0.202
5	C_6H_5	isopentyl	4.269	9.010	0.409	0.145	0.094
6^a	2-naphthyl	C_6H_5	5.114	8.890	-0.389	-0.689	--
7	$CH_2C_6H_5$	C_6H_5	4.206	8.852	0.319	0.029	-0.019
8	$CH_2C_6H_5$	isobutyl	3.968	9.101	0.585	0.493	0.473
9	$CH_2C_6H_5$	CH_2-isopropyl	3.464	9.097	1.076	0.908	0.875
10^a	cyclohexyl	C_6H_5	4.015	9.065	0.319	0.415	--
11	cyclohexyl	isobutyl	3.776	9.075	0.495	0.625	0.642
12	cyclohexyl	CH_2-cyclopropyl	3.272	9.071	0.833	1.039	1.097
13	cyclohexyl	CH_2-cyclopropyl	4.065	9.077	0.267	0.387	0.412
14	cyclopentyl	cyclopentyl	3.345	9.060	0.648	0.967	1.041
15	cyclopentyl	isobutyl	3.380	9.042	1.237	0.918	0.849
16^a	cyclopentyl	CH_2-cyclopropyl	2.876	9.067	1.161	1.364	--

(CI0), First-order connectivity index (CI1), Second-order connectivity index (CI2), dipole moment (DM), total energy at its current geometry after optimization of structure (TE), heat of formation at its current geometry after optimization of structure (HF), ionization potential (IP), electron affinity (EA), octanol-water partition coefficient(logP), molar refractivity(MR), shape index order 1 (SI1), shape index order 2 (SI2), shape index order 3 (SI3), Zero-order valance connectivity index (VCI0), First-order valance connectivity index (VCI1), Second-order valance connectivity index (VCI2). (Physicochemical parameters data will be provided on request).

Results and Discussion

The QSAR studies of the thiomethane series resulted in several QSAR equations. Inter-correlation between the descriptors involved in the QSAR model is ≤ 0.57. The best equation when we considered only one parameter is Eq. 1.

$$pIC_{50} = 4.336 \, (\pm 0.596) - 1.004 \, (\pm 0.151) \, \log P \quad (1)$$

$n = 13$, $R = 0.895$, $R^2 = 0.802$, $R^2_{adj} = 0.783$, SEE = 0.264, $F = 44.42$, $P < 0.001$, $q^2 = 0.726$, $S_{PRESS} = 0.309$, SDEP = 0.297.

The above equation is statistically significant one. The R^2 and internal predictivity of the model is good. When we have considered the best equation containing two parameters is Eq. 2.

$$pIC_{50} = -5.993 \, (\pm 4.613) - 0.831 \, (\pm 0.165) \, \log P + 1.075 \, (\pm 0.581) \, IP \quad (2)$$

$n = 13$, $R = 0.923$, $R^2 = 0.852$, $R^2_{adj} = 0.823$, SEE = 0.238, $F = 28.80$, $P < 0.001$, $q^2 = 0.743$, $S_{PRESS} = 0.299$, SDEP = 0.287.

When we considered three parameters for developing model, there was no significant improvement in R^2 and q^2. Eq. 2 was selected as the best model on the basis of high q^2 values and

R^2 value. The values given in the parentheses are 95% confidence intervals of the regression coefficients. Eq. 2 could explain 85.2% and predict 74.3% of the variance of the HIV-1 protease inhibitory activity data. The calculated HIV-1 protease inhibitory activity values by Eq.2 are given in table1. This model showed good correlation coefficient (R) of 0.923 between descriptors [logP and IP] and HIV-1 protease inhibitory activity. This model also indicates statistical significance > 99.9% with F value $F_{(2,10)} = 28.80$. The residual of the observed and calculated activities are shown in fig. 1. The predictive ability of the selected model was also confirmed by external r^2_{CVext} method. According to Tropsha *et al.*, the proposed QSAR model is predictive as it satisfies the conditions $r^2_{CVext} > 0.5$ and $R^2_{Pred} > 0.6$ ($r^2_{CVext} = 0.885$, $R^2_{Pred} = 0.991$) (22). The robustness of this model was checked by Y–randomization test. The low R^2 and q^2 values indicate that the good results in our original model are not due to a chance correlation or structural dependency of the training set.
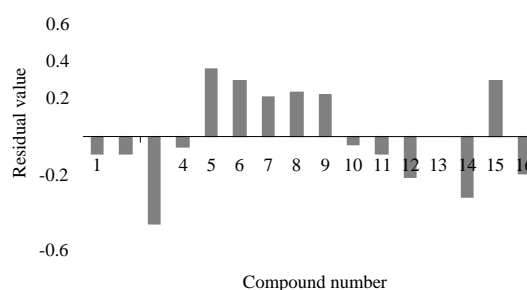
The QSAR shows a linear relationship of HIV-1 protease inhibitory activity with the logP. Its negative sign indicates that highly hydrophobic groups are not good for improving the activity of the series. The positive coefficient of IP showed that the presence of electron donating groups is favor for activity. Thus we conclude that the biological activity will be increased if substituents that bring about changes in the molecule as mentioned above are attached to it.

References

1. Gallo, R. C., Salahuddin, S. Z, Popovic, M., Shearer, G. M, Kaplan, M., Haynes, B. F, Palker, T. J., Redfield, R., Oleske, J. and Safai, B. (1984) Frequent detection and isolation of cytopathic retroviruses (HTLV-III) from patients with AIDS and at risk for AIDS. Science, 224: 500-503.

2. De Clercq, E. (1995) Toward improved anti-HIV chemotherapy: therapeutic strategies for intervention with HIV infections. J. Med. Chem., 38: 2491-2517.

3. Pungpo, P. and Hannongbua, S. (2000) Three-dimensional quantitative structure-activity relationships study on HIV-1 reverse transcriptase inhibitors in the class of dipyridodiazepinone derivatives, using comparative molecular field analysis. J. Mol. Graphics & Modell., 18: 581-590.

4. Jayatilleke, P.R.N., Nair, A.C., Zauhar, R. and Welsh, W.J. (2000) Computational studies on HIV-1 protease inhibitors: Influence of calculated inhibitor-enzyme binding affinities on the statistical quality of 3D-QSAR CoMFA models. J. Med. Chem. , 43: 4446-4451.

5. Nair, A.C., Jayatilleke, P., Wang, X., Miertus, S. and Welsh, W.J. (2002) Computational studies on tetrahydropyrimidine-2-one HIV-1 protease inhibitors: improving three-dimensional quantitative structure-activity relationship comparative molecular field analysis models by inclusion of calculated inhibitor-and receptor based properties. J. Med. Chem., 45: 973-983.

6. Buolamwini, J.K. and Assefa, H. (2002) CoMFA and CoMSIA 3D QSAR and docking studies on conformationally-restrained cinnamoyl HIV-1 integrase inhibitors: Exploration of a binding mode at the active site. J. Med. Chem., 45: 841-852.

7. Raghavan, K., Buolamwini, J.K., Fesen, M.R., Pommier, Y. and Kohn, K.W. (1995) Three dimensional quantitative structure-activity relationships (QSAR) of HIV integrase inhibitors: A comparative molecular field analysis (CoMFA) study. J. Med. Chem., 38: 890-897.

8. Debnath, A.K., Jiang, S., Strick, N., Lin, K. and Haberfield, P. (1994) Three dimensional structure-activity analysis of a series of porphyrin derivatives with anti-HIV-1 activity targeted to the V3 loop of the gp 120 envelope glycoprotein of the human immunodeficiency virus type 1. J. Med. Chem., 37: 1099-1108.

9. Thomas, J.T. and Roy, K. (2006) QSAR by LFER model of HIV protease inhibitor mannitol derivatives using FA-MLR, PCRA and PLS techniques. Bioorg. Med. Chem., 14: 1039-1046.

10. Thomas, J.T. and Roy, K. (2006) Comparative QSAR modeling of CCR5 receptor binding affinity of substituted 1-(3,3-diphenylpropyl)-piperidinyl amides and ureas. Bioorg. Med .Chem. Lett., 16: 4467-4474.

11. Ravichandran, V., Jain, P.K., Mourya, V.K. and Agrawal, R.K. (2008) QSAR study on some arylsulfonamides as anti-HIV agents. Med. Chem. Res., 16: 342-351.

12. Ravichandran, V. and Agrawal, R. K. (2007) Predicting anti-HIV activity of PETT derivatives:CoMFA approach. Bioorg. Med. Chem. Lett., 17: 2197-2202.

154

13. Ravichandran, V., Mourya, V.K. and Agrawal, R.K. (2007) QSAR study of novel 1, 1, 3 – trioxo [1, 2, 4] - thiadiazine (TTDs) analogues as potent anti-HIV agents. Arkivoc, XIV: 204-212.

14. Ravichandran, V.; Prashanthakumar, B.R., Sankar, S. and Agrawal, R.K. (2008) Comparative molecular similarity indices analysis for predicting anti-HIV activity of phenyl ethyl thiourea (PET) derivatives. Med. Chem. Res., 17: 1-11.

15. Ravichandran, V., Mourya, V.K. and Agrawal, R.K. (2007) QSAR prediction of HIV–1 reverse transcriptase inhibitory activity of benzoxazinone derivatives. Internet Electron. J. Mol. Des., 6: 363-374.

16. Ravichandran V, Mourya VK, Agrawal RK (2008) QSAR modeling of hiv-1 reverse transcriptase inhibitory activity with PETT derivatives. Digest J. Nanomat. Biostruct., 3: 9-17.

17. Ravichandran, V., Mourya, V.K. and Agrawal, R.K. (2008) Prediction of HIV-1 protease inhibitory activity of 4-hydroxy-5,6-dihydropyran-2-ones: QSAR study. J. Enzyme Inhib. Med. Chem., (Inpress).

18. Ravichandran, V., Mourya, V.K. and Agrawal, R.K. (2008) QSAR analysis of 6-aryl-2,4-dioxo-5-hexenoic acids as HIV–1 integrase inhibitors. Indian J. Pharm. Edu. Res., 42: 40-47.

19. Sahu, K.K., Ravichandran, V., Jain, P.K., Sharma, S., Mourya, V.K. and Agrawal, R.K. (2008) QSAR analysis of chicoric acid derivatives as HIV–1 integrase inhibitors. Acta Chimi. Slov., 55:138-145.

20. Sahu, K.K., Ravichandran, V., Mourya, V.K. and Agrawal, R.K. (2007) QSAR analysis of caffeoyl naphthalene sulphonamide derivatives as HIV-1 Integrase inhibitors. Med. Chem. Res., 15: 418-430.

21. Prasad, J.V.N.V., Para, K.S., Tummino, P.J., Fergusion, D., McQuade, T.J., Lunney, E.A., Rapundalo, S.T., Bately, B.L., Hingoram, G., Domagala, J.M., Gracheck, S. J., Bhat, T.N., Liu, B.L., Baldwin, E.T., Erickson, J.W. and Sawyer, T.K. (1995) Nonpeptidic potent HIV-1 protease inhibitors: (4-hydroxy-6-phenyl-2-oxo-2h-pyran-3-yl) thiomethanes that span $P_1 – P_2'$ subsites in a unique mode of active site binding. J. Med. Chem., 38: 898-905.

22. Tropsha, A., Gramatica, P., Gombar, V.K. (2003) The importance of being earnest: Validation is the absolute essential for successful application and interpretation of QSPR models. Quant. Struct. Act. R el., 22: 1-9.

Comparative UV-spectra of fermented cultural extract of antifungal-active *Streptomyces* isolates recovered from different ecological habitats

[1]Ismail Saadoun, [1]Fouad AL-Momani, [1]Qotaiba Ababneh and [2]Shahidi Bonjar

[1]Dept. of Biological Sciences, Jordan Univ. of Science and Technology, Irbid-22110, Jordan
[2]Department of Plant Pathology, College of Agricultural Sciences, Bahonar University of Kerman, Kerman-Iran
* For Correspondence : isaadoun@just.edu.jo

Abstract

UV-spectra of antifungal-active *Streptomyces* isolates were compared to previously reported spectra and analyzed under different extraction conditions. MU123 *Streptomyces* isolate from Turkey exhibited a UV spectrum similar to 23_7 isolate from Jordan with 2 maximum absorbance peaks at (226 and 260 nm) and at (220 and 260 nm), respectively. This spectrum was repeated by the C5P1-6 isolate from Jordan with 2 maximum absorbance peaks at 225-250 and 300 nm. The aquatic species identified as *S. violaceusniger* showed 2 maximum absorbance peaks at 231 and 258 nm similar to the UV spectrum of a clinical isolate of actinomycetes (*Streptomyces* sp. 96.0333) that exhibited 2 absorbance peaks at 220-225 and 262 nm. When C1P2-6 isolate from Jordan was compared to Ir 102 from Iran under same cultural, extraction and UV analysis conditions, data revealed similar UV spectra with 2 absorbance peaks for both isolates at 200-225 and 275-300 nm. Approximately 50% of reported active screened isolates exhibit similar UV-spectra which might reflect their habitats, culture and UV analysis conditions. Comparison of UV-spectra and absorption peaks of known antibiotics to that of active *Streptomyces* isolates might explain the ability of the same *Streptomyces* sp. to produce several antibiotics.

Introduction

Members of the order *Actinomycetales* are the most abundant soil microorganisms under a wide variety of conditions. They include many species that are characterized by the production of extracellular important bioactive compounds. Majority of those strains belong to species within the genus *Streptomyces* which produce two–thirds of the naturally occurring antibiotics world wide. Such strains were advocated as promising agents against several pathogens and are well known for their potential to produce a large number of inhibitory metabolites used in industry, pharmacy, including: antihelminthic, antitumor, antifungal agents (3, 4, 23). Several studies on the isolation, characterization and genotyping of soil streptomycetes of Jordan have already been conducted (11, 13, 14, 15). Other studies showed the ability of different streptomycetes isolates to inhibit the growth of several multi-resistant Gram-positive and Gram-negative pathogens (18, 19, 20). Experiments on the nature of the inhibitory metabolite produced by *S. violaceusniger* showed a maximum absorption in the UV region at 210-260 nm (16). In another study, *Streptomyces* isolates active against *Candida albicans* determined with UV-spectra absorbance peaks were either at 230 nm or 300 nm or in between (17). Some of these spectra were similar to the UV-spectra of the active

extracts of clinical isolates of actinomycetes with indication of similarities in the maximum absorbance peaks (8). Similarly, a study by Iliæ *et al*. (7) on 20 different *Streptomyces* isolates from the soils of Southeastern Serbia indicated that the UV spectra of the culture extracts for the active isolates showed absorbance peaks ranging between 221 and 240 nm. The UV spectra of the active compounds in methanol showed peaks at 217 and 221 nm.

In this investigation we are comparing the UV-spectra of some extracted culture broths of active *Streptomyces* isolates with each other as well as with other reported isolates obtained from different habitats and analyzed under different extraction and instrumental conditions.

Materials and Methods
Isolation and characterization of the active strains

The procedures were performed as described by Saadoun and Al-Momani (12) and Saadoun *et al*. (21).

Antibacterial and antifungal agents

The activity of the *Streptomyces* isolates towards bacteria and *Candida albicans* was performed as described by Saadoun *et al*. (16) and Saadoun and Al-Momani (17), respectively.

Table 1: Comparison of the UV-spectra of different *Streptomyces* isolates recovered from different habitats and analyzed by different UV spectroscopic instruments.

Isolate	Antibiosis		Figure	Reference	Maximum Absorbance (nm)		Culture Broth Extracted in	UV-Spectrophotometer
	ID[a]	Fungus[b]			Peak 1	Peak 2		
23₇			1a	17	223	250	n-butanol	DSM-100
	16-20	*C. albicans*		18				
	25-30	*T. harasmii*						
		As. flavus						
MU123	11-20	*C. albicans*	1b	22	226	260	n-butanol	Shimadzu 1601
23₇			1c	This study	220	260	n-butanol	Jenway/UK
	16-20	*C. albicans*		17				
		T. harasmii		22				
	25-30	*As. flavus*						
C5P1-6	ND[c]	ND	1d	This study	225-250	300	n-butanol	Unicam
No. 22	ND	*C. albicans*	-	9	229	260	n-butanol	DSM-100
A1	35-40	*C. albicans*	2a	17	236	262	n-butanol	DSM-100
S. violaceusniger	10	*C. albicans*	2b	16	231	258	n-butanol	Shimadzu
Sp. 96.0333			2c	8	220-225	262	Ethyl acetate	Kontron Instruments /Uvikon 932
	42-52	*C. albicans*						
	65	*C. tropicalis*						
	33	*As. fumaigatus*						
	30	*Tr. rubrum*						
A1	35-40	*C. albicans*	2d	This study	240	278	n-butanol	Jenway/UK
C1P2-6	ND	ND	3a	This study	200-225	275-300	n-butanol	Unicam
Ir 102			3b	This study	200-225	275-300	n-butanol	Unicam
	>20	*Al. solani*		1				
		Al. alternate						
S. hygroscopicus	>31	*C. albicans*	-	7	217	221	methanol	-

[a]ID: Inhibition zone diameter in mm as determined by agar disc diffusion method. [b]C: *Candida*; T: *Trichoderma*; Tr : *Trichophyton rubrum* ; Al: *Alternaria*; As : *Aspergillus* [c]ND: Not determined

UV-Spectra of bioactive fermented *Streptomyces* broths

UV-spectra of different streptomycetes isolates obtained from previous studies (16, 17) and those obtained from Dr. Shahidi (Bahonar University of Kerman, Kerman-Iran) or from this study were compared for general pattern, maximum absorbance peaks and range of wave length. Streptomycetes isolates were grown in submerged culture in 250 ml flasks containing 50 ml liquid medium (per 1/l, beef extract 3.0 g; peptone 5.0 g; glucose 2.0 g; pH 7.5). Flasks were inoculated with 1 ml of *Streptomyces* spores suspension (10^7 CFU/ml) and incubated at 28 °C for 7 days with shaking at 100 rpm. Control flasks were not inoculated with the *Streptomyces* spores

and were treated as above. After growth, the content of each flask was centrifuged at 2000 g/ 10 min. Approximately 20 ml of each of the centrifuged fermentation broth was extracted with 15 ml of n-butanol after which absorption spectra in UV region (200-450 nm) were determined using a Jenway or Unicam UV-visible spectrophotometer. The organic solvent for extraction of the culture broth and UV spectrophotometer used in different studies are mentioned in Table (1).

Results and Discussion

This work introduces the inference of strains and antibiotics from the UV spectra of fermented cultural extract of bioactive
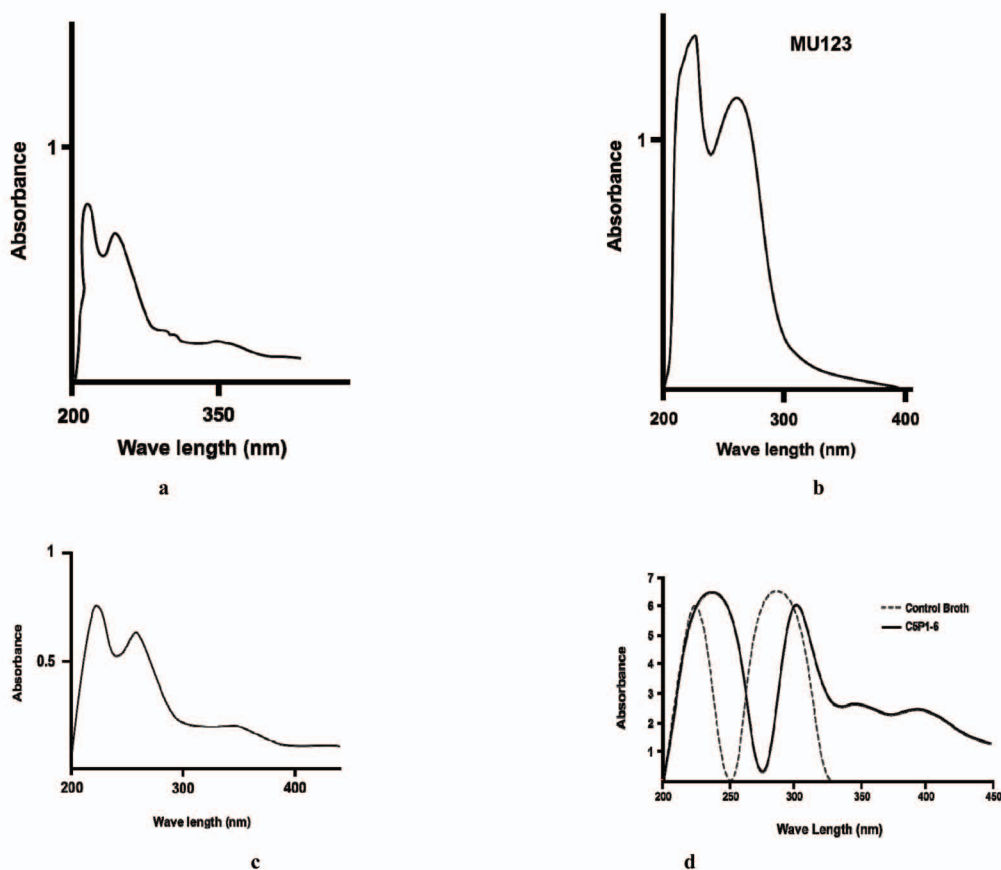

Fig. 1: UV spectra for the active fermentation broth of isolates of 237 (a, Saadoun and Al-Momani, 2000); MU123 (b, Sahin and Ugur, 2003); 237 (c, this study) and C5P1-6 (d, this study).

Comparison of UV spectrum analysis of active streptomycetes

Streptomyces. Several investigators determined the UV spectra for the active fermented broths of different *Streptomyces* isolates on the basis that future studies may answer the question whether the metabolites produced by these isolates responsible for these absorbance peaks or not (6, 7, 8, 16, 17). Furthermore, the use of spectroscopy to distinguish polyenic from nonpolyenic substances were used by several authors (2, 6, 10). When Sahin and Ugur (22) investigated the antimicrobial activity of some *Streptomyces* isolates that were obtained from the soils of Mugla province/Turkey, they observed that MU123 isolate exhibited antifungal activity against *C. albicans* (ATCC 10239) and *C. tropicalis* (RSKK 665) with an inhibition zone diameter of 11-20 mm and ≥ 31 mm, respectively. This isolate showed a UV spectrum (Fig. 1b) similar to what was reported for the isolate 23_7 from Jordan (16) (Fig. 1a) with 2 maximum absorbance peaks at 226 and 260 nm (Table 1). The isolate 23_7 exhibited an inhibition zone diameter of 16-20 mm against *C. albicans* (17) and 25-30 mm against *Trichoderma harasmii* and *Aspergillus flavus* (18). The two maximum absorbance peaks by 23_7 isolate were at 223 and 250 nm (Table 1). This difference in the maximum absorbance peaks might be explained by spectroscopic instrument used in the analysis, culture and extraction conditions. To confirm that similarity, the UV-spectrum of the extracted broth for the 23_7 isolate was repeated by using Jenway/UK UV-visible spectrophotometer (Table 1, Fig. 1c). Data revealed a UV-spectrum similar to what was reported for the isolate 23_7 (17) (Fig. 1a) with 2 maximum absorbance peaks at 220 and 260 nm (Table 1). By using Unicam UV-spectrophotometer, the isolate (C5P1-6) of this study was analyzed and a similar spectrum exhibited with 2 maximum absorbance peaks at 225-250 and 300 nm (Table 1, Fig. 1d).

Saadoun *et al*. (16) in their analysis of the UV-spectrum (200-500) of n-butanol extract of yeast dextrose broth culture of *Streptomyces violaceusniger* showed 2 maximum absorbance peaks at 231 and 258 nm (Table 1, Fig. 2b). This *Streptomyces* sp. was isolated from a sediment sample, collected from a stream, Auburn, Alabama-USA (13). *S. violaceusniger* exhibited a 10 mm inhibition zone diameter against *C. albicans* (16). In another study, Saadoun and Al-Momani (17) determined the UV-spectra of the fermented broth for the most active *Streptomyces* isolates against *C. albicans*. They showed absorbance peaks ranging between 230 and 300 nm and with the isolate A1 exhibiting similar UV-spectra and 2 absorbance peaks at 236 and 262 nm (Table 1, Fig. 2a). A1 was among the isolates that was recovered from soils of North Jordan with an activity of 35-40 mm against *C. albicans* (17). Similarly, Lemriss and his colleagues (8) when screened for nonpolyenic antifungal metabolites in clinical isolates of actinomycetes found that *Streptomyces* sp. 96.0333 exhibiting antifungal activity of ≥ 30 mm against all the tested fungi (Table 1) and a UV spectrum (Fig. 2c) as the one reported by Saadoun and Al-Momani (17) and Saadoun *et al*. (16) with 2 absorbance peaks at 220-225 and 262 nm (Table 1). To confirm that, the UV-spectrum of the extracted broth for the A1 isolate was repeated by using Jenway/UK UV-visible spectrophotometer (Table 1, Fig. 2d). Data revealed a UV-spectrum similar to what was reported for the isolate A1 by Saadoun and Al-Momani (17) (Fig. 2a) and Saadoun *et al*. (16) with 2 absorbance peaks at 240 and 280 nm (Table 1). Also isolates from this study (C1P2-6) and from Iran (Ir 102) were compared under the same cultural, extraction and UV analysis conditions. Data indicated a similar UV spectrum with 2 absorbance peaks for both isolates at 200-225 and 275-300 nm (Table 1, Fig 3a and Fig 3b, respectively). The isolate Ir 102 exhibited ≥ 20 mm against *Alternaria solani* and *A. alternate* (1). The wide peaks exhibited by the Ir 102 and C5P1-6 isolates may be explained by the
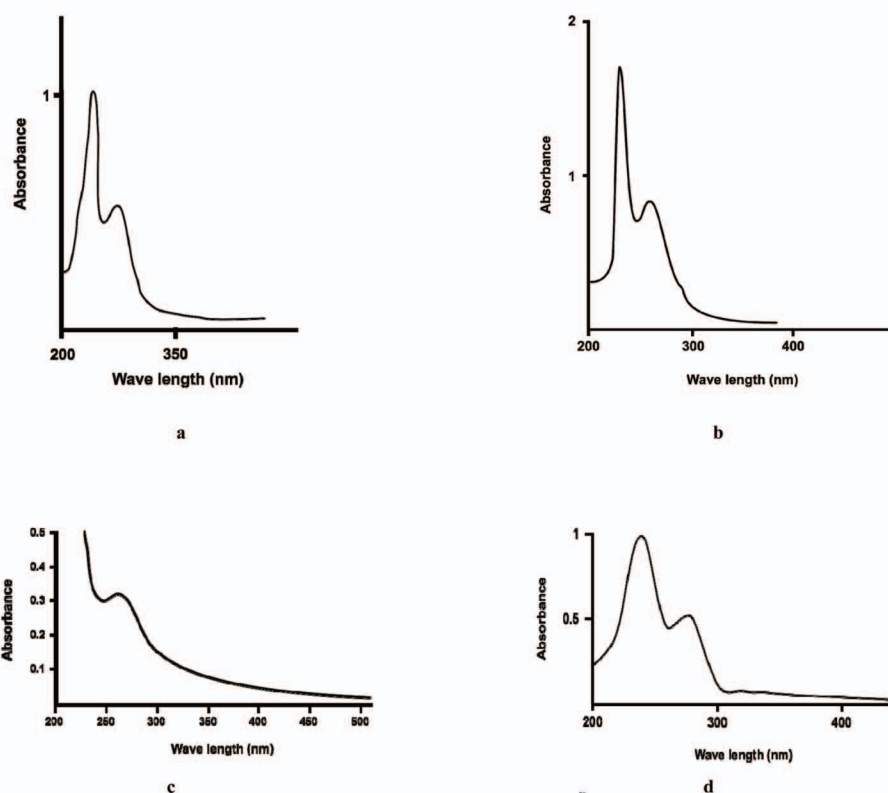
Fig. 2: UV spectra for the active fermentation broth of isolates of A1 (a, Saadoun and Al-Momani, 2000); *Streptomyces violaceusniger* (b, Saadoun *et al.,* 1999) and *Streptomyces* sp. 96.0333 (c, Lemriss *et al.*, 2003) and A1 (d, this study).

saturation of the detector during the measurements.

Results obtained from several investigations revealed that the UV-spectrum activity ranged between 200 and 300 nm. The C5P1-6 isolate of this study showed similar spectrum (Fig. 1d) to isolate 23₇ (Fig 1c) that

was obtained from soils of North Jordan. Similar UV-spectra and absorbance peaks were shown in studies by Msameh (9) and Saadoun and Al-Momani (17) and those exhibited by *S. violaceusniger* recovered from an aquatic habitat in Alabama-USA (13). The similarity between the Jordanian isolates might be
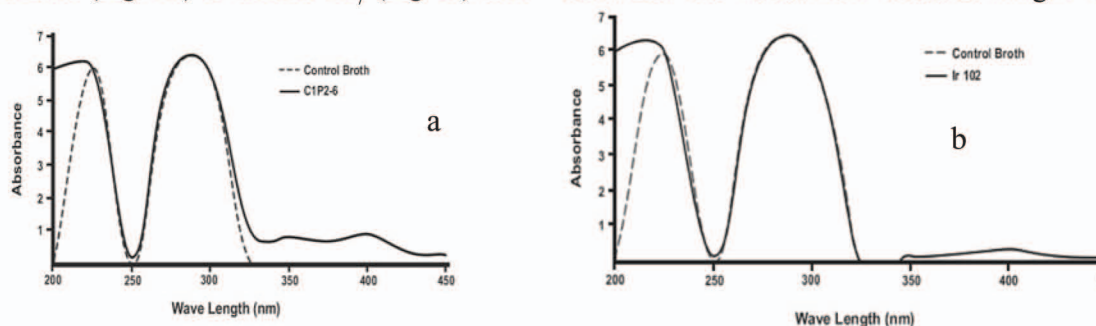
Figure 3: UV spectra for the active fermentation broth of isolates of C1P2-6 (a, This study); Ir 102 (b, This study).

Comparison of UV spectrum analysis of active streptomycetes

explained by the susceptibility of the tested *C. albicans* pathogen to similar bioactive compounds produced by the *Streptomyces* isolates were recovered from the same environment and to their active broths that were extracted under the same conditions and analyzed using the same kind of UV spectrophotometer. Msameh (9) in his investigation showed 12 out of 26 UV spectra (46%) that are similar to each other, Saadoun and Al-Momani (17) showed 12 UV spectra (46%) that are similar to what was reported by Msameh (9).

Although the UV-spectra is one of the basic evidences to identify an antibiotic, similarities in the UV spectra might explain that compounds produced by strains from various areas have similar structure. Similarities in the general UV spectra and maximum absorbance peaks presented in this investigation could explain the ability of the *Streptomyces* sp. to produce antibiotics. Betina (5) reported that several antibiotics can be produced by the same microbial species. For example, *S. hygroscopicus*, *S. griseus*, *S. lavendulae*, *S. albus* and *S. aureofaciens* produced a total of 58, 48, 39, 31 and 21 different antibiotics respectively (5). Some secondary metabolites are produced as a group of closely related structures; one strain of *Streptomyces* produces 32 different anthracyclines. Therefore, further investigation is encouraged on the HPLC profile of the *Streptomyces* extracts and HPLC-MS by comparing with known standards. Some antibiotics as cyclohexamide and actidione have similar UV-spectra (9) and these spectra were similar to the metabolites produced by *S. violaceusniger* (16) and by *Streptomyces* isolate A1 (17).

Although the active *Streptomyces* strains reflect different ecological habitats, culture, and UV analysis conditions, screened isolates showed similar UV-spectra. Similarities in the general UV spectra and/or absorbance peaks could explain

the ability of the various tested and reported *Streptomyces* strains to produce similar active compounds.

Acknowledgements

References

1. Aghighi, S., Shahidi, G.H., Rawashdeh, R., Bataineh, S. and Saadoun, I. (2004). First report of antifungal spectra of activity of Iranian actinomycetes strains against *Alternaria solani*, *Alternaria alternate*, *Fusarium solani*, *Phytophthora megasperma*, *Verticillium dahliae* and *Saccharomyces cervisiae*. Asian Journal of Plant Sciences 3, 463-471.

2. Barakate, M., Ouhdouch, Y., Oufdou, K.H., and Beaulieu, C. (2002). Characterization of rhizospheric soil Strteptomycetes from Moracon habitats and their antimicrobial activities. World Journal of Microbiology and Biotechnology 18, 49-54.

3. Blatz, R. H. (1998). Genetic manipulation of antibiotic producing *Streptomyces*. Trends in Microbiology 6, 76-83.

4. Berdy, J. (1995). Are actinomycetes exhausted as a source of secondary metabolites? *Proceeding of the nine symposiums on the actinomycetes*, pp. 13-34.

5. Betina, V. (1983). The chemistry and biology of antibiotics. Elsevier Scientific Publishing Company, The Netherlands, pp 35-58

6. Hacene, H., Sabaou, N., Bounage, N. and Lefevre, G. (1994). Screening for non-polyenic antifungal antibiotics produced by rare actinomycetales. Microbios 79, 81-85.

7. Iliæ, S.B., Konstantinoviæ, S.S., Todoroviæ, Z.B. (2005). UV/VIS analysis and

antimicrobial activity of *Streptomyces* isolates. Facta universitatis - series: Medicine and Biology 12 (1): 44-46.

8. Lemriss, S., Laurent, F., Couble, A., Casoli, E., Lancelin, J.M., Saintpierre-Bonaccio, D., Rifai, S., Fassouane, A. and Boiron, P. (2003). Screening of nonpolyenic antifungal metabolites produced by clinical isolates of actinomycetes. Canadian Journal of Microbiology 49, 669-674.

9. Msameh, Y. (1992). Streptomycetes in Jordan; distribution and antibiotic activity. M.Sc. Thesis, Yarmouk University, Irbid-Jordan.

10. Ouhdouch, Y., Barakate, M, and Finance, C. (2001). Actinomycetes of Moracon habitats: isolation and screening for antifungal activities. Europian Journal of Soil Biology 37, 69-74.

11. Saadoun, I. and Al-Momani, F. (1996). Bacterial and *Streptomyces* flora of some Jordan Valley soils. Actinomycetes 7, 95-99.

12. Saadoun, I. and Al-Momani, F. (1997). Studies on soil Streptomycetes from Jordan. Actinomycetes 8, 42-48.

13. Saadoun, I., Schrader, K.K. and Blevins, W.T. (1997). Identification of 2-methylisoborneol (MIB) and geosmin as volatile metabolites of *Streptomyces violaceusniger*. Actinomycetes 8, 37-41.

14. Saadoun, I., Mohammad, M.J., Malkawi, H.I., Al-Momani, F. and Meqdam, M. (1998). Diversity of soil streptomycetes in Northern Jordan. Actinomycetes 9, 52-60.

15. Saadoun, I., Al-Momani, F., Malkawi, H. and Mohammad, M.J. (1999). Isolation, identification and analysis of antibacterial activity of soil streptomycetes isolates from North Jordan. Microbios 100, 41-46.

16. Saadoun, I., Hameed, K.M. and Moussauui, A. (1999). Characterization and analysis of antibiotic activity of some aquatic actinomycetes. Microbios 99, 173-179.

17. Saadoun, I. and Al-Momani, F. (2000). Activity of North Jordan soil streptomycetes against *Candida albicans*. World Journal of Microbiology and Biotechnology 16, 139-142.

18. Saadoun, I., Hameed, K., Al-Momani, F., Malkawi, H., Meqdam, M. and Mohammad, M.J. (2000). Characterization and analysis of antifungal activity of soil streptomycetes isolated from North Jordan. Egyptian Journal of Microbiology 35, 463-471.

19. Saadoun, I. and Gharaibeh, R. (2002). The *Streptomyces* flora of Jordan and its' potential as a source of antibiotics active against antibiotic-resistant Gram-negative bacteria. World Journal of Microbiology and Biotechnology 18, 465-470.

20. Saadoun, I. and Gharaibeh, R. (2003). The *Streptomyces* flora of Badia region of Jordan and its' potential as a source of antibiotics active against antibiotic-resistant bacteria. Journal of Arid Environments 53, 365-371.

21. Saadoun, I., Wahiby, L., Ababneh, Q., Jaradat, Z., Massadeh, M. and Al-Momani, F. (2008). Recovery of soil streptomycetes from arid habitats in Jordan and their potential to inhibit multi-drug resistant *Pseudomonas aeruginosa* pathogens. World Journal of Microbiology and Biotechnology 24: 157-162.

22. Sahin, N. and Ugur, A. (2003). Investigation of the antimicrobial activity of some *Streptomyces* isolates. Turkish Journal of Biology. 27, 73-78.

23. Seto, H., Fujioka, T., Furihatha, K., Kaneko, J. and Takahkashi, S. (1989). Structure of complestain a very strong inhibitor of protease activity of complement in the human complement system. Tetrahedron Letters 37, 4987-4990.

Use of Soybean Oil Fry Waste for Economical Biosurfactant Production by Isolated *Pseudomonas aeruginosa* Using Response Surface Methodology

C. J. B. de Lima and J. Contiero[*]

Department of Biochemistry and Microbiology
Biological Sciences Institute, Rio Claro, São Paulo, University - Unesp - CEP 13506-900
Rio Claro, São Paulo, Brazil

*For correspondence - jconti@rc.unesp.br

Abstract

The present study sought biotensoactive production from soybean oil fry waste using *Pseudomonas aeruginosa* ATCC 10145 and *Pseudomonas aeruginosa* isolated from the soil of a petroleum station having undergone gasoline and diesel oil spills. The results of the experiments were analyzed using a complete factorial experimental design, investigating the concentration of soybean oil waste, ammonia sulfate and residual brewery yeast. Assays were performed in 250-mL Erlenmeyer beakers containing 50 mL of production medium, maintained on a rotary shaker at 200 rpm and a temperature of 30 ± 1 °C for a 48-hour fermentation period. Biosurfactant production was monitored through the determination of rhamnose, surface tension and emulsification activity. The *Pseudomonas aeruginosa* ATCC 10145 strain and isolated *Pseudomonas aeruginosa* were able to reduce the surface tension of the initial medium from 61 mN/m to 32.5 mN/m and 30.0 mN/m as well as produce rhamnose at concentrations of 1.96 and 2.89 g/L with emulsification indices of 96% and 100%, respectively.

Keywords: *Pseudomonas aeruginosa*, Biosurfactant, Rhamnose, Surface-active, Emulsification index, Soybean oil.

Introduction

Surfactants are an important class of chemical compounds widely used in different industries, acting as dispersants and/or solubilizers of organic compounds. The vast majority of commercially employed surfactants are synthesized from petroleum derivatives (1). In the past few decades, however, the interest in surfactants of a microbial origin has increased significantly, above all, due to their biodegradability (2,3,4).

Compounds of a microbial origin that exhibit surfactant properties (reduction of surface tension and/or high emulsifying capacity) are denominated biosurfactants and are metabolic byproducts of bacteria and fungi (5). Glycolipids are the best known microbial surfactants. These compounds are made up of carbohydrates associated to a long chain of aliphatic or hydroxy-aliphatic acids. Rhamnolipids are among the most-studied glycolipids and are compounds that have one or two rhamnose molecules linked to one or two α-hydroxydecanoic acid molecules (6).

Surfactants produced microbiologically offer a number of advantages over their chemical equivalents, such as low toxicity, tolerance to temperature, pH and ionic strength as well as the possibility of being produced from renewable substrates (7,8,9). Biosurfactants can be applied in fields such as agriculture for the formulation of

pesticides and herbicides; the food industry as additives in condiments; and in pharmaceutical, textile, cosmetic and petroleum industries, where there are employed for the secondary recovery of petroleum, such as in the removal and mobilization of oil residuals and bioremediation (10).

Despite their advantages, biosurfactants are not widely used by industries due to the high production costs associated to low productivity and the use of expensive substrates. One possible strategy for reducing production costs is the use of alternative substrates, such as agricultural or food industry wastes, which generally contain the high levels of carbohydrates and lipids necessary for the biosynthesis of biosurfactants (11). Moreover, the use of wastes contributes toward a reduction in environmental pollution and the economic valuation of such products. Alternative substrates, such as oil dregs, used oils, molasses and wastes from the processing of cheese, potatoes and cassava, are examples of byproducts with potential for the production of biosurfactants (12,13,14,15).

The aim of the present study was to determine suitable replacements for chemical surfactants byproducts with either low or no toxicity using wastes as raw materials to reduce the cost of these byproducts. The main objectives of the study were to determine the potentiality of an isolated strain of *Pseudomonas aeruginosa* in producing biosurfactant from soybean oil waste used in the frying of different foods, ammonia nitrate and residue from an autolyzed brewery biomass; and compare its performance to that of *Pseudomonas aeruginosa* ATCC 10145, using a complete factorial experimental design.

Materials and Methods

Microrganism

P. aeruginosa ATCC 10145 was kindly donated by Dr. Ivano de Fillipis from the Instituto Nacional de Controle de Qualidade em Saúde (INCQS/FIOCRUZ) – Rio de Janeiro, Brazil. *P. aeruginosa* was isolated from the soil of a petroleum station having undergone gasoline and diesel oil spills located in the city of Uberlândia, Minas Gerais, Brazil. The bacterial strain was identified as *P. aeruginosa* called strain UFU. The cultures were maintained at 4°C in a bacto nutrient broth (BD, cod. 234000) supplied by the Becton Dickinson and Company, USA.

Culture Isolation

The medium proposed by Vecchioli (16), added with 0.5% (v/v) of soybean oil fry waste as the sole carbon source, was used for the bacterial cultures using the pour-plate technique. Among the isolated microorganisms, the one that demonstrated the best surface tension reduction of the culture medium after fermentation was selected and identified. The isolated microorganism was identified at the Enterobacteria Laboratory of the Oswaldo Cruz Institute (Rio de Janeiro, Brazil), following traditional procedures based on bacterial cytomorphology, biochemistry and physiology.

Growth Medium and Conditions

Growth of the bacterial culture was performed on the medium proposed by Santos (17), consisting of (g/L) NH_4NO_3 (1.7), Na2HPO4 (7.0), KH_2PO_4 (3.0), $MgSO_4.7H_2O$ (0.2), yeast extract (5.0) and glucose (10.0). Biosurfactant production assays were conducted on the same mineral medium used for microbial growth, with the addition of soybean oil fry waste (g/L between 5 and 15), residual brewery yeast (g/L between 0 and 10), NH_4SO_4 (g/L between 1 and 13). The residual brewery yeast, consisting of 100% inactivated, dried cells of *Saccharomyces cerevisiae* was provided by a local brewery. The product composition was 8.0% moisture, 40.0% protein, 3.0% fibrous matter, 8.0% mineral matter and aflatoxin (50 ppb). All media were autoclaved at 121°C for 15 min after adjusting the pH to 7.0 with 0.1 N HCl.

The inoculum was prepared by adding three loopfuls of cells from the stock culture to a 500 mL Erlenmeyer beaker containing 100 mL of the growth medium. The inoculated medium was incubated at 30 ± 1°C for 24 hours on a rotary shaker (New Brunswick, USA) at 170 rpm. Afterwards, optical density (600 nm) of bacterial suspension was adjusted to 0.4 and an aliquot of 1 mL of inoculum (2%) was transferred to a 250-mL Erlenmeyer beaker containing 50 mL of medium and incubated at 30°C for 48 hours on a rotary shaker at 170 rpm. Samples were collected at defined time intervals and submitted to analysis.

Complete Factorial Experimental Design

The literature indicates that carbon and nitrogen sources play a critical role in the performance of rhamnose production by *P. aeruginosa* strains (17). To investigate the effects of soybean oil fry waste (WFSO), ammonium sulfate (AS) and residual brewery yeast (RBY) on the selected dependent variables (rhamnose synthesis, emulsification index and surface tension), a complete factorial experimental design (CFED) was used on two levels (18). Statistical calculations were performed using the Statistic 5.1 software program (State Ease Inc.,

Table 1. Real values of variables used in complete factorial experimental design

Independents		Range and levels	
Variables		-1	+1
WFSO (g/L)	X_1	5	15
SA (g/L)	X_2	1	13
RBY (g/L)	X_3	0	10
Microorganism *isolated*	X_4	*P. aeruginosa* ATCC 10145	*P. aeruginosa*

Minneapolis, MN, USA). Using the CFED method, a total of 16 experiments were conducted with combinations of FSOW, AS, RBY and the two *Pseudomonas aeruginosa* strains. Table 1 displays the range and levels of the variables investigated.

Analytical Methods

Cell growth was determined by measuring the optical density of samples, using a UV-160A visible spectrophotometer (Shimadzu, Co., Tokyo, Japan) at 540 nm. Cell concentration was determined by dry weight filtering through a 0.45 μm previously weighed Millipore membrane (19).

Surface tension (ST) was measured at 25°C using a Tensiometer (Fisher Scientific, USA), which was previously calibrated with surveyor weights. A decrease in surface tension was used as a qualitative measurement of surfactant concentration and a quantitative indicator of efficiency.

The biosurfactant emulsification index (EI) was determined according to Cooper and Goldenberg (20). Cell-free culture samples and kerosene (at a ratio of 4:6) were vigorously mixed for 2 min using a vortex (Phoenix, Brazil, model AP-56) and left undisturbed for 24 h at room temperature. EI 24 is the percentage of the height

of the emulsified layer (cm) relative to the total height of the liquid column, determined at the 24-h time point.

The rhamnose concentration was determined according to the methodology described by Rahman et al. (21).

Results and Discussion

Effects of carbon and nitrogen concentrations on rhamnose production

Table 2 displays the results of the complete factorial designs from the FSOW, AS and RBY concentrations.

Table 2. Results of rhamnose production (RM), EI (E24) and ST obtained in the Experiments with *P. aeruginosa* ATCC 10145 and isolated *P. aeruginosa* UFU

Experiments	WFSO (g/L)	SA (g/L)	RBY (g/L)	Microorganism	RM (g/L)	E24[a] (%)	ST[b] (mN/m)
1	5	1	0	ATCC 10145	0.56±0.02	60±0.0	38.5±0.5
2	5	1	0	Isolated	0.79±0.02	71±0.0	36.5±0.5
3	5	1	10	ATCC 10145	0.73±0.01	71±2.0	36.5±0.5
4	5	1	10	Isolated	0.98±0.03	75±3.0	34.0±1.0
5	5	13	0	ATCC 10145	0.25±0.02	40±2.0	41.0±0.0
6	5	13	0	Isolated	0.36±0.01	42±1.0	40.5±1.0
7	5	13	10	ATCC 10145	0.41±0.04	41±2.0	40.5±1.0
8	5	13	10	Isolated	0.59±0.01	60±1.0	39.5±0.0
9	15	1	0	ATCC 10145	1.43±0.01	96±1.0	32.5±0.0
10	15	1	0	Isolated	1.89±0.03	100±0.0	30.5±1.0
11	15	1	10	ATCC 10145	1.96±0.04	96±0.0	32.5±0.0
12	15	1	10	Isolated	2.81±0.03	100±0.0	30.0±0.0
13	15	13	0	ATCC 10145	0.82±0.02	67±1.0	35.5±0.5
14	15	13	0	Isolated	0.91±0.03	67±2.0	35.5±0.5
15	15	13	10	ATCC 10145	1.07±0.03	81±2.0	33.5±1.0
16	15	13	10	Isolated	1.15±0.05	85±1.0	33.0±1.0

EI[a] 24 emulsification index measured after 24-h incubation in kerosene

Inicial ST[b] do meio de produção was 61mN/m

Table 2 displays the statistical delineation used in the production of rhamnose by *P. aeruginosa* ATCC 10145 and isolated *P. aeruginosa* UFU under the different conditions. Both strains were able to use the residue tested (FSOW) and synthesize the biosurfactant. Experiments 11 and 12 employed extreme FSOW, RBY values and a minimal concentration of AS, obtaining the highest production of rhamnose and emulsification index as well as the lowest surface tension value. According to Lang and Wullbrant (22), high concentrations of carbon and nitrogen in the fermented medium are needed for the obtainment of high concentrations of rhamnose. In the present study, the highest amount of rhamnose (2.81 g/L), highest emulsification index (100%) and lowest surface tension (30.5 mN/m) were obtained from the isolated *P. aeruginosa*

UFU, whereas the least adequate condition occurred for *P. aeruginosa* ATCC 10145, with the lowest production of rhamnose (0.25 g/L), lowest emulsification index (40%) and highest surface tension (41.1 mN/m).

Haba et al. (14) selected the *P. aeruginosa* 47T2 NCIB 40044 strain from 36 screened strains due to its capacity to produce 2.7 g/l of rhamnose from FSOW. Previous studies found that this strain produced only 6.4 g/l of rhamnose through cultivation in olive oil waste (23). De Lima et al. (24) obtained a final concentration of 2.3 g/L of rhamnose when *P. aeruginosa* PACL was cultivated in WFSO.

As Table 2 shows, both strains are able to reduce surface tension to below 35 mN/m. According to Cooper (25), an organism is considered a promising biosurfactant producer when it produces tensoactive compounds with a surface tension below 40 mN/m. In order for a biosurfactant to be considered efficient, however, this value must be below 35 mN/m. Studies on rhamnolipid homologues extracted and purified from the fermentation broth by *Pseudomonas aeruginosa* 47T2 cultivated in oil dregs have described a value of 32.8 mN/M for surface tension (26). In a study carried out with vegetable oils (olive, soybean and sunflower) at a concentration of 20 g/L, Andrés et al. (27) found that the broth fermented by *P. aeruginosa* 42 A2 achieved surface tension values of 32.0, 34.0 and 335.5 mN/m, respectively.

For all experiments, the biosurfactant produced had intense emulsification properties. The complete kerosene in water emulsions proved stable for 24 hours. This analysis is a practical measurement of biosurfactant use, as it gives the compound the ability to emulsify non-miscible liquids with the formation of a stable emulsion. The results obtained in the present experiment suggest that isolated *Pseudomonas aeruginosa* UFU has both a better degradation capability regarding soybean oil waste in fermented media as well as a greater potential for producing biosurfactant.

Statistical analysis of the data

From the CFED, the operational conditions of the WFSO (X_1), AS (X_2), RBY (X_3) and *P. aeruginosa* strains (X_4) were determined. As X_4 is a qualitative variable and the equation of the empirical model must be in function of the quantitative variables, it was necessary to perform a correction of the adjusted equation, replacing the X_4 variation with either –1 or 1 in order to maximize the response. Thus, the adjusted empirical model for rhamnose synthesis containing only significant parameters (p=0.05; Student's t test) is represented by Equation 1. Table 3 displays the parameters and significance levels of the model variables.

$$RM = 1.185 + 0.48X_1 - 0.33X_2 + 0.187X_3 - 0.187X_1X_2 \qquad (1)$$

The results show that X_1 and X_3 are highly significant among the independent variables, as they have positive coefficients (Eq. 1), according to which an increase in their concentration increases the production yield. The X_2 variable and the X_1X_2, interaction also have a significant effect, as their negative signs initiate when their concentrations are lower in the system, thereby promoting an increase in the response (RM).

Table 3. Results of the regression for rhamnose synthesis

Codified Factor	Parameter	T Studant	Probability
Constant	1.0250	22.2485	0.0000
X_1	0.4800	10.4188	0.0004
X_2	-0.3300	-7.1629	0.0020
X_3	0.1875	4.0698	0.0152
X_4	0.1600	3.4729	0.0255
X_1X_2	-0.1875	-4.0698	0.0152

$R^2 = 0.9832$; Adjusted $R^2 = 0.9414$; R =0.9916

The goodness-of-fit of the model was checked by determining the coefficient (R^2) and the multiple correlation coefficient (R). The R^2 value (0.9832) for the complete equation (data not shown) indicates that the sample variation of 98.32% for rhamnose was attributed to the independent variables and only 1.68% of the total variation cannot be explained by the model. The value of the adjusted determination coefficient (adjusted $R^2 = 0.9414$) for Equation (1) is also high, which demonstrates the high significance of the model. The high R value (0.9916) demonstrates high agreement between the experimental observations and predicted values. This correlation is also evident on the plot of predicted versus experimental rhamnose values in Figure 1, as all points cluster around the diagonal line, meaning that no significant violations of the model were found.
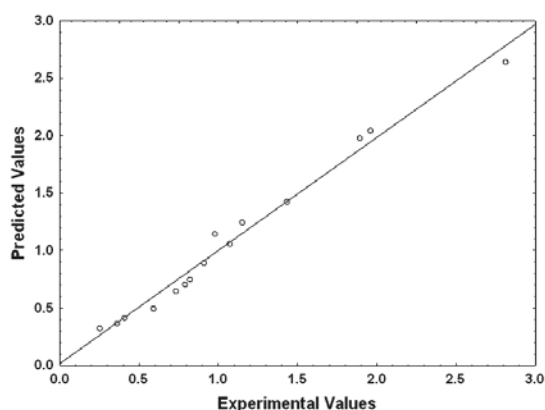

Fig 2. Response surface for rhamnose in relation to WFSO and AS.

Kinetics of rhamnose production by isolated *P. aeruginosa* **UFU and** *P. aeruginosa* **ATCC 10145**

Figure 3 illustrates the kinetics of rhamnose production from the best results obtained by *P. aeruginosa* ATCC 10145 (Experiment 11) and isolated *P. aeruginosa* UFU (Experiment 12)

Fig 1. Predicted vs. experimental values plotted for rhamnose

The 3D response surface (Fig. 2) represents the empirically adjusted equation (Eq. 1) and is plotted to visualize the interactions of the independent variables (WFSO, AS) as well as locate the optimum level of each variable for maximum response (rhamnose synthesis).

The response surface in Figure 2 reveals that an increase in FSOW concentration and a decrease in AS concentration cause an increase in rhamnose synthesis.
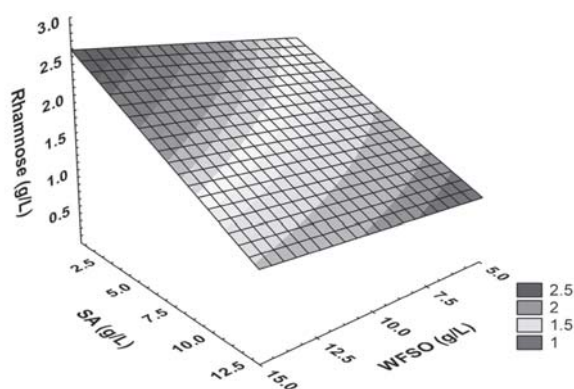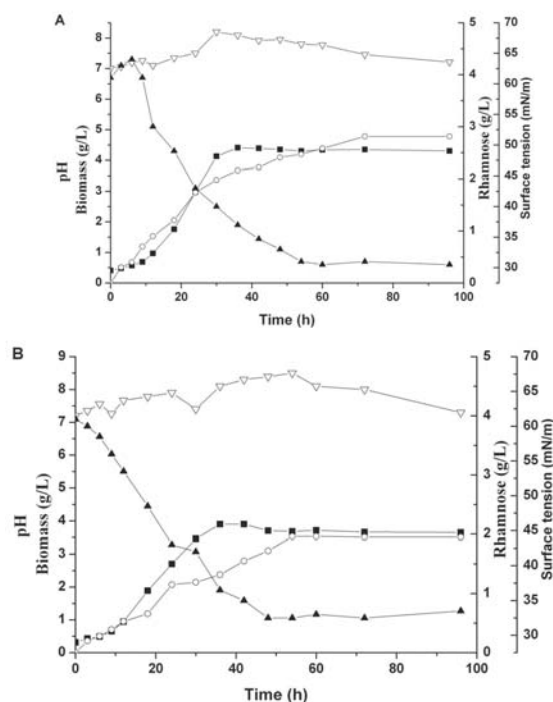

Fig. 3. Kinetics of growth (┆), rhamnose (○), pH (▲) and surface tension (▽): (A) Isolated *P. aeruginosa* UFU and (B) *P. aeruginosa* ATCC 10145 cultivation from soybean oil fry waste.

de Lima *et al*

using soybean oil waste from fried food preparation as the carbon source.

There was intense cell growth up to 36 h of fermentation, when the stationary phase was established, corresponding to biosurfactant production (Yp/x) of 0.54 for the isolated strain (Fig.3A) and 0.36 g rhamnose/g cells for the ATCC 10145 strain (Fig.3B). At 72 h, the isolated strain a achieved rhamnose synthesis level of 2.81 g/L, while the ATCC 10145 reached 1.96 g/L of rhamnose at 54 h. In previously published studies, Guerra-Santos et al. (28), Haba et al. (14) and Dubey et al. (29) achieved 0.97-2.7 g/L of biosurfactant production with different strains of *P. aeruginosa* using glucose and fry oil waste as carbon sources.

As Figure 3 shows, biosurfactant production initially follows an exponential growth phase, but when microbial growth ceases and a stationary phase is achieved, rhamnose synthesis continues, which suggests biotensoactive production partially associated with microbial growth. These observations were also described by Mayer et al. (30), Benincasa et al. (31) and Yu-Hong et al. (32). Perhaps the production of biosurfactant can be classified as a secondary metabolite. Biossurfactant production accompanies bacterial growth in fry oil waste, which may help in the adherence of cells to the substrate molecules and their metabolism (33,34).

Due to the biotensoactive accumulation in the medium, there was also a drop in surface tension (Fig.3). Regarding pH, there was a variation ranging from 7.01 to 8.5 and a tendency toward final values greater than 7.2.

The type of carbon source affects the properties (surface tension and emulsification activity) and final concentration of the rhamnose produced. These differences may be associated to the composition of triglycerides in the substrates used (35) as well as the activity of the microbial lipase on these substrates (36).

Differences were found between the two microorganisms tested in the present study with regard to rhamnose production when the same substrate was used. Differences in rhamnose number in the composition of the rhamnolipids may also result in differences in biotensoactive properties (15).

Conclusion

With the complete factorial experimental design, it was possible to determine the behavior of the independent variables on rhamnose production, the emulsification index and surface tension. The present study demonstrated the biosurfactant-producing potential from the re-use of a fried soybean oil substrate by *P. aeruginosa* ATCC10145 and a new isolated strain, which obtained the best results regarding rhamnose production (2.89 g/L), surface tension (30 mN/m) and emulsification index (100%).

Acknowledgements

References

1. Fiechter, D. (1992). Biosurfactants: moving towards industrial application. Trends in Biotechnology, 10: 208-216.

2. Ishigami Y., Gama Y., Nagahara H., Motomiya T. and Yamaguchi M. (1988). Liposome containing rhamnolipids. Japanese Patent Kokai, 29: 63–182.

3. Makkar, R.S. and Cameotra, S.S. (1999a). Biosurfactant production by microorganisms on unconventional carbon sources – a review. Journal of Surfactants and Detergents 2: 237–241.

4. Makkar, R.S. and Cameotra, S.S. (1999b). Biochemical and structural characterization of biosurfactant produced by *Bacillus*

subtilis at *thermophilic* conditions. Journal of Surfactants and Detergents, 2: 371–376.

5. Nitschke, M and Pastore, G.M. (2002). Biosurfactantes: Propriedades e aplicações. Química Nova, l25: 772-776.

6. Desai, J.D. and Banat, I.M. (1997). Microbial production of surfactants and their commercial potential. Microbiology and Molecular Biology Reviews, 61: 47-64.

7. Banat, I.M., Rhaman, K.S.M., Rhaman, T.J., Marchant, R. and Mcclean, S. (2002). Rhamnolipid biosurfactant production by strains of *Pseudomonas aeruginosa* using low-cost raw materials. Biotechnology Progress, 18: 1277-1281.

8. Kim, S.H., Lim, E.J., Lee, J.D. and Lee, T.H. (2000). Purification and characterization of biosurfactants from *Nocardia* sp. L-417. Biotechnology Applied Biochemistry, 31: 249-253.

9. Mulligan, C.N., Mahmourides, G. and Gibbs, B.F. (1989). Biosurfactant production by chloramphenicol tolerant strain of *Pseudomonas aeruginosa*. Journal of Biotechnology, 12: 37-44.

10. Ron, E.Z. and Rosenberg, E. Biosurfactants and oil bioremediation. (20002). In: Current Opinion in Biotechnology. Editora Elsevier, 13: 249-252.

11. Cameotra, S.S. and Makkar, R.S. (1998). Synthesis of biosurfactants in extreme conditions. Applied microbiology and Biotechnology, 50: 520-529.

12. Abalos, A., Pinazo, A., Infante, M.R., Casals, M., Garcia, F. and Manresa, A. (2001). Physicochemical and antimicrobial properties of new rhamnolipid produced by *Pseudomonas aeruginosa* AT10 from oil refinery wastes. Langmuir, 17: 1367-1371.

13. Siddhartha, G.V.A.O., Nitschke, M., Haddad, R., Eberlin, M.N. and Contiero, J. (2006). Production of *Pseudomonas aeruginosa* LBI rhamnolipids following growth on Brazilian native oils. Process Biochemistry, 41: 483-488.

14. Haba, E., Espuny, M.J., Busquets, M. and Manresa, A. (2000). Screening and production if rhamnolipids by *Pseudomonas aeruginosa* 47T2 NCIB 40044 from waste frying oil. Journal of Applied Microbiology, 88: 379-387.

15. Nitschke, M., Siddhartha, G.V.A.O., Gonçalves, L.A., Haddad, R., Eberlin, M.N. and Contiero, J. (2005). Oil wastes as unconventional substrates for rhamnolipid biosurfactant production by *Pseudomonas aeruginosa* LBI. Biotechnology Program, 21: 1562-1566.

16. Vecchioli, G.I., Del Panno, M.T. and Painceira, M.T. (1990). Use of selected autochthonous soil bacteria to enhance degradation of hydrocarbons in soil. Environmental Pollution 67: 249-258.

17. Santos, A.S., Sampaio, A.P., Vasquez, G.S., Santa Anna, L.M., Pereira, N. and Freire, D.M.G. (2002), Applied Biochemimestry Biotechnology 98: 1025-1035.

18. Jeff Wu, C.F. and Hamada, M. (2000). Experiments: Planning, analysis, and parameter design optimization. New York: Wiley Series in Probability and Statistics.

19. Reis, F.A.S.L., Servulo, E.F.C. and França, F.P. (2004). Lipopeptide surfactant production by *Bacillus subtilis* grown on low-cost raw materials. Applied Microbiology and Biotechnology, 115: 899-912.

20. Cooper, D.G. and Goldenberg, B.G. (1987). Surface-Active Agents from Two *Bacillus*

Species. Applied Environment Microbiology, 53: 224-229.

21. Rahman, K.S.M., Banat, I.M., Thahira-Rahaman, J., Thayumanavan, T. and Lakshmanaperumalsamy, P. (2002). Bioremediation of gasoline contaminated soil by a bacterial consortium amended whit poultry litter, coir pith and rhamnolipids biosurfactant. Bioresource Technology, 81: 25-32.

22. Lang, S. and Wullbrandt, D. (1999). Rhamnose lipid – Biosynthesis, Microbial Production and Application Potential. Applied Microbiology Biotechnology, 51: 22-32.

23. Mercadé, M.E., Manresa, M. A., Robert, M., Espuny, M. J., Andrés C. and Guinea, J. (1993). Olive oil mill effluent (OOME): New substrate for biosurfactant production. Bioresource Technology, 43: 1-6.

24. De Lima, C.J.B., De França, F.P., Sérvulo, E.F.C., Resende, M.M. and Cardoso, V. L. (2007). Enhancement of rhamnolipids production in residual soybean oil by an isolated strain of *Pseudomonas aeruginosa*. Applied Biochemistry and Biotechnology, 137: 463–470.

25. Cooper, D.G. and Paddock, D.A. (1984). Production of a biosurfactant from *Torulopsis bombicola*. Applied and Environmental, 47: 173-176.

26. Haba E., Pinazo, A.O., Jauregui M.J., Espuny M.R. and Manresa, A. (2002). Physicochemical characterization and antimicrobial properties of rhamnolipids produced by *Pseudomonas aeruginosa* 47T2 NCBIM 40044. Biotechnology and bioengineering, 81: 316-322.

27. Andrés, C., Mercadé, E., Guinea, J. and Manresa, A. (1994). 7,10-Dihydroxy-8 (E)
–octadecanoic acid produced by *Pseudomonas* 42 A2: Evaluation of different cultural parameters of the fermentation. World Journal of Microbiology and Biotechnology, 10: 106-109.

28. Guerra-Santos, L.H., Kappeli, O. and Fiechter, A. (1986). Dependence of *Pseudomonas aeruginosa* continuous culture biosurfactant production on nutritional and environmental factors. Applied Microbiology and Biotechnology, 24: 443-448.

29. Dubey, K. and Juwakar, A. (2001). Distillery and curd whey wastes as viable alternative sources for biosurfactant production. World Journal Microbiology Biotechnology, 17: 61-69.

30. Mayer, R.M. and Soberón-Chavez, G. (2000). *Pseudomonas aeruginosa* rhamnolipids: Biosynthesis and potential applications. Applied Microbiology and Biotechnology, 54: 625-633.

31. Benincasa, M., Contiero, J., Manresa, M.A., and Moraes, I.O. (2002). Rhamnolipid production by *Pseudomonas aeruginosa* LBI growing on soapstock as the sole carbon source. Journal of Food Engineering, 54: 283-288.

32. Yu-Hong, W., Chien-Liang, C. and Jo-Shu, C. (2005). Rhamnolipid production by indigenous *Pseudomonas aeruginosa* J4 originating from petrochemical wastewater. Biochemical Engineering Journal, 27: 146–154.

33. Baldi, F., Ivosevic, N., Minaui, A., Pepi, M., Fani, R., Svetlicii, V. and Zutii V. (1999). Adhesion of Acinetobacter venetians to diesel fuel droplets studied with in situ electrochemical and molecular probes. Applied Environmen Microbiology, 65: 2041-2048.

34. Rosenberg, M. and Rosenberg, E. (1981). Role of adherence in growth of *Acinetobacter calcoaceticus* RAG-1 on hexadecane. Journal Bacteriology, 148: 51-57.

35. Kosaric, N. (1993). Biosurfactants: Production, Properties, Applications (1th edition), Marcel Dekker, INC., New York, USA, pp.504.

36. Shabtai, Y. and Daya-Mishne, N. (1992). Production, purification, and properties of a lipase from a bacterium (*Pseudomonas aeruginosa* YS-7) capable of growing in water-restricted environments. Applied Environment Microbiology, 58: 174-180.

Production of á-amylase from agricultural byproducts by *Humicola lanuginosa* in solid state fermentation

Ravi Kant Singh*[a], Shashi Kumar[b], and Surendra Kumar[b]

[a]Department of Biotechnology, IMS Engineering College, Ghaziabad, U.P. India
[b]Chemical Engineering Department, Indian Institute of Technology Roorkee, Roorkee 247 667, Uttarakhand, India
*For correspondence - rksingh.iitr@hotmail.com

Abstract

In this study α-amylase activity expression in *Humicola lanuginosa* was evaluated under different environmental conditions using solid state fermentation (SSF) on different agricultural byproducts. The solid supports for α-amylase production in SSF process were wheat bran, wheat straw, rye straw, and corncob leaf. Wheat bran has been found to yield maximum production of á-amylase among these solid substrates. Effects of process variables, namely incubation time & temperature, initial moisture content, pH, supplementary carbon source, and inoculum level, on production of α-amylase have been studied, and accordingly optimum conditions have been determined. It has been found that the á-amylase production is the highest at 144 hr incubation period, 50ºC incubation temperature, 90% initial moisture contents, pH of 6 and 20% inoculum level. Soluble starch has been found the best supplementary carbon source.

Key words: solid state fermentation, *Humicola lanuginosa,* agricultural byproducts, α–amylase, process optimization, solid support.

Introduction

Enzyme production is an emerging field of biotechnology. At industrial scale, most of the enzymes are manufactured by submerged fermentation (SmF) techniques. However, in the last decades, there has been an increasing trend towards the utilization of the solid state fermentation (SSF) technique to produce several enzymes from thermophilic microorganisms (1-8). Few important advantages of solid state fermentation (SSF) over the traditionally employed submerged fermentation (SmF) are higher yields in a shorter time period, better oxygen circulation, resemblance to natural habitats for filamentous fungi, less effects in downstream processing, and low energy consumption (9).

Amylases are a group of enzymes that have been found in several microorganisms like bacteria (1,2,10,11) and fungi (3,12). α-amylases can be derived from plants, animals and microbes but its production from microbial sources are cost effective and fulfill the industrial demands. The large number of α- amylases are available commercially and they have almost completely replaced chemical hydrolysis of starch (13). Amylases are useful in a broad range of industrial applications which include food, fermentation, textile and paper industries.

Fungal α-amylases are produced by different fermentation techniques. Production of these α-amylases has been investigated through submerged fermentation (SmF) and solid state

fermentation (SSF) (14). The major factors that affect microbial production of á-amylase in a solid state fermentation (SSF) system include selection of a suitable substrate and microorganism, particle size of the substrate, inoculum concentration and moisture level of the substrate. Out of these, the selection of suitable solid substrate is a critical factor (6,15). The production of α-amylase by submerged fermentation (SmF) using synthetic media has been reported by many workers (16-18). The contents of synthetic media are very expensive and uneconomical. Therefore, it needs to be replaced by the more economically available substrates to reduce the cost. In this regard, agro-industrial residues are generally considered as the best substrate for the production of amylases. Table 1 provides few such substrates and microorganisms for the production of different types of amylases (19-29). Thus the use of solid state fermentation (SSF) for α-amylase production has many advantages over submerged fermentation (SmF) due to its simple techniques, low capital investment, lower levels of catabolite repression and better product recovery (5).

The thermal stability is an important feature of most of the enzymes sold in bulk for industrial application. So the selection of thermophilic microorganisms is of particular interest for the production of thermophilic á-amylases (30). The thermophilic fungus *H. lanuginosa* is selected for the production of thermostable á- amylase in the present study.

The purpose of the present study is to investigate the production of á-amylase under solid state fermentation (SSF) process conditions. In this paper the influence of pH, temperature, initial moisture content, inoculation size and incubation time on á-amylase production by *H. lanuginosa* through SSF using four agriculture byproducts viz. wheat bran, corncob leaf, rye straw and wheat straw has been investigated. The effect of supplementary carbon sources (i.e. soluble starch, sucrose, maltose, and glucose).

Materials and Methods
Microbial strain

The thermophilic fugal strain *Humicola lanuginosa* was isolated from the soil (MIET, Meerut) on glucose-peptone medium containing

Table 1: Amylase produced by SSF technique (19-29)

Support	Microorganism	Amylase	Reference
Starch waste	*Bacillus megatarium*	β- amylase	(19)
Wheat bran	*Pycnoporus sanguineus*	α- amylase	(20)
Sorghum Starch	*Trichoderma* sp.	α- amylase	(21)
Wheat bran	*A. niger*	Glucoamylase	(22)
Wheat bran	*Bacillus amyloliquefaciens*	α- amylase	(23)
Polyurethane foam	*A. oryzae*	α- amylase	(24)
Corn floor	*Saccnaromycopsis capsrasis*	α- amylase	(25)
Rice bran	*A. niger*	α- amylase	(26)
Wheat bran	*A. niger*	Glucoamylase	(27)
Urethane foam	*A. oryzae*	Glucoamylase	(28)
Wheat bran	*Rhizopus sp.*	Glucoamylase	(29)

100 g/l of NaCl, purified on the same medium and maintained on 1% malt extract agar slant at 4 ^{0}C.

Preparation of substrates

Different agricultural byproducts, wheat bran (WB), wheat straw (WS), rye straw (RS) and corncob leaf (CL) were obtained from local market. These waste materials were washed first with tap water followed by distilled water to remove the adhered surface dust particles. Then bleaching operation was carried out by immersing them in hot water (75-80^{0}C) for 20 minutes followed by oven drying at 45^{0}C. The dried material was grinded in a mixer grinder (Remi) then sterilized at 121^{0}C, 15 psi pressure for 15 minutes and stored at 4 ^{0}C before further use.

Inoculum preparation

Actively growing and heavily sporulating (ten days) old malt agar slant culture was added to 10 ml sterile distilled water. The spores were gently scraped off with the help of a sterile needle and contents were passed through glass wool so as to obtain spore inoculums free from mycelia bits (31-33). A volume of one ml of spore suspension contained more than 10^6 spores. They were cultured in a medium containing soluble starch 5 g., yeast extract 2 g., KH_2PO_4 1 g., $MgSO_4.7H_2O$ 0.5 g., distilled water 1000 ml. The medium was autoclaved (121^{0}C for 15 minutes), allowed to cool, then aseptically added to sterile 500 ml Erlenmeyer flasks (100 ml added per flask).These flasks with 100 ml liquid medium were incubated with 2 ml spore suspension with autoclaved distilled water and incubated at 50 ± 2 ^{0}C and 120 rpm for 2-3 days in the preliminary experiments and only two days in all subsequent experiments. All chemicals used were of reagent grade.

Solid state fermentation

Four agriculture byproducts; wheat bran, corncob leaf, rye straw, wheat straw was considered as substrate. Five gm of each substrate was taken into 250 ml conical flasks. To adjust percentage moisture levels (w/v), 0.1M acetate buffer, pH = 6.0 was added. The content of the flasks were mixed thoroughly and sterilized in the autoclave at 121 ^{0}C temperature and 1 atmospheric pressure for 20 min and then cooled at room temperature. Each flask was incubated with one ml of inoculum and subsequently rotated in a rotary incubator shaker at 50 ^{0}C.

Optimization of process parameters

Various process parameters affecting á-amylase production in solid state fermentation (SSF) are optimized. The strategy was to optimize each parameter independently and subsequently optimum conditions were employed in each experimental run. The best solid substrate was selected for optimum production of á-amylase production and the suitable solid substrate was used in subsequent experiments. The tested process parameters in this study were initial moisture content (20, 30, 40, 50, 60, 70, 80, 90, 100, 110%, w/v), inoculum concentration (5, 10, 15, 20, 25, 30%, v/w), incubation time (24, 48, 72, 96, 120, 144, 168, 192 h), incubation temperature (30, 40, 50, 60, 70, 80 ^{0}C), initial pH (4, 5, 6, 7, 8), and supplementary carbon sources (soluble starch, sucrose, maltose, glucose). On the basis of experimental data wheat bran was found to be the best solid substrate in solid state fermentation (SSF) process (details are mentioned in result and discussion section).

Determination of dry weight of substrate

All four substrates are not available in completely dried form. They generally contain moisture. Prior to utilize them in bioprocess, it is necessary to dry these solid substrates. Therefore, in the present study the amount of wet solid substrate was kept in the oven at 70 ^{0}C for 24 h to remove the moisture from the solid substrate. After drying, the mass of solid substrate was measured.

Enzyme extraction

At the end of solid state fermentation, the solid substrates were mixed thoroughly with acetate buffer (pH 6, 50 ml) containing 0.1 % tween 80 surfactant (14). The contents were mixed by shaking for two hours at 50 ^{0}C on a rotary shaker at 200 rpm. The slurry was squeezed by muslin cloths. The extract was filtered with a Whatman No. 1 filter paper and the filtrate was used as a crude á-amylase.

Enzyme assay

The α-amylase enzyme was assayed accordingly to the method described by Miller (34). The reaction mixture contained 200 µl soluble starch in phosphate buffer (0.1M, pH = 6); 200 µl of diluted enzyme and 300 µl phosphate buffer. The reaction was incubated for 15 minutes at 30 ^{0}C, 300 µl dinitrosalicylic acid (DNS) solution were added and boiled for 15 minutes. Before cooling 100 µl Rochelle salt (40 % sodium potassium tartarate) was added and colour was measured at 575 nm. One unit of á-amylase activity was defined as the amount of enzyme that releases 1 mg of reducing sugar as glucose per ml per minute under the assay conditions. All data points correspond to triplicates of independent experiments.

Estimation of moisture content

The moisture content of the wheat bran was estimated by drying 10 g of wheat bran to a constant weight at 70 ^{0}C for 24 h and the dry weight was recorded. To fix the initial moisture content of the solid medium, wheat bran was soaked with the desired quantity of water. After soaking, the sample was again dried as described above and the percent moisture content was calculated by the following formula (35). % moisture content (initial) of solid medium = (wt. of the wheat bran – dry wt.) x 100/ dry wt.

Result and Discussion

Screening of agriculture byproducts as substrates for SSF

The selection of a suitable solid substrate in solid state fermentation (SSF) is a critical factor. In this study, four solid substrates are taken for growth and enzyme fermentation by the selected culture. In literature different solid substrates were found to affect the production of enzymes (35-36). In view of this the amylase activity in U/g was measured for all four substrates at temperature of 50 ^{0}C and pH 6. These amylase activities are illustrated in Figure 1. It is evident from this figure that the maximum amount of amylase activity (267 U/g) is obtained in presence of wheat bran alone. The activity decreases in order of wheat bran (WB)> wheat straw (WS)> rye straw (RS)> corncob leaf (CL). In previous studies also (36,37) wheat bran was found to be best substrate for glucoamylase production by an
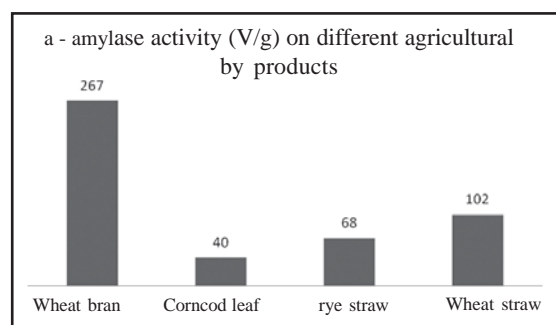

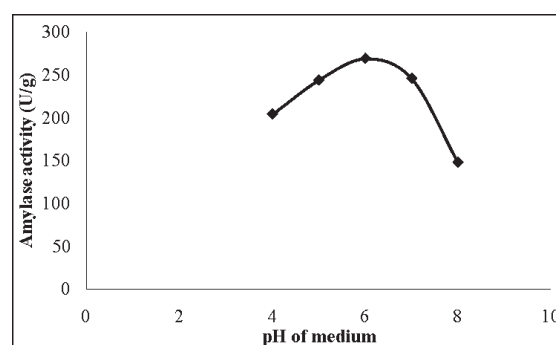**Fig. 1.** Effect of solid substrates on á-amylase activity

Fig. 2. Effect of initial pH of medium on á-amylase activity

Ravi *et al*

Aspergillus sp. and suitable for necessary manipulation. In further experiments, therefore, wheat bran has been used as most suitable substrate out of four selected substrates for the production of á-amylase.

Effect of initial pH of the medium on á-amylase activity

The pH of the growth medium is one of the physio-chemical parameters responsible for morphological changes in the organism and in enzyme secretion. In the present study the influence of pH on amylase activity has been studied by varying pH from 4 to 8. The variation in pH is carried out by adding acid or base buffer as per requirement. The trend in Figure.2 indicates that amylase activity first increases on increasing pH of medium, reaches maximum (269 U/g) at pH of 6 and then decreases. The variation in amylase activity from 4 to 7 is small, indicating excellent buffering properties of wheat bran used in SSF. A similar study has been reported by Gangadharan et al. (23).

Influence of incubation temperature on á-amylase activity

The growth of the microorganism is related to temperature which in turn influences the amylase production (23). The Fig.3 shows the variation in amylase activity at different temperatures varying from 30 to 80 ^{0}C. The
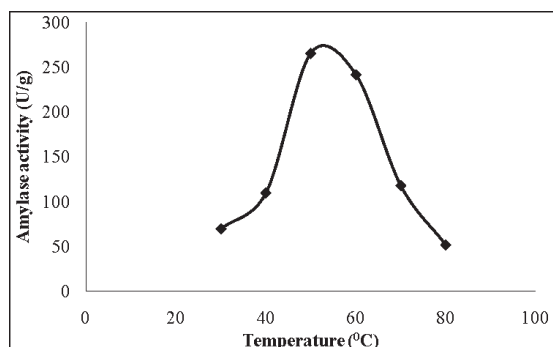
Fig. 3. Effect of incubation temperature on á-amylase activity

maximum amylase production (266 U/g) has been observed at 50 ^{0}C. It has also been reported that the metabolic heat generated during microbial cultivation in SSF exerts harmful effects on the microbial activity (38) and thus the initial set temperature is vital.

Effect of initial moisture content of the medium on the production of á-amylase

The maximum amylase activity (288 U/g) has been attained at the initial moisture content level of 90% (Fig.4). The critical importance of moisture level in SSF media and its influence on the biosynthesis and selection of enzymes can be
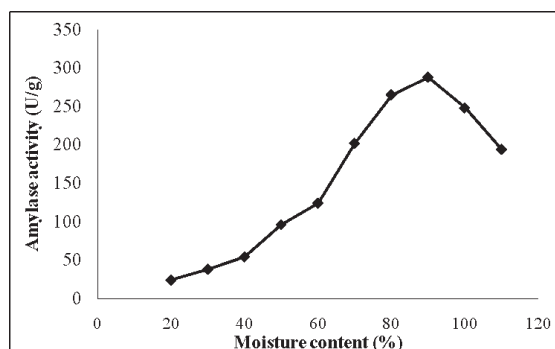
Fig. 4. Effect of initial moisture content of the medium on á-amylase activity

attributed to the interference of moisture in the physical properties of the solid particles. An increase in moisture level is believed to reduce the porosity of the wheat bran, resulting in limited oxygen transfer (8). Low moisture content causes reduction in the solubility of nutrients of the substrates and the low degree of swelling (39).

Influence of inoculum size on á-amylase activity

The inoculum level is an important factor for the production of á- amylase. Higher inoculum concentration increases the moisture content to a significant extent. The free excess liquid present in an unabsorbed form, therefore, gives rise to an additional diffusional barrier together with that

imposed by the solid nature of the substrate and leads to a decrease in growth and enzyme production (5). Lower inoculum level results in a lower number of cells in the production medium. This requires a longer time to grow to an optimum number to utilize the substrate and to form the desired product (40). In the present study, the maximum amylase activity was found at 20 % of inoculum level. After this inoculum concentration no significant increase in enzyme activity has been found (Fig.5). This may be due to the limiting nutrients at higher inoculum size.
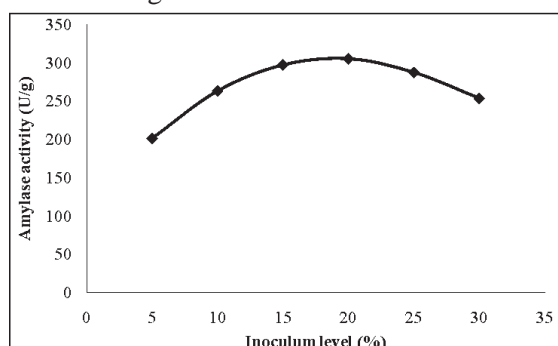
Fig. 5. Effect of inoculum size on á-amylase activity
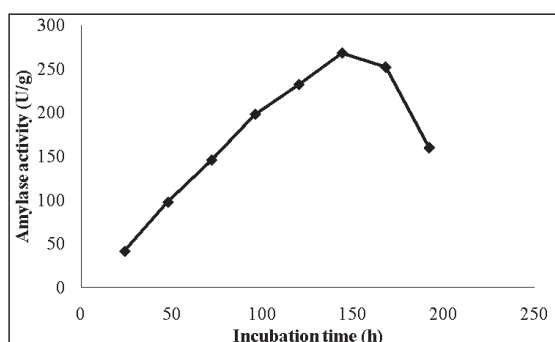
Fig. 6. Effect of incubation time on α-amylase activity

Effect of incubation time on á-amylase activity

Figure.6 shows the variation in amylase activity with incubation time at temperature 50 ^{0}C and pH 6.The trend indicates that the amylase production increases with the increase in incubation time and after 144 h the enzyme production decreases due to substrate inhibition. Thus, the maximum enzyme has been produced at 144 h of incubation time. A similar result has been reported by Ellaiah et al. (37).

Effect of supplementation of carbon sources on á-amylase activity

The influence of four supplementary carbon sources has been studied. These carbon sources are soluble starch, sucrose, maltose, glucose. Among all supplementary carbon sources, the soluble starch has been found to be the best source for maximum amylase production (Fig.7).
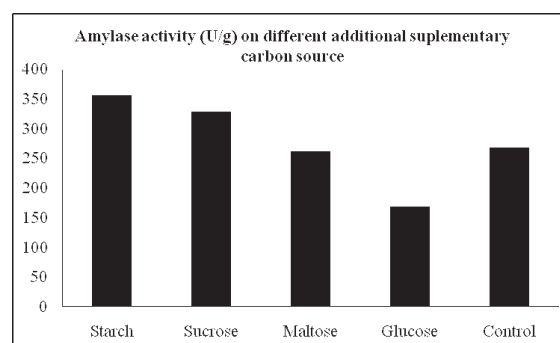
Fig. 7. Effect of supplementary carbon sources on á-amylase activity

The data corresponding to control in figure-7 indicates the production without additional carbon source. In previous studies, the soluble starch was also reported as the best carbon supplement for amylase production in *M. thermophila* D14 (8) and *A. fumigatus* (41,42).

Conclusion

The use of solid state fermentation (SSF) for production of á-amylase using *Humicola lanuginosa* is an economical process and is very simple to apply. All the solid substrates wheat bran, corncob leaf, wheat straw, rye straw can be used for supported biosynthesis of α-amylase using *H. lanuginosa* under SSF. However, these

substrates did not cause enzyme productions as high as wheat bran. Therefore, wheat bran has been superior to other solid substrates for the synthesis of á-amylase from *Humicola lanuginosa* by solid state fermentation. The maximum productivity of á-amylase (356 U/g) was achieved by utilizing wheat bran as the solid substrate with soluble starch as an additional carbon source in 144 h at temperature 50 ^{0}C and moisture content of 90%, pH of 6, and inoculum level of 20 % (w/v). Although the results of these investigations are based on experiments conducted in flasks, they provide valuable information for the production of á-amylase by solid state fermentation process at a larger scale.

Acknowledgement

References

1. Busch, J.E. and Stutzenberger, F.J. (1997). Amyloytic activity of *Thermomonospora fusca*. World J. Microbial. Biotechnol., 13(6): 637-642.

2. Haseltine, C., Rolfsmeier, M. and Blum P. (1996). The glucose effect and regulation of á-amylase synthesis in the hyperthermophilic archaeon *Sulfataricus solfataricus*. J. Bacteriol., 178: 945-950.

3. Fadel-M. (2000). Production of Thermostable amylolytic enzyme by *Aspergillus* higher F-909 under solid state fermentation. Egyptian J.Microbial., 35: 487-505.

4. Lonsane, B.K. and Rames, M.V. (1990). Production of bacterial thermostable á-amylase by solid state fermentation: a potential tool for achieving economy in enzyme production and starch hydrolysis. Adv. Appl. Microbial., 35: 1-56.

5. Baysal, Z., Uyar, F. and Aytekin, C. (2003). Solid-state fermentation for production of á-amylase by a thermotolerant *Bacillus subtillis* from hot-spring water. Process Biochem., 38 (12): 1665-1668.

6. Sodhi, H.K., Sharma, K., Gupta, J.K. and Soni, S.K. (2005). Production of a thermostable á-amylase from *Bacillius sp.* PS-7 by solid-state fermentation and its synergistic use in the hydrolysis of malt starch for alcohol production. Process Biochem., 40 (2): 525-534.

7. Babu, K.R. and Satyanarayana, T. (1995). á-amylase production by thermophilic Bacillus coagulance in solid-state fermentation. Process Biochem., 30 (4): 305-309.

8. Sadhukhan, R.K., Manns, S., Roy, S.K. and Chakraborty, S.L. (1990). Thermostable amyloytic amylase enzyme from a celluolytic fungus *Myceliophthora thermophilla* D14 ATCC 48104. Appl. Microbioal. Biotechnol., 33: 692-696.

9. Robinson, T, Mchnlan, G, Marchant, R. and Nigam, P. (2001). Remediation of dyes in textile effluent: a critical review on current treatment technologies with a proposed alternative. Biosensor. Technol., 77: 247-255.

10. Lealom, F. and Gashe, B.A. (1994). Amylase production by a from gram- positive bacterium isolated from fermenting tef (Eragrostis tef). J. Appl. Bacteriol., 77 (3): 348-352.

11. Young, M.H., Gun, L.D., Hoon, Y.J., Ha, P.Y. and Jae, K.Y. (2001). Rapid and simple purification of a novel extracellular beta-amylase from *Bacillus sp.,* Biotechnology Letters, 23 (17): 1435-1438.

12. Wang, B.D., Chen, D.C. and Kuo, T.T. (2001). Characterization of a *Saccharomyces cerevisiae* mutant with over

secretion phenotype. Appl. Microbiol. Biotechnol., 55 (6): 712-720.

13. Pandey, A., Nigam, P., Soccol, C. R., Soccol, V. T., Singh, D. and Mohan, R. (2000). Advances in microbial amylases. Biotechnol. Appl. Biochem., 31: 135-152.

14. Ramachandran, S., Patel, A.K., Nampoothiri, K.M., Chandran, S., Szakacs, G, Soccol, C.R. and Pandey, A. (2004). á-amylase from a fungal culture grown on oil cakes and its properties. Braz. Arch. Biol. Technol., 47: 309-317.

15. Pandey, A., Soccol, C.R., Nigam, P., Soccol, V.T., Vandenbegh, L. and Mohan, R. (2000). Biotechnological potential of agro-industrial residues II: Cassava bagasse. Bioresour. Technol., 74 (1): 81-87.

16. Hamilton, L.M., Fogarty, W.M. and Kelly, C.T. (1999). Purification and properties of the raw starch degrading alpha amylase of *Bacillus sp.* IMD-434. Biotechnol. Lett., 21 (2): 111-115.

17. Haq, I., Ashraf, H., Ali, S. and Qadeer, M.A. (1997). Submerged fermentation of alpha amylase by *Bacillus licheniformis* GCB-36. Biologia., 43 (2): 39-45.

18. Mc Tigue, M.A., Kelly, C.T., Doyle, E.M. and Fogarty, W.M. (1995). The alkaline amylase of the alkalophilic sp. IMD 370. Enzyme Microbial. Technol., 17: 570-573.

19. Ajayi, A.O. and Fagade, O.E. (2003). Utilization of corn starch as substrate for â-amylase by *Bacillus sp.,* African J. Biomed. Res., 6 (1): 37-42.

20. De, A.S.E.M., Mizuta, K. and Giglio, J.R. (1997). *Pycnoporus sanguineus*: a novel source of á- amylase. Mycol. Res., 101 (2): 188-190.

21. Pacheco-Chavez, R.A., Carvalho, J.C.M., Tavares, L.C., Vessoni-Penna, T.C., Converti, A. and Sato, S. (2004). Production of á- Amylase and Glucoamylase by a new isolate of *Trichoderma* sp. using sorghum starch as a carbon source. Engg, in Life Sciences, 4 (4): 369-372.

22. Hema, A., Trivedi, U.B. and Patel, K.C., (2006). Glucoamylase production by solid state fermentation using rice flake manufacturing waste products as substrate. Bioresour. Technol., 97 (10): 1161-1166.

23. Gangadharan, D., Sivaramakrishnan, S., Madhavan, K. N. and Pandey, A. (2006). Solid Culturing of *Bacillus amyloliquefaciens* for alpha amylase production. Food Technol. Biotechnol. 44 (2): 269–274.

24. Murado, M.A., Gonzalez, M.P., Torrado, A. and Pastrana, L.M. (1997). Amylase production by solid sate culture of *Aspergillus oryzae* on polyurethane foams, some mechanistic approaches from an empirical model. Process Biochem., 32 (1): 35-42.

25. Tsuyoshi, N., Fudou, R., Yamanaka, S., Kozaki, M., Tamang, N., Thapa, S. and Tamang, J.P. (2005). Identification of yeast strains isolated from marcha in Sikkim, a microbial starter for amylolytic fermentation. Int. J. Food Microbiol., 99 (2): 135-146.

26. Oshoma, C.E. and Ikenebomeh, M.J. (2005). Production of *Aspergillus niger* biomass from rice bran. Pakistan J. Nutrit., 4 (1): 32-36.

27. Arasaratnam, V., Mylvaganam, K. and Balasubramaniam, K. (1997). Paddy husk support and rice bran for the production of Glucoamylase by *Aspergillus niger*. Intern. J. Food Sci. Technol., 32 (4): 299-304.

28. Morita, M., Shimamura, H., Ishida, N., Imamura, K., Sakiyama, T. and Nakanishi,

K. (2004). Characterization of á- glucosidase production from recombinant *Aspergillus oryzae* by membrane surface liquid culture in comparison with various cultivation methods. J. Biosci. Bioengg., 98 (3): 200-206,

29. Morita, H. and Fujio, Y. (1999). Polygalacturonase production of *Rhizopus sp.*MKU 18 using a metal ion regulated liquid medium. J. Gen. Appl. Microbiol., 45 (4): 199-201.

30. Selvakumar, P., Ashakumary, L. and Pandey, A. (1996). Microbial synthesis of starch saccharifying enzyme in solid-state fermentation, J. Sci. Ind. Res.*,* 55, 443-449.

31. Adams, P.R. (1981). Amylase production by *Mucor pusillus* and *Humicola lanuginosa* as related to mycelial growth. Biomed. Life Scien.*,* 76 (2): 97-101.

32. Kamra, P. and Satyanarayana, T. (2004). Xylanase production by the thermophilic mold *Humicola lanuginosa* in solid-state fermentation. App. Biochem. Biotechnol., 119: 145-157.

33. Morinaga, T., Kanda, S. and Nori, R. (1986). Lipase production of a new thermophilic fungus, *Humicola lanuginosa* var. catenulate. J. Fermentation Technolo.*,* 64 (5) : 451-453.

34. Miller, G.L. (1959). Use of dinitrosalicylic acid reagent for determination of reducing sugar. Anal. Chem, 31: 426-429.

35. Satyanarayana, T. (1994). Production of bacterial extracellular enzymes by solid-state fermentation, 122-129, In Pandey, A. (ed.) solid-state fermentation, Wiley Eastern Limited, New Delhi.

36. Beckord, L.D., Kneen, E. and Lewis, K.H. (1945). Bacterial amylases production on wheat bran. Ind. Eng. Chem.,Ind. Ed., 37: 692-696.

37. Ellaiah, P., Adinarayana, K., Bhavani, Y., Padmaja, P. and Srinivasulu, B. (2002). Optimization of process parameters for glucoamylase production under solid-state fermentation by a newly isolated *Aspergillus sp.*, Process Biochem.*,* 38 (4): 615-620.

38. Pandey, A. (1990). Improvement in solid state fermentation for glucoamylase production. Biol. Wastes, 34: 11-19.

39. Feniksova, R.V., Tikhomirova, A.S. and Rakhleeva, E.E., (1960). Conditions for forming amylase and proteinase in surface cultures of *Bacillus subtilis*. Microbiologia, 29: 745-748.

40. Kashyap, P., Sabu, A., Pandey, A., Szakas, G. and Soccol, C.R. (2002). Extracellurar L-glutaminase production by *Zygosaccharomyce rouxii* under solid-state fermentation. *Process Biochem.,* 38: 307-312.

41. Goto, C.E., Barbosa, E.P., Kistner, L.C.L., Gandra, R.F., Arrias, V.L. and Peralta, R.M. (1998). Production of amylase by *Aspergillus fumigates*. Revista de Microbiologia, 29: 99-103.

42. Mukherjee, S.K. and Majomdar, S.K. (1993). Fermentative production of á-amylase by *Aspergillus flavus*, Indian J. Exp. Biol., 11: 436-438.

Association of CYP3A5*3 and CYP3A5*6 Polymorphisms with Breast Cancer Risk

Surekha D, Sailaja K, Nageswara Rao D, Padma T,
Raghunadharao D[1] and Vishnupriya S*
Department of Genetics, Osmania University, Hyderabad, India
[1]Department of Medical Oncology, Nizams Institute of Medical Sciences
Hyderabad, India
*For Correspondence - sattivishnupriya@gmail.com

Abstract

CYP3A5 gene is located on chromosome 7q21.1 and is responsible for the metabolism of over 50% of all clinically used drugs. 250 breast cancer and same number of healthy age matched controls were analyzed for the polymorphisms of CYP3A5*3 and CYP3A5*6 by polymerase chain reaction-restriction fragment length polymorphism. The normal wild type allele CYP3A5*1 produces correct transcript and individuals with at least one CYP3A5*1 allele can express CYP3A5 at higher levels. In the present study, the frequency of heterozygotes for CYP3A5*1 (1/3) was significantly increased in breast cancer (53.0%) when compared to controls (41.4%) with corresponding increase in CYP3A5*1 allele frequency. The frequency of 3/3 genotype was increased in postmenopausal (40.0%) patients with high BMI, ER, PR and HER2/neu positive status and in housewife group. There was an increase of 1/3 genotype frequency in patients with positive family history and agricultural laborers (55.6%). In conclusion our results suggested that the CYP3A5*3 polymorphism might influence the breast cancer etiology which mainly depends on the type of exposure. CYP3A5*6 allele was not observed in cases as well as in controls.

Keywords: Polymorphisms; Breast cancer; Receptor status

Introduction

CYP3A enzymes are the most abundantly expressed cytochrome P450 enzymes in liver and are responsible for the metabolism of over 50% of all clinically used drugs (1) Gellner et al (2) had identified a 231-kb region on chromosome 7q21.1 containing 3 CYP3A genes: CYP3A4, CYP3A5 and CYP3A7, as well as 3 pseudogenes and a novel CYP3A gene, which they termed CYP3A43. Jounaidi et al (3), isolated the 5-prime flanking region of CYP3A5 from a genomic clone on chromosome 7. Promoter analysis determined that CYP3A5 uses a CATAA box, rather than a TATA box at positions -23 to -28 and has a basic transcription element from -35 to -50.

Kuehl et al (4) stated that variation in the CYP3A enzymes could influence circulating steroid levels and responses to 50% of oxidatively metabolised drugs. CYP3A activity was the sum activity of the family of CYP3A genes, including CYP3A5, which was polymorphically expressed at high levels in a minority of Caucasians. Only individuals with at least one CYP3A5*1 (wild type) allele express large amounts of CYP3A5. Kuehl et al (4) demonstrated that SNPs in CYP3A5*3 (6986A-G) and CYP3A5*6 (a G-to-A transition in exon 7 resulting in deletion of that exon) cause alternative splicing and protein truncation, resulting in the absence of CYP3A5 from tissues of some people. Because CYP3A5

represents at least 50% of the total hepatic CYP3A content in people polymorphically expressing CYP3A5, it might be the most important genetic contributor to interindividual and interracial differences in CYP3A-dependent drug clearance and in responses to many medicines. There are substantial interindividual differences in CYP3A expression, exceeding 30-fold in some populations like African Americans, Southeast Asians, Pacific Islanders and Southwestern American Indians. The higher prevalence of CYP3A5 expression in non-Caucasians indicated that they are more likely to experience higher clearance of drugs principally inactivated by CYP3A so less likely to experience dose-limiting toxicities, and have different risks of diseases that are associated with the CYP3A5 expressor phenotype. The relatively low levels of metabolic activity of CYP3A5 protein as observed in Korean population suggested that they would be at greater risk for drug toxicity even at conventional doses (5).

Similar frequencies of CYP3A5*3 were observed in the leukemic patients and normal controls. Consequently, the finding suggested that the CYP3A5 polymorphism was not associated with the risk of myeloid leukemia (6). CYP3A5*6 was not found in Asian population.

Materials and Methods

A group of 250 breast cancer patients were selected for the present study. 250 healthy and age matched women without family history of breast cancer or any other cancers were selected to serve as control group. Cases were chosen from Nizam's Institute of Medical Sciences after confirmed diagnosis and controls included healthy volunteers. The diagnosis of breast cancer was established by pathological examination, mammography, Fine needle aspiration (FNAC) and biopsy. Epidemiological history such as age at onset of breast caner, diet, socioeconomic status, occupation, reproductive history, family history and consanguinity was taken through personal interview with breast cancer patients using specific proforma. The patients were screened for receptor status of estrogen, progesterone and HER-2/neu by immunohisto chemical assay. Clinical history such as size of the tumor, presence of auxiliary nodes, extent of metastasis, stage and type of the breast cancer, chemotherapeutic drugs used and prognosis of the disease was collected with the help of oncologist. Informed consent was taken from all patients and controls included in the study. The approval of ethical committee was taken before initiation of the work.

Five milliliters of blood was collected in an EDTA vaccutainer from patients as well as controls. DNA was isolated (7) and used for amplification of CYP3A5*3 and CYP3A5*6 by PCR-RFLP (8). CYP3A5*3 polymorphism

This polymorphism was detected by using modified primers. The polymorphism of the CYP3A5*3 (nt 22893 G) with the mutagenic base C at nt 22889 was introduced as the fourth base at 3' end of the forward primer created the Dde I site after PCR (Fig 1) The 155 bp product was digested into 121 and 34 bp fragments for CYP3A5*1 and 97, 34 & 24 bp fragments for CYP3A5*3 allele. The heterozygote is identified by the presences of 121, 97, 34 & 24 bp fragments. CYP3A5*6 polymorphism

PCR-RFLP was done for identification of CYP3A5*6 polymorphism using specific primers. The amplified product (268 bp) was digested with 1 unit of Dde I enzyme (New England biolabs) at 37^0C for overnight and electrophoresed on 14% PAGE (Fig 2) and noticed DNA fragments of size 120, 103, 25 &20 for CYP3A5*1 and 128, 120 & 20 for CYP3A5*6 allele.

Statistical analysis

The results were analyzed using appropriate statistical tests by SPSS Version 14. Odds ratio was estimated to calculate the relative risk for

each genotype to develop disease. Differences in genotype frequency distribution between disease and control groups was done using 2*2 χ^2 and χ^2 test for heterogeneity.

Results and Discussion

The cytochrome P450 (CYP) catalyzes the metabolism of numerous exogenous and endogenous molecules. CYP3A5 was found to be more efficient in activating aflotoxin B1 to carcinogenic form (9). CYP3A5 was considered as a candidate gene for prostate cancer as the expression was observed in both normal as well as in tumor tissue, whereas CYP3A4 expression was limited to normal prostate tissue. The hypothesis that prostate cancer risk might be associated with CYP3A5 genotype had been strengthened by the report of linkage disequilibrium between CYP3A5 and CYP3A4 alleles (10). The proportion of CYP3A4*1B and CYP3A5*1 alleles was found to be increased in liver, gastric and colorectal cancer patients (11) and these findings were in accordance with other studies from Caucasian population (12).

In the present study, the frequency of heterozygotes for CYP3A5*1 (1/3) was significantly increased in breast cancer (53.0%) when compared to controls (41.4%) with corresponding increase in 3A5*1 allele frequency (Table 1). The study group showed deviation from Hardy-Weinberg equilibrium but not controls ($\div 2=0.58$) indicating selective forces operating in disease group ($\div 2=5.09*$) (Table 1). The frequency of CYP3A5*3 allele was found to be similar in both leukemia (CML, AML) group and controls (7). Nogal et al (13) had reported that

Table 1. CYP3A5*3 polymorphism with respect to breast cancer and epidemiological parameters

Parameters	1/1		1/3		3/3		Allele Frequency	
	n	%	n	%	n	%	1	3
Disease (249)	25	10.0	132	53.0	92	37.0	0.37	0.63
Controls (249)	28	11.2	103	41.4	118	47.4	0.32	0.68
Menopausal Status								
Premenopausal (124)	10	8.1	72	58.1	42	33.9	0.37	0.63
Postmenopausal (125)	15	12.0	60	48.0	50	40.0	0.36	0.64
Familial History								
Familial (74)	2	2.7	32	43.2	40	54.1	0.24	0.76
Non-Familial (176)	2	1.1	70	39.8	104	59.1	0.21	0.79
BMI								
<20 (14)	2	14.3	11	78.6	1	7.1	0.54	0.46
20-26.4 (27)	5	18.5	14	51.6	8	29.6	0.44	0.56
26.4-30 (104)	11	11.0	61	59.0	32	31.0	0.40	0.60
>30 (45)	4	8.9	21	46.7	20	44.5	0.32	0.68
Occupation								
Housewives (173)	2	1.2	66	38.2	105	60.7	0.20	0.80
Agriculture (27)	0	0	15	55.6	12	44.4	0.28	0.72
White-Collar Jobs (43)	2	4.7	17	39.5	24	55.8	0.24	0.76
Others (7)	0	0	4	57.1	3	42.9	0.21	0.79

CYP3A5*3 and CYP3A5*6 Polymorphisms and Breast Cancer

functional polymorphisms, such as CYP3A5*3 could alter individual susceptibility to lung cancer. The results of their study suggested that the carriers of this allele are at lower risk of developing advanced lung caner probably due to decreased activation of procarcinogens present in the tobacco smoke.

The CYP3A5*1 allele represent wild type which has faster kinetics of metabolising various drugs and environment carcinogens. In general, when chemical compounds enter the body, the phase I enzymes will metabolize these compounds into procarcinogens and they are more active than parent compounds. This indicates the possibility that wild type allele with faster kinetics can form more active procarcinogens leading to development of breast cancer. The CYP3A5*3 allele cannot metabolize compounds and results in accumulation of environmental compounds which might also act as carcinogens (2).

The frequency of 3/3 genotype was increased in postmenopausal women (40.0%) with breast cancer. Postmenopausal women tend to have prolonged exposure to carcinogens during lifetime, which might predispose them to develop breast cancer especially with CYP3A5*3 allele as it is inefficient to metabolize the carcinogenic compounds. There was a slight increase of 1/3 genotype in patients with positive family history, which suggest that these genes might play important role in causing germline mutations in major candidate genes leading to familial susceptibility to develop cancer.

Higher frequency of 3/3 genotype was found to be present in patients with obesity. The environmental carcinogens, which enter into body, are generally stored in adipose tissue and may form DNA adducts in individuals who has lower activity of CYP3A5 gene. So the patients with 3/3 genotype as well as elevated BMI carry increased risk to develop breast cancer. When

occupation of breast cancer was considered, the frequency of homozygous (3/3) genotype was increased in patients who are housewives (60.7%) and heterozygous (1/3) genotype was increased in agricultural laborers (55.6%) which suggested that the CYP3A5 dependent risk of developing breast cancer depends on the type of exposure to different environmental compounds as well as drugs used for various medical reasons (Table 1).

The frequency of 3/3 genotype was increased in patients with estrogen and progesterone receptor positive status indicating that individuals with positive hormonal receptor status and 3/3 genotype carry higher risk to develop cancer. Higher frequency of patients with 3/3 genotype were found to be positive HER2/neu status. No significant association was observed when CYP3A5*1 gene with respect to stage of the breast cancer and nodal status of the patients, which indicated that CYP3A5*3 polymorphism might not be a contributing factor in the progression of the disease (Table 2).

In the present study, the CYP3A5*6 allele was not observed in breast cancer cases as well as in controls. Our results are in accordance with other studies on Taiwan and Korean population who did not report the CYP3A5*6 allele (6,7).

In conclusion our results suggested that the CYP3A5*3 polymorphism might influence the breast cancer etiology which mainly depends on the type of exposure.

Table 2. CYP3A5*3 polymorphism with respect to Clinical parameters

Parameters	1/1		1/3		3/3		Allele Frequency	
	n	%	n	%	n	%	1	3
Estrogen receptor								
Positive (90)	7	7.8	45	50	38	42.2	0.33	0.67
Negative (97)	14	14.4	50	51.5	33	34.0	0.40	0.60
Progesterone receptor								
Positive (87)	6	6.9	45	51.7	36	41.4	0.33	0.67
Negative (100)	15	15	50	50	35	3	0.40	0.60
HER2/neu								
Positive (26)	0	0	7	26.9	19	73.1	0.13	0.87
Negative (27)	3	11.1	4	14.8	20	74.1	0.19	0.81
Node Status								
Positive (121)	1	0.8	52	42.6	69	56.6	0.22	0.78
Negative (74)	2	2.7	31	41.3	42	56.0	0.23	0.77
Stage								
I (11)	0	0	7	63.6	4	36.4	0.32	0.68
II (96)	8	8.3	50	52.1	38	40	0.34	0.66
III (72)	7	9.7	41	56.9	24	33.3	0.38	0.62
IV (48)	8	16.7	21	43.8	19	40.0	0.39	0.61

Table 3. Chi Square and Odds Ratios (OR) for CYP3A5*3 polymorphism with respect to Breast cancer, Epidemiological and Clinical parameters

Parameters	Chi Square	P	OR	CI Intervals (1/3 Vs 3/3)
Breast cancer	6.968	0.03*	1.6437	1.1296-2.3918
Menopausal Status	2.783	0.25	1.4286	0.8371-2.438
Familial History	1.182	0.554	1.1886	0.6824-2.0703
BMI	8.715	0.19	-	-
Occupation	6.859	0.334	-	-
Estrogen receptor	2.69	0.26	0.7816	0.4221-1.4474
Progesterone receptor	3.246	0.19	0.875	0.4729-1.619
HER2/neu	3.826	0.148	1.8421	0.4636-7.3197
Node Status	1.061	0.588	1.021	0.5675-1.8369
Stage	5.196	0.52	-	-

*Significant Chi –Square value ($P < 0.05$)

CYP3A5*3 and CYP3A5*6 Polymorphisms and Breast Cancer
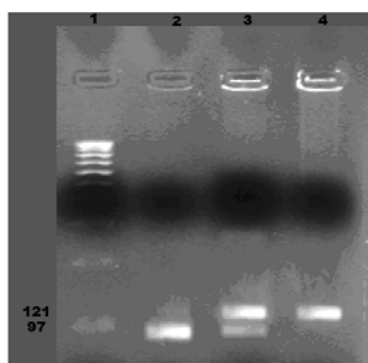
Fig. 1: Electrophoretogram of *Dde* I digested PCR product generated by amplification of genomic DNA using CYP3A5*3 gene specific primers.
Lane # 1: 100 bp DNA ladder
lane # 2: 3/3Genotype
lane # 3,: 1/3Genotype
lane # 4: 1/1Genotype
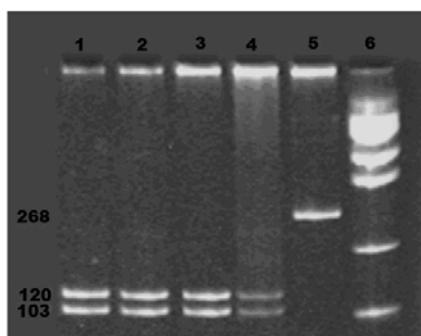
Fig. 2: Electrophoretogram of *Dde* I digested PCR product generated by amplification of genomic DNA using CYP3A5*6 gene specific primers.
Lane # 1-4: 1/1
lane # 5: Uncut band
lane # 6,: 100 bp DNA ladder

Reference

1. Paulussen A., Lavrijsen K., Bohets H., Hendrickx J., Verhasselt P., Luyten W., Konings F. and Armstrong M. (2000). Two linked mutations in transcriptional regulatory elements of the CYP3A5 gene constitute the major genetic determinant of polymorphic activity in humans. Pharmacogenetics, 10: 415-424.

2. Gellner K., Eiselt R., Hustert E., Arnold H., Koch I., Haberl M., Deglmann CJ., Burk O., Buntefuss D., Escher S., Bishop C., Koebe HG., Brinkmann U., Klenk HP., Kleine K., Meyer UA. and Wojnowski L. (2001). Genomic organization of the human CYP3A locus: identification of a new, inducible CYP3A gene. Pharmacogenetics, 11: 111-121.

3. Jounaidi Y., Guzelian PS., Maurel P. and Vilarem MJ. (1994). Sequence of the 5-prime-flanking region of CYP3A5: comparative analysis with CYP3A4 and CYP3A7. *Biochem.* Biophys Res Commun, 205: 1741-1747.

4. Kuehl P., Zhang J., Lin Y., Lamba J., Assem M., Schuetz J., Watkins PB., Daly A., Wrighton SA., Hall SD., Maurel P., Relling M., Brimer C., Yasuda K., Venkataramanan R., Strom S., Thummel K., Boguski MS. and Schuetz E. (2001). Sequence diversity in CYP3A promoters and characterization of the genetic basis of polymorphic CYP3A5 expression. Nature Gene, 27: 383-391.

5. Park SY., Kang YS., Jeong MS., Yoon HK. and Han KO. (2008). Frequencies of CYP3A5 genotypes and haplotypes in a Korean population. Pharmacogenetics, 33 (1): 61-65.

6. Liu TC., Lin SF., Chen TP. and Chang JG. (2001). Polymorphism analysis of CYP3A5 in myeloid leukemia. Oncol Rep, 9(2):327-9.

7. Nuremberg JI. and Lahari D KJr. (1991). A rapid non-enzymatic method for the

preparation of HMW DNA from blood RFLP studies. Nucleic Acid Research, 19: 5444.

8. Ta-Chih Liu., Sheng-Fung Lin., Tyen-Po Chen. and Jan-Goeth Chang. (2002). Polymorphism analysis of CYP3A5 in myeloid leukemia. Oncology reports, 9: 327-329.

9. Gillam EMJ., Guo Z., Ueng YF., Yamazaki H., Cock I., Reilly PE. and Hooper WD. and Guengerich FP. (1995). Expression of cytochrome P450 3A5 in Escherichia coli: effects of 5' modification, purification, spectral charecterization, reconstitution condition and catalytic activities. Arch Biochem Biophys, 318**:** 374-384.

10. Wojnowski L., Hustert E., Klein K., Goldhammer M., Haberl M., Kiechheiner J., Koch L., Klattig J., Zanger U. and Brock moller J.Re. (2002). Modification of clinical presentation of prostrate tumors by a novel genetic variant in CYP2A4.J Natl Cancer Inst, 94:630-631.

11. Gervasini G., Marti E., Ladero M., Pizarro R., Sastre J., Martinez C., Gracia M., Diaz-Rubio M. and Agundez AG. (2007). Genetic variability in CYP3A4 and CYP3A5 in primary liver, gastric and colorectal cancer patients. BMC Cancer, 7: 118.

12. Wilkinson GR. (2004). Genetic variabilityin cytochrome P4503A5 and invivo cytochrome cytochrome P4503A activity: some answers but still questions. Clin Pharmacol Ther, 76:99-103.

13. Nogal A., Coelho A., Araujo A., Azevedo I., Faria A., Soares M., Catarino R. and Medeiros R. (2007) CYP3A5*3 genotypes and advanced non-small cell lung cancer development. Journal of clinical Oncology, 25(18S): 21030.

Transdermal Drug Delivery System for Atomoxetine Hydrochloride – *In vitro* and *Ex vivo* Evaluation

Mamatha T[1], Venkateswara Rao J[1*], Mukkanti K[2] and Ramesh G[3]
[1]Sultan–Ul–Uloom College of Pharmacy, Road No.3, Banjarahills, Hyderabad-500034, (A.P.), India
[2]Centre for Environment, Jawaharlal Nehru Technological University, Kukatpally
Hyderabad-500072 (A.P.), India
[3]Centre for Biopharmaceutics and Pharmacokinetics, University College of Pharmaceutical Sciences
Kakatiya University, Warangal- 506 009 (A.P.), India
*For Correspondence: jvrao1963@yahoo.co.in

Abstract

Monolithic matrix type transdermal drug delivery systems (TDDS) of atomoxetine hydrochloride (A-HCl) were prepared by the film casting on a mercury substrate and characterized by physicochemical characteristics like thickness, weight variation, drug content, flatness, folding endurance and *in vitro* drug release studies, *ex vivo* skin permeation studies. Eight formulations (carrying Eudragit RL100 and Hydroxypropyl methyl cellulose 15 cps in the ratios of 8:2, 6:4, 4:6, 2:8 in formulations A-1, A-2, A-3, A-4 and Eudragit RS 100 and Hydroxypropyl methyl cellulose 15 cps in the same ratios in formulations B-1, B-2, B-3, B-4 respectively) were prepared. All formulations carried 20 mg of drug, A-HCl, 10% w/w of propylene glycol as penetration enhancer, 10% w/w of dibutyl phthalate as plasticizer in ethanol. The formulations exhibited uniform thickness, weight and good uniformity in drug content. The maximum drug release in 24 hrs for A-series formulations was 95.52 % (A-3) and for B-series, it was 89.55 % (B-4). Again formulations A-3 (Kp = 3.53 X 10^{-2} cm h^{-1}) and B-4 (Kp = 3.20 X 10^{-2} cm h^{-1}) exhibited the best skin permeation potential in the respective series. On the basis of *in vitro* drug release and *ex vivo* skin permeation performance, formulation A-3 was found to be better than the other seven formulations. The results of the study show that A-HCl could be administered transdermally through the matrix type TDDS for effective control of attention-deficit/hyperactivity disorder (ADHD) in children, adolescents, and adults.

Keywords: Transdermal, atomoxetine hydrochloride, propylene glycol, Eudragit, HPMC.

Introduction

Delivery of drugs into systemic circulation via skin has generated a lot of interest during the last decade as transdermal drug delivery systems (TDDS) offer many advantages over the conventional dosage forms and oral controlled release delivery systems notably avoidance of hepatic first pass metabolism, decrease in frequency of administration, reduction in gastrointestinal side effects and improves patient compliance (1). Matrix based transdermal formulations have been developed for a number of drugs such as metoprolol (2), nitrendipine (3), ephedrine (4), ketoprofen (5), propranolol (6), labetolol hydrochloride (7) and triprolidine (8).

Atomoxetine hydrochloride (A-HCl) is a potent inhibitor of the presynaptic norepinephrine transporter with minimal affinity for other monoamine transporters or receptors and is the first non-stimulant medication approved for the management of attention-deficit/hyperactivity disorder (ADHD) in children, adolescents, and adults.

A-HCl is well absorbed after oral administration with peak plasma concentrations in 1 to 2 hours after a dose. Bioavailability is about 94% in poor metabolisers but only 63% in extensive metabolisers. Atomoxetine is metabolized primarily via the cytochrome P450 isoenzyme CYP2D6 to the active metabolite 4-hydroxyatomoxetine; a minority of the population are poor metabolisers and experience plasma concentrations about 5 times those in extensive metabolisers. The half life of atomoxetine is about 5.2 hours in extensive and 21.6 in poor metabolisers (9). A-HCl due to its low therapeutic dose (10-100 mg) and substantial biotransformation in liver becomes it ideal candidate for design and development of transdermal therapeutic system. A-HCl in transdermal formulations provides sustained blood levels over a prolonged period, which is required for control of ADHD.

In spite of several advantages offered by transdermal route, only a few drug molecules are administered transdermally because the formidable barrier nature of stratum corneum. Two major approaches to increase transdermal permeation rate include physical techniques (iontophoresis, electroporation, sonophoresis, and microneedles) and use of chemical penetration enhancers (PE) such as solvents, surfactants, fatty acids, and terpenes.

Propylene glycol (PG) is the most commonly used pharmaceutical excipients and have been widely employed to enhance the transdermal flux of many drugs (10-14). Various mechanisms of action have been attributed to the PG for its penetration enhancement capabilities such as increased thermodynamic activity (15), increased skin/vehicle partitioning of the drug (16), and alteration of barrier property by interacting with skin components. PG may reduce barrier property of skin by causing conformational changes either in lipid acryl chains (17) or protein domains (18) or by partial lipid extractions (19).

The objective of this study was to formulate transdermal patches of A-HCl and to evaluate the effect of PG in drug release.

Materials and Methods

Materials

Atomoxetine HCl, Eudragit RL 100 (ERL) (Rohm Pharma GmbH, Germany) and Eudragit RS 100 (ERS) (Rohm Pharma GmbH, Germany) were procured from Aurobindo Pharmaceuticals (Hyderabad, India). Liquid mercury, dibutyl phthalate (DBP), hydroxypropyl methyl cellulose (HPMC), propylene glycol (PG), disodium hydrogen phosphate, potassium dihydrogen phosphate, sodium chloride were purchased from S.D. Fine Chemicals Limited, India. All the materials used were of analytical grade.

Preparation of TDDS

The composition of various formulations is given in Table 1. The polymeric solution (10% w/v) was prepared by dissolving ERL-100/ ERS-100 and HPMC in different ratios, along with A-HCl, DBP and PG in ethanol. The solution was poured into a glass ring placed on the surface of liquid mercury kept in a petridish. The solvent was allowed to evaporate under ambient conditions (temperature 32^0C and relative humidity 45%) for 24 hours. Aluminum foil was used as backing film. The polymer was found to be self sticking due to the presence of eudragit polymers along with plasticizer. The patches were cut to give required area and stored in airtight container till further use.

Physicochemical Evaluation
Thickness and Weight Variation
The thickness of the patches was assessed at 6 different points using screw gauze. For each formulation, three randomly selected patches were used. For weight variation test, 3 films from each batch were weighed individually and the average weight was calculated (Table 2).

Table 1. Composition of Atomoxetine HCl Transdermal Delivery Systems

S.No	Formulation Code	A-HCl (mg)	Polymer	
			ERL100:HPMC	ERS100:HPMC
1	A - 1	20	8 : 2	-
2	A - 2	20	6 : 4	-
3	A - 3	20	4 : 6	-
4	A - 4	20	2 : 8	-
5	B - 1	20	-	8 : 2
6	B - 2	20	-	6 : 4
7	B - 3	20	-	4 : 6
8	B - 4	20	-	2 : 8

Note: All the formulations carried 10 % w/w propylene glycol as penetration enhancer. All the formulations carried 10 % w/w dibutyl phthalate as plasticizer

Table 2. Physicochemical Characteristics of Prepared Films

Formulation	Cumulative % of drug released (Q^r_{24}[a])	Cumulative % of drug permeated (Q^p_{24}[a])	Flux (mcg/cm^2/h)(J[a])	Permeability Coefficient (cm h^{-1}) (Kp X 10^{-2}[a])
A-1	70.70 ± 1.13	61.94 ± 1.27	139.83 ± 0.31	2.60 ± 0.067
A-2	91.6 ± 1.24	75.55 ±1.87	168.23 ± 0.32	3.13 ± 0.054
A-3	95.52 ± 1.76	84.89 ±1.89	183.87 ± 0.24	3.43 ± 0.024
A-4	94.4 ± 1.54	80.97 ± 1.43	177.83 ± 0.27	3.31 ± 0.032
B-1	58.02 ± 1.89	44.40 ± 2.09	101.73 ± 0.25	1.89 ± 0.032
B-2	63.24 ± 1.75	45.70 ±1.74	103.87 ± 0.33	1.93 ± 0.024
B-3	85.07 ± 1.65	62.31 ±1.67	143.07 ± 0.23	2.66 ± 0.035
B-4	89.55 ±1.97	71.45 ±1.04	162.23 ± 0.27	3.02 ± 0.028

[a] Values presented are mean ± S.D (n=3)

Table 3. *In vitro* drug release and skin permeation of the developed TDDS

S.No.	Formulation code	Mean Thickness [a] (μ)	Weight [a] (mg)	Folding Endurance [a]	Drug Content [a] (%)
1	A-1	125 ± 1	19.1 ± 2.67	238 ± 4.55	97.7 ± 0.11
2	A-2	129 ± 2	20.8 ± 1.87	227 ± 3.20	99.4 ± 0.16
3	A-3	138 ± 3	24.4 ± 1.65	249 ± 1.00	97.1 ± 0.19
4	A-4	142 ± 3	24.9 ± 3.76	209 ± 5.34	98.0 ± 0.26
5	B-1	122 ± 1	21.7 ± 1.23	215 ± 2.90	98.3 ± 0.18
6	B-2	127 ± 4	23.1 ± 2.90	218 ± 3.76	97.2 ± 0.11
7	B-3	133 ± 2	19.6 ± 3.78	230 ± 5.00	98.1 ± 0.13
8	B-4	134 ± 3	21.3 ± 2.00	240 ± 3.76	99.2 ± 0.19

[a] Values presented are mean ± S.D (n=3)

Flatness

Longitudinal strips were cut from each film, one from the centre and two from either side. The length of each strip was measured and the variation in the length because of uniformity in flatness was measured by determining percent constriction, considering 0 % constriction equivalent to 100% flatness (20).

$$\% \text{ Constriction} = l_1\text{-}l_2/ l_2 \times 100$$

Where l_1 is initial length of each strip, l_2 is final length of each strip.

Folding Endurance

The folding endurance was measured manually as per the reported method (21). Briefly, a strip of the film (4 x 3 cm) was cut evenly and repeatedly folded at the same place till it broke. The thinner the film more flexible it is.

Drug Content Determination

The patch (1 cm^2) was cut and added to a beaker containing 100 ml of phosphate buffered saline pH 7.4 (PBS). The medium was stirred (500 rpm) with teflon coated magnetic bead for 5 hours. The contents were filtered using whatman filter paper and the filtrate was analysed by U.V.spectrophotometer (Elico, SL-164, Hyderabad, India) at 269 nm for the drug content against the reference solution consisting of placebo films.

In vitro drug release studies

The *in vitro* release was carried out with the dialysis membrane using Franz diffusion cell. The cell consists of two chambers, the donor and the receptor compartment. The donor compartment was open at the top and was exposed to atmosphere. The temperature was maintained at 37 ± 0.5° C and receptor compartment was provided with sampling port. The diffusion medium used was PBS pH 7.4 solution. The drug containing film with a support of backing membrane was kept in the donor compartment and it was separated from the

receptor compartment by dialysis membrane with molecular weight cut off between 12000 to 14000 (Himedia, Mumbai, India). The dialysis membrane was previously soaked for 24 hours in PBS pH 7.4. The donor and receptor compartment hold together using clamp. The receptor compartment with 15 ml of PBS pH 7.4 was maintained at 37 $\pm$ 0.5 °C and stirred with magnetic capsule operated by magnetic stirrer, to prevent the formation of concentrated drug solution layer below the dialysis membrane. Samples of 3 ml, were collected at predetermined time intervals and replaced with fresh buffer. The concentration of drug was determined by UV. spectrophotometrically at 269 nm. Cumulative percentage drug released were calculated (Table 3) and plotted against time (Fig. 1 and 2). The data was fitted to different kinetic models to explain the release mechanism and pattern using the following equations.

$$\text{Zero order equation } Q = Q_o = Kt$$
$$\text{First order equation } Q = Q_o = e^{-Kt}$$
$$\text{Higuchi equation } Q = Kt^{1/2}$$

Where, Q is the cumulative amount of drug released, Q_0 is the initial amount of drug, k is release constant and t is time.
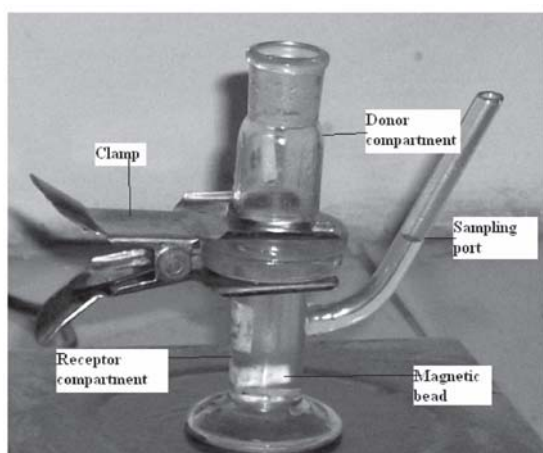

Fig. 1. Schematic diagram of Franz diffusion cell

Preparation of Skin

Prior approval by Institutional Animal Ethics Committee was obtained for conduction of experiment (Ref: IAEC/SUCP/03/2007). The albino rats were obtained from Sainath Animal Agency, Hyderabad, India. Albino rats weighing 170-190 gm were sacrificed using anesthetic ether. The hair of test animals was carefully removed with the help of depilatory and the full thickness skin was removed from the abdominal region. The epidermis was prepared surgically by heat separation technique (22), which involved soaking the entire abdominal skin in water at 60 °C for 45 sec, followed by careful removal of the epidermis. The epidermis was washed with water and used for *ex vivo* permeability studies.

***Ex vivo* Skin Permeation Studies**

The *ex vivo* skin permeation studies were carried out using Franz diffusion cell (Fig. 1) with a diffusional area of 3.73 cm². Rat abdominal skin was mounted between the compartments of the diffusion cell with stratum corneum facing the donor compartment. The receiver phase is 15 ml of PBS pH 7.4, stirred at 300 rpm on a magnetic stirrer. The stratum corneum side of the skin was kept in intimate contact with the film and over that placed a backing membrane. The whole assembly was kept in a water bath at 37 $\pm$ 0.5 °C. Samples (3 ml) were collected at predetermined time intervals and replaced with fresh buffer. The concentration of drug was determined by U.V. spectrophotometrically at 269 nm. Cumulative percentage drug permeated was calculated and plotted against time (Fig. 3 and 4). Flux was determined directly as the slope of the curve between the steady state values of the amount of drug permeated (mg cm⁻²) v/s time (hours) (23) and permeability coefficients were deduced by dividing the flux by the initial drug load (mg cm⁻²) as shown in Table 3.
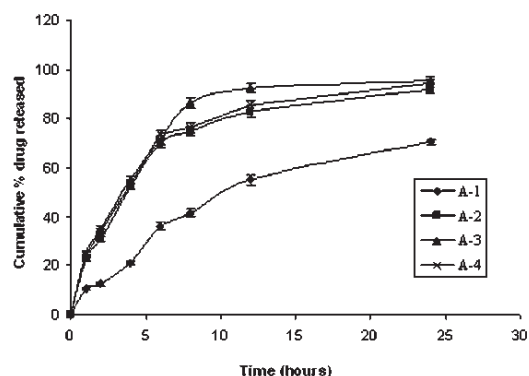
Fig. 2. *In vitro* release profiles of atomoxetine hydrochloride from TDDS using Franz diffusion cell.
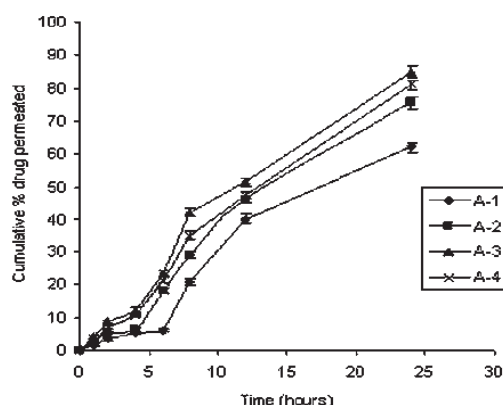
Fig. 4. *Ex vivo* permeation profiles of atomoxetine hydrochloride from TDDS using Franz diffusion cell.
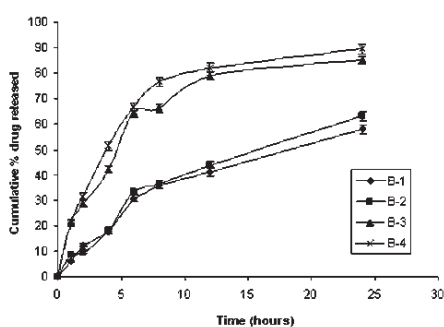
Fig. 3. *In vitro* release profiles of atomoxetine hydrochloride from TDDS using Franz diffusion cell.
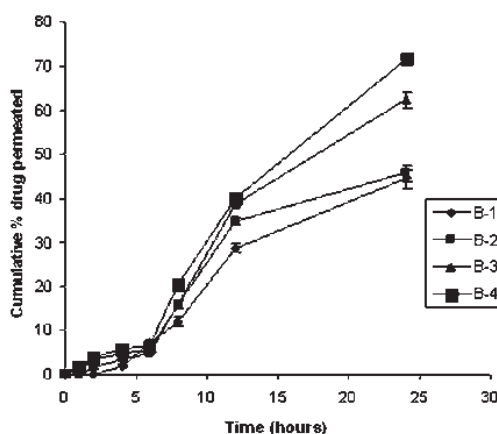
Fig. 5. *Ex vivo* permeation profiles of atomoxetine hydrochloride from TDDS using Franz diffusion cell.

Results and Discussion

The results of physicochemical characteristics are depicted in Table 2. The weights are ranged from 19.1 ± 2.67 to 24.9 ± 3.76 mg and 19.6 ± 3.78 to 23.1 ± 2.90 for formulation A and B series respectively. Thickness ranged from 125 ± 1 ì to 142 ± 3 ì (A series) and 122 ± 1 ì to 134 ± 3 ì (B series). The weights are found to be high with films prepared with higher proportions of HPMC as

one of two polymers. As the proportion of HPMC was decreased, the thickness was also decreased. Good uniformity in drug content was observed and it ranged from 97.1 ± 0.19 mg to 99.4 ± 0.16 mg (A series) and 97.2 ± 0.11 mg to 99.2 ± 0.19 mg (B series).

The results of flatness study showed that none of the formulations had the difference in the strip lengths before and after their cuts, thus

In vitro and *Ex vivo* Evaluation

indicating 100% flatness. It shows that no amount of constriction in the patches and thus they could maintain a smooth surface when applied onto the skin. The folding endurance was found to be between 209 ± 5.34 to 249 ± 1.00 and it was found to be satisfactory.

In vitro release studies

The results of in vitro drug release studies from transdermal patches are depicted in Fig 2 and 3. The cumulative percent of drug release from formulations of A-series was 70.70, 91.60, 95.52 and 94.4 respectively from A-1, A-2, A-3 and A-4 and of B-series was 58.02, 63.24, 85.07 and 89.55 respectively from B-1, B-2, B-3 and B-4 (Table 3). The drug release from different formulations was increased in the following order: A-3>A-4>A-2>B-4>B-3>A-1>B-2>B-1.

Variable release profiles of A-HCl from different experimental patches composed of various blends of ERL/HPMC and ERS/HPMC were observed. The process of drug release in most controlled release devices is governed by diffusion, and the polymer matrix has a strong influence on the diffusivity as the motion of a small molecule is restricted by the three-dimensional network of polymer chains (24).

Release rates were increased when the concentration of HPMC increased in the formulations. This is because as the proportion of this polymer in the matrix increased, there was an increase in the amount of water uptake and hydration of the polymeric matrix and thus more drug was released (25). Formulation A4 showed less drug release compared to formulation A3, this is because the high proportion of HPMC swellable polymer further increases the tartuosity and diffusional path length, resulted in decreased drug release. However the difference was statistically insignifinacant (p>0.05).

The data was fitted to different kinetic models to explain drug release mechanism. The results suggested that the drug release followed Higuchi model as it was evidenced from correlation coefficients and indicating that the drug release was taking place by the process of diffusion. The correlation coefficients (0.87 to 0.97 in A4 and A1; 0.86 to 0.98 in B4 to B1) were greater than the correlation coefficients of zero order (0.67 to 0.65 in A4 and A1; 0.68 to 0.88 in B4 to B1) and first order kinetics (0.56 to 0.71 in A4 to A1, 0.57 to 0.72 in B4 to B1). As the concentration of HPMC increases in the formulations

Ex vivo skin permeation studies

The results of *ex vivo* permeation of A-HCl from patches are shown in Fig 4 and 5. The cumulative percent of drug permeation from formulations of A-series was 61.94, 75.55, 84.89 and 80.97 respectively from A-1, A-2, A-3 and A-4 and of B-series was 44.4, 45.7, 62.31 and 71.45 respectively from B-1, B-2, B-3 and B-4 (Table 3). The order of drug permeation from different formulations was increased in the following order: A-3>A-4>A-2>B-4>B-3>A-1>B-2>B-1

Formulations A-3 (84.89 %) and B-4 (71.45 %) showed maximum drug permeation in their respective series with permeability coefficients of 3.43×10^{-2} cm h^{-1} and 3.02×10^{-2} cm h^{-1} (Table 3). The skin permeation profiles of the test formulations were in conformity to the *in vitro* drug release pattern. The cumulative amount of drug permeated as well as the permeability coefficient (Kp) for TDDS were in the order of A-3>A-4>A-2>A-1 and B-4>B-3>B-2>B-1 for the A and B series, respectively. The results corroborated that higher the drug release from the formulation, higher was the rate and extent of drug permeation. Again the Kp for formulation A-3 was high than B-4 leading to conclusion that ERL 100 and HPMC combination is better than ERS 100 and HPMC as the polymeric precursor for the A-HCl transdermal formulation. As the concentration of hydrophilic polymer was

increased, the amount of drug permeated was increased. This may be a result of the initial rapid dissolution of the hydrophilic polymers when the patch is in contact with the hydrated skin, which results in accumulation of high amounts of drug on the skin surface and thus leads to the saturation of the skin with drug molecules at all times (26). Drug release rate from films containing higher proportions of lipophilic polymer ERL 100 and ERS 100 may be contributed to the relatively hydrophobic nature of polymer which has less affinity for water. This results in decrease in the thermodynamic activity of the drug in the film and decreased drug permeation.

Comparison between the best formulations of respective series (A-3 and B-4) revealed that extent of drug release was higher in case of A-3 (polymers ERL 100 and HPMC) than B-4 (polymers ERS 100 and HPMC). The maximum drug permeation from formulation A-3 might be due to higher permeability characteristics of ERL 100 in comparison to ERS 100. The formulation A-3 showed an increase in permeation than the A-4 may be due to decreased in path length to the movement of drug, as it is inversely proportional to diffusion rate.

Any vehicle can have three models of penetration enhancement that is by changing thermodynamic activity or by improving skin/ vehicle partition coefficient or by altering the barrier property of stratum corneum.

Propylene glycol (PG) action as a sorption promoter has been explained in the literature on the basis of its co solvency effect. Where thermodynamic activity is considered as main driving force and also by carrier mechanism, in which PG partition into the skin and thereby promotes the movement of the drug into and through the skin. PG shows penetration enhancement activity towards 5-fluorouracil (27), progesterone (28) and estradiol (29).

Conclusions

Ex vivo permeation of A-HCl shows that patches of ERL 100:HPMC is suitable compared to ERS 100:HPMC patches. The results of the study show that A-HCl could be administered transdermally through the matrix type TDDS for effective control of ADHD. Further work is recommended in support of its efficacy by long term pharmacokinetics and pharmacodynamic studies on human beings.

References

1. Robinson, J. R and Lee, H.L. (1987) Controlled Drug Delivery Fundamentals and Applications 2nd edi, Marcel Dekker, New York. pp. 524-552.

2. Aquil, M., Sultana, Y. and Ali, A. (2003). Matrix type transdermal drug delivery systems of metoprolol tartrate: In vitro characterization. Acta Pharm, 53: 119-125.

3. Ramesh, G., Vamshi Vishnu, Y., Kishan, V and Madhusudan Rao, Y. (2007). Development of nitrendipine transdermal patches: *in vitro* and *ex vivo* characterization. Current Drug Del, 4: 69-76.

4. Singh, J., Tripathi, K.P. and Sakia, T.R. (1993). Effect of penetration enhancers on the in vitro transport of ephedrine through rat skin and human epidermis from matrix based transdermal formulations. Drug Dev. Ind. Pharm, 19: 1623-1628.

5. Valenta, C. and Almasi-Szabo, I. (1995). In vitro diffusion studies of ketoprofen

transdermal therapeutic system. Drug Dev.Ind. Pharm, 21:1799-1805.

6. Krishna, R. and Pandit, J.K. (1994). Transdermal delivery of propranolol. Drug Dev.Ind. Pharm, 20: 2459-2465.

7. Aqil, M., Zafar, S., Ali, A. and Ahmad, S. (2005). Transdermal drug delivery of labetolol hydrochloride: system development, in vitro; ex vivo and in vivo characterization. Curr Drug Deliv, 2(2): 125-31.

8. Shin, S. and Lee, H. (2002). Enhanced transdermal delivery of triprolidine from the ethylene-vinyl acetate matrix. Eur. J. Pharm. Biopharm, 54: 161-164.

9. Sweetman S.C. (2005). Martindale – The Complete Drug Reference, 34th edi, Pharmaceutical Press, London (U.K), pp. 1055.

10. August, B.J., Blake, J.A. and Hussain, M.A. (1990). Contributions of drug solubilization, partitioning, barrier disruption and solvent permeation to the enhancement of skin permeation of various compounds with fatty acids and amines. Pharm. Res, 7: 712-718.

11. Cho,Y.J. and Choi, H.K. (1998). Enhancement of percutaneous absorption of ketoprofen: effect of vehicles and adhesive matrix. Int. J. Pharm.169: 95-104.

12. Kim, J., Cho, Y.J. and Choi, H. (2000). Effect of vehicles and pressure sensitive adhesives on the permeation of tacrine across hairless mouse skin. Int. J. Pharm. 196: 105-113.

13. Panchangula, R., Salve, P.S., Thomas, N.S., Jain, A.K. and Ramarao, P. (2001). Transdermal delivery of naloxone: effect of water, propylene glycol, ethanol and their binary combinations on permeation through rat skin. Int. J. Pharm, 219: 95-105.

14. Manvi, F.V., Dandagi, P.M., Gada, A. P., Mastiholimath, V.S. and Jagadeesh, T. (2003). Formulation of a transdermal drug delivery system of ketotifen fumarate. Indian J. Pharm. Sci, 65(3): 239-243.

15. Mollgaard, B. and Hoelgaard, A. (1983). Permeation of estradiol through the skin-effect of vehicles. Acta Pharm. Suec, 20: 443-450.

16. Barry, B.W. (1987). Mode of action of penetration enhancers in human skin J. Control. Release, 6: 85-97.

17. Rowe, E.S. (1985). Lipid chain length and temperature dependence of ethanolphosphatidylcholines. Biochem. Biophys. Acta, 813: 321-330.

18. Kurihara-Bergstrom, T., Knutson, K., Denoble, L.J. and Goates, C.Y. (1990). Percutaneous absorption enhancement of an ionic molecule by ethanol-water systems in human skin. Pharm. Res. 7:762-766.

19. Kim, Y.H., Ghanem. A.H., Mahmoud, H.and Higuchi, W.I. (1992). Short chain alkanols as transport enhancers for lipophilic and polar/ionic permeants in hairless mouse skin: Mechanism(s) of action. Int. J. Pharm, 80: 17-31.

20. Arora, P. and Mukherjee, B. (2002). Design, development, physicochemical, and in vitro and in vivo evaluation of transdermal patches containing diclofenac diethylammonium salt. J Pharm Sci, 9: 2076-2089.

21. Devi, K., Saisivum, S., Maria, G.R. and Deepti, P.U.(2003). Design and evaluation of matrix diffusion controlled transdermal patches of verapamil hydrochloride. Drug Dev Ind Pharm, 5: 495-503.

22. Kaidi, Z and Jagdish, S (1999). In vitro per-cutaneous absorption enhancement of pro-

pranolol hydrochloride through porcine epidermis by terpenes/ethanol. J. Control. Rel, 62: 359-366.

23. Bonina, F.P., Carellii, V., Cols, G.D., Montenegro, L. and Nannipieri, E. (1993). Vehicle effects on in vitro skin permeation of and stratum corneum affinity for model drugs caffeine and testosterone. Int. J. Pharm, 100: 41-47.

24. Fan, L.T. and Singh, S.K. (1989). Controlled release: A quantitative treatment. Springer-Verlag, New York. 13-56, 85-129.

25. Vamshi Vishnu, Y., Ramesh, G., Chandrasekhar, K., Bhanoji rao, M.E. and Madhusudan Rao, Y. (2007). Development and *in vitro* evaluation of buccoadhesive carvedilol tablets Acta Pharm, 57:185–197.

26 Rama Rao, P. and Diwan, P.V. (1998). Formulation and in vitro evaluation of polymeric films of diltiazem hydrochloride and indomethacin for transdermal administration. Drug Dev. Ind. Pharm, 24: 327-336.

27. Rigg, P.C. and Barry, B.W. (1990). Shed snake skin and hairless mouse skin as model membranes for human skin during permeation studies. J. Invest. Dermatol, 94: 234-240.

28. Valenta, C. and Wedding, C. (1997). Effects of penetration enhancers on the in vitro percutaneous absorption of progesterone. J. Pharm. Phamacol, 49: 955-959.

29. Goodman, M. and Barry, B.W. (1988). Action of penetration enhancers on human skin as assessed by the permeation of model drugs 5-fluorouracil and estradiol.1. Infinite dose technique. J. Invest. Dermatol, 91: 323-327.

Antibacterial activity of bacterial isolates of soil bacteria collected from Palestine

Thaer Abdelghani* , Bapi Raju Kurad[1] and Ellaiah Poluri [2]
Department of Medical Lab Sciences, Faculty of Allied Medical Sciences
Arab American University, P.O. Box 240, Jenin , Palestine
[1] College of Medicine, University of Illinois at Chicago, Chicago, Illinois, USA
[2] College of Pharmaceutical Sciences, Andhra University, Visakhapatnam -530003
A.P., India
* For correspondence - t.abdelghani@aauj.edu

Abstract

A total of 51 *Actinomycetes* were isolated from different soil samples of Palestine. Preliminary screening by cross-streak method was carried out for all the 51 isolates. After preliminary screening, 17 isolates which showed antimicrobial (antibacterial, antifungal) activity were selected for further study. Among these 17 isolates tested, 5 isolates which were found to be promising were subjected to detailed taxonomic studies. A novel strain of *S. albovinaceus* (isolate 10/2) which was found to be maximum antibiotic producer and which has shown both broad spectrum antibacterial and antifungal activities was isolated and is been selected for further detailed optimization studies.

Key words

Actinomycetes / S. albovinaceus / Antibacterial / Isolation / Soil samples

Introduction

Ever since mankind started suffering from ailments, the quest for finding remedies to treat the diseases started. The science of antibiotics has remained and will remain for many years, one of the most interesting natural sciences, in both theoretical and practical aspects. Microbial natural products still appear as the most promising source of the future antibiotics that society is expecting (1). Antibiotics are produced by bacteria, fungi, actinomycetes, algae, lichens and green plants. Since the isolation of actinomycin in 1940 and streptomycin in 1944 by Waksman (2,3), the *Actinomycetes* have received tremendous attention of the scientists. The genus *Streptomyces* was proposed by Waksman & Henrici (4) for aerobic, spore-forming *Actinomycetes* . Members of *Streptomyces* are a rich source of bioactive compounds, notably antibiotics, enzymes, enzyme inhibitors and pharmacologically active agents (5-10). About 75 % of the known commercially and medically useful antibiotics are produced by *Streptomyces* (11,12). Waksman (13) recognized the natural substrates that are ideal sources for the isolation of *Actinomycetes*. Among these, they are quite commonly found in soil, water and other environments (14). In 1900 Beijerinck (15) established that *Actinonomycetes* occur in great abundance in the soil. The first quantitative enumeration of *Actinomycetes* in the soil was made by Hiltner and Stormer (16).There is now good evidence also for the growth of *Actinomycetes* in marine soils (14, 17, 18). Goodfellow and Haynes (19) reviewed the literature on the isolation of *Actinomycetes* from marine sediments. The screening programs for new *Actinomycetes* and for their antibiotics are

still proceeding at a very rapid pace. There is a need for the development of new antibiotics to overcome the problems associated with the existing antibiotics. To discover the new antibiotics it will be necessary to continue the use of conventional screening programs. Different soils all over the world had been exploited in search of bioactive *Actinomycetes*. So, in order to discover new antibiotics, our approach is to investigate unexplored regions of the world with the aim of isolating bioactive *Actinomycetes* from these regions and from those organisms whose potential was neglected through out the history. The aim of our work is to conduct intensive screening program on different soil samples of Palestine which is an unexplored territory and which is likely to yield purposeful results towards isolation of either new species of *Actinomycetes* and /or new antibiotics. As such, we felt that systematic screening of Palestine soil samples is very much necessary. The selected isolates were identified by morphological, biochemical and other criteria and finally screened for the production of novel antibiotics and pharmacological active compounds. This investigation may yield a few new species of *Actinomycetes* leading to the isolation of new antiviral and antibacterial antibiotics with desired antimicrobial spectrum and therapeutic use. It may lead to the isolation of new species producing already known and clinically useful antibiotics, but with high yield in a simple medium which facilitate the purification procedure and reduce the cost.

Materials and Methods

Several methods have been developed to identify *Streptomyces* species (20 – 27). In a systematic screening program for isolation of bioactive *Actinomycetes*, a total of 8 different soil samples were collected into sterile boiling tubes with a sterile spatula. Care was taken to see that the points of collection had as widely varying characteristics as possible with regard to the organic matter, moisture content, particle size and colour of soil.

Isolation of *Actinomycetes* from soil samples

About 1gm of sample was transferred to a sterile Erlenmeyer (E.M) flask containing 50 ml sterile water. The flasks were shaken on rotary shaker for 30 min for the detachment of the spore chains, if any. The flasks were kept aside for 30 min to settle down the particulate matter. The clear supernatant was diluted with sterile water. These dilutions (10^{-1}-10^{-3}) were used as inocula. One ml of each of these dilutions were pipetted out into the medium, plated into petridishes 6 inches diameters and incubated at 28 °C for 2-3 weeks. For the isolation of *Actinomycetes* from the above mentioned samples, the following media were used : starch casein agar medium (28) , potassium tellurite agar medium, oat meal agar medium , bennets agar medium.

Physiological, biochemical, and cultural (morphological) properties

Media used were those recommended by the International Streptomyces Project (ISP) (22) and by Waksman (29). Mycelium was observed after incubation at 28 °C for 2 weeks. Colors were determined according to Prauser (30). Reduction of nitrate and production of melanoid pigment were determined by the method of ISP (22). Carbohydrate utilization was determined by growth on carbon utilization medium (ISP 9) (22) supplemented with 1 % carbon sources at 28 °C. Liquefaction of gelatin was evaluated by the method of Waksman (29). Hydrolysis of starch and milk were evaluated by using the media of Gordon et al. (31). All cultural characteristics were recorded after 2 weeks.

Cell wall composition (chemotaxonomic analysis): Cells used for chemotaxonomic analysis were obtained after incubation at 28 °C for 3 days in yeast extract-glucose broth (pH 7.0) containing 10 g/l of yeast extract and 10 g/l of glucose. Isomers of diaminopimelic acid in the whole-cell

hydrolysates were determined by thin-layer chromatography according to the method of Hasegawa et al. (32). Whole-cell sugars were analyzed according to the method of Becker et al. (33).

Study of antimicrobial activity: All selected isolates were subcultured onto YEME agar slants and incubated at 28 ℃ for about 7-10 days. The following production medium was used to test antibiotic production: soyabean meal (1.0 %), corn steep liquor (0.5 %), soluble starch (1.0 %), dextrose (0.5 %), calcium carbonate (0.7 %) with pH (7.2) .Antimicrobial activity of the strain was determined by standard cup plate method using Gram (+) and (-) bacteria, fungi and yeast as test organisms. Assay plates were prepared by inoculating 20 ml of Mueller - Hinton agar medium with test organism. Agar-cups (6mm diameter) were filled with 50 ml of mycelia -free culture filtrate in triplicate and the plates were incubated at 37 ℃ for 24 h. Inhibition zone diameters were measured.

Results and Discussion

Isolation of *Actinomycetes* from soil samples: A total of 8 different soil samples were collected and used for screening and isolation of *Actinomycetes*. A brief description of soil samples is given in Table 1.The selected *Actinomycetes* isolates from the above soil samples are shown in Table 2. A total of 51 *Actinomycetes* were isolated from different soil samples of Palestine after discarding isolates with identical characteristics. The criteria chosen were the color of the aerial mycelium, substrate mycelium and the pigmentation. Preliminary screening by cross-streak method was carried out for all the 51 isolates. After preliminary screening, 17 isolates which showed antimicrobial (antibacterial, antifungal) activity were selected for further study. Among these 17 isolates tested, 5 isolates (7/2, 8/7, 10/2, 12/2 and 13/2) which were found to be

promising were subjected to detailed taxonomic studies. The results of the taxonomic studies of the selected isolates are described in the following individual monographs.

Taxonomic studies on isolate no. 10/2

Morphological and cultural characteristics: Aerial mycelium is white in color. Raised growth was observed. Short straight sporophores were also seen. Detail taxonomic studies are shown in Tables 3 and 4**.**

Antimicrobial activity: Antimicrobial spectrum of the culture filtrate was studied and the results are shown in Table 5.

The above information indicates that this isolate belongs to the family Streptomycetaceae. As such the taxonomic characters of our isolate 10/2 is compared with that of the *Streptomyces* species reported in the existing literature and found to be closer to *S. albovinaceus* (34). The comparative data is given in Table 6. Our isolate 10/2 and reference strain have the following similarities: color of aerial mycelium, sporophore morphology, melanin pigmentation and utilization of glucose, fructose, arabinose, mannitol, xylose as a carbon source. Our isolate 10/2 differs from the reference strains in utilization of raffinose , sucrose , inositol and rhamnose . In view of the large number of similarities with the reference strain our isolate 10/2 is considered to be a strain closer to *S. albovinaceus*

Taxonomic studies on isolate no. 7/2

Morphological and cultural characteristics : Aerial mycelium was grey in color. Raised growth was observed. Short spirals with two to three turns' sporophores were also observed. Detail taxonomic studies are shown in Tables 3 and 4.

Antimicrobial activity: Antimicrobial spectrum of the culture filtrate was studied and the results are shown in Table 5.

The above information indicates that this isolate belongs to the family Streptomycetaceae. As such the taxonomic characters of our isolate 7/2 is compared with that of the *Streptomyces* species reported in the existing literature and found to be closer to *S. violaceoruber* (35). The comparative data is given in Table 7. Our isolate 7/2 and reference strain have the following similarities : color of aerial mycelium , sporophore morphology , melanoid pigments on ISP – 6 , utilization of D-glucose , D- fructose , L(+) arabinose , D- mannitol , xylose , inositol , rhamnose , gelatin , liquefaction , coagulation and peptonization of milk. Our isolate 7/2 differs from the reference strains in utilization carbon sources raffinose and sucrose. In view of the large number of similarities with the reference strain our isolate 7/2 is considered to be a strain to be close to *S. violaceoruber.*

Taxonomic studies on isolate no. 12/2

Morphological and cultural characteristics: Aerial mycelium was grey in color. Raised growth was observed. Long and straight sporophores were seen. Detail taxonomic studies are shown in Tables 3 and 4.

Antimicrobial activity: Antimicrobial spectrum of the culture filtrate was studied and the results are shown in Table 5.

The above information indicates that this isolate belongs to the family Streptomy cetaceae. As such the taxonomic characters of our isolate 12/2 is compared with that of the *Streptomyces* species reported in the existing literature and found to be closer to *S. tanashiensis* (20, 36 – 38). The comparative data is given in Table 8. Our isolate 12/2 and reference strain have the following similarities: color of aerial mycelium, sporophore morphology, utilization of glucose, arabinose , xylose , and rhamnose. Our isolate 12/2 differs from the reference strains in melanoid pigmentation on ISP – 6, utilization of fructose, mannitol , raffinose , sucrose , and inositol. In

view of the large number of similarities with the reference strain our isolate 12/2 is considered to be a strain to *S. tanashiensis*

Taxonomic studies on isolate no. 13/2

Morphological and cultural characteristics: Aerial mycelium was whitish grey in color. Raised growth was observed. Long and straight sporophores were observed. Detail taxonomic studies are shown in Tables 3 and 4.

Antimicrobial activity: Antimicrobial spectrum of the culture filtrate was studied and the results are shown in Table 5.

The above information indicates that this isolate belongs to the family Streptomycetaceae. As such the taxonomic characters of our isolate 13/2 is compared with that of the *Streptomyces* species reported in the existing literature and found to be closer to *S. setonii* (13,20, 36, 39) . The comparative data is given in Table 9. Our isolate 13/2 and reference strain have the following similarities: color of aerial mycelium, sporophore morphology, melanoid pigments on ISP-1 and ISP-7, utilization of glucose, fructose, arabinose , mannitol , xylose , starch hydrolysis , gelatin liquefaction, coagulation and peptonization of milk and nitrate reduction. Our isolate 13/2 differs from the reference strains in melanoid pigments on ISP-6, utilization of raffinose , sucrose , inositol , and rhamnose. In view of the large number of similarities with the reference strain our isolate 13/2 is considered to be a strain to *S. setonii*

Taxonomic studies on isolate no. 8/7

Morphological and cultural characteristics: Aerial mycelium was light grey in color. Growth was not raised. Sporophore was short with very short branches. Detail taxonomic studies are shown in Tables 3 and 4.

Antimicrobial activity: Antimicrobial spectrum of the culture filtrate was studied and the results are shown in Table 5.

The above information indicates that this isolate belongs to the family Streptomycetaceae. As such the taxonomic characters of our isolate 8/7 is compared with that of the *Streptomyces* species reported in the existing literature and found to be closer to *S. longisporus* (20 , 36, 37). The comparative data is given in Table 10.Our isolate 8/7 and reference strain have the following similarities : color of aerial mycelium , morphological section, utilization of D-glucose , D-fructose , L(+) arabinose , D-mannitol , D-xylose , raffinose , and sucrose. Our isolate 8/7 differs from the reference strains in utilization of carbon sources like inositol and rhamnose. In view of large number of similarities with the reference strain our isolate 8/7 is considered to be a strain close to *S. longisporus*

Conclusion

In the present study effort was mainly directed towards the isolation of *Actinomycetes* from soil samples of Palestine, an unexplored territory for study of their morphological, cultural, physiological, biochemical and antimicrobial activities.

Detailed taxanomical studies were carried out and it was concluded that 5 different new strains were isolated of which one isolate (10/2) was found to be excellent antibacterial producer. Isolate no (10/2) *S. albovinaceus* which was found to be maximum antibiotic producer and which has shown both broad spectrum antibacterial and antifungal activities is been selected for detailed optimization studies. Further works on isolate no (10/2) like optimization studies, studies on anticancer activity and purification of the active principle which are under progress. Toxicology and commercial viability study will be submitted in a separate article.

References

1. Fernando Pela´ ez (2006). The historical delivery of antibiotics from microbial natural products—Can history repeat?. Biochemical Pharmacology, 71: 981- 990.

2. Waksman, S.A. and Woodruff, H.B. (1940). Bacteriostatic and bactericidal substances produced by a soil *actinomyces*. Proceeding of the Society for Experimental Biology and Medicine, 45: 609 - 614.

3. Schatz, A., Bugie, E. and Waksman, S.A. (1944). Streptomycin, a substance exhibiting antibiotic activity against gram-positive and gram-negative bacteria. Proceeding of Society for Experimental Biology and Medicine, 55: 66 - 69.

4. Waksman, S.A. and Henrici, A. (1943). The nomenclature and classification of the *actinomycetes* . J Bacteriol.*,* 46: 337 - 341.

5. Be´rdy, J. (1995). Are *actinomycetes* exhausted as a source of secondary metabolites? Biotechnologia, 7-8: 13 - 34.

6. Ping, X., Wen-Jun, L., Wen-long, W., Dong, W., Li-Hua, X. and Cheng-Lin, J. (2004).Streptomyces hebeiensis sp. nov. International Journal of Systematic and Evolutionary Microbiology, 54: 727–731.

7. Kazuki, Y., Hiroaki, O., Hiro-omi, O., Kuniaki, H., Fumie, S., Hideaki, T., Shohei, S., Teruhiko, B. and Kenji, U. (2005). Desferrioxamine E produced by Streptomyces griseus stimulates growth and development of Streptomyces tanashiensis, Microbiology, 151: 2899–2905.

8. Goodfellow, M., Williams, S.T. and Mordarski, M. (1988). Introduction to and importance of actinomycetes, pp. 1-5. In: Goodfellow, M., Williams, S.T. and Mordarski, M. (Eds), Actinomycetes in biotechnology. Academic Press, New York.

9. Sanglier, J.J., Hagg, H., Huck, T.A. and Fehr, T. (1993 a). Novel bioactive

compounds from *actinomycetes*: a short review (1982 - 1992). Res Microbiol., 144**: 633 – 642.

10. Sanglier, J.J., Wellington, E.M., Behal, V., Fiedler, H.P., Ellouz, G.R., Finance, C., Hacene, M., Kamoun, A., Kelly, C., Mercer, D.K. , et al. (1993 b). Novel bioactive compounds from *actinomycetes*. Res Microbiol., 144: 661 – 663.

11. Sujatha, P., Bapi Raju, K.V.V.S.N. and Ramana, T. (2005).Studies on a new marine *Streptomycete* BT-408 producing polyketide antibiotic SBR - 22 effective against methicillin resistant *Staphylococcus aureus* Microbiological Research, 160:119-126**.**

12. Eriko, T. (2002). ã -Butyrolactones: Streptomyces signalling molecules regulating antibiotic production and differentiation. Current Opinion in Microbiology, 9:287–294.

13. Waksman, S.A.(Eds), (1959). The Actinomycetes. Isolation, identification, cultivation and preservation, pp.17-28. Vol I, Williams & Wilkins Company Baltimore, USA.

14. Nevine, B.G., Soraya, A.S., Zeinab, M.E. and Gehan, A.A. (2000). Isolation and enumeration of marine *actinomycetes* from seawater and sediments in Alexandria. J Gen Appl Microbiol., 46: 105 - 111.

15. Beijerinck, M.W.(1900). Ueber Chinonbildung durch *Streptothrix chromogena* und In *Proceeding of the National Academy of the United States of America*: 25ᵗʰ November, Volume 100. Suppl 2, pp.14555 - 14561

18. Tracy, J.M., Paul, R.J., Christopher, A.K. and William, F. (2002). Widespread and Persistent Populations of a Major New Marine *Actinomycete* Taxon in Ocean Sediments. Applied and Environmental Microbiology, 68 (10): 5005 – 5011

19. Goodfellow, M. and Haynes, J.A. (1984). *Actinomycetes* in marine sediments, pp. 453. In: Ortiz, L.O., Bojalil, L.F. and Yakoleff, V. (Eds), Biological, Biochemical and Biomedical Aspects of Actinomycetes, Academic Press Inc, Orlando, Fla,

20. Buchanan, R.E. and Gibbons, N.E. (Ed.) (1974). In Bergey's Manual of Determinative Bacteriology, 8ᵗʰ edition, The Williams and Wilkins Company, Baltimore, USA.

21. Pridham, T.G. and Gottlieb, D. (1948). The utilization of carbon compounds by some Actinomycetales as an aid for species determination. J Bacteriol., 56: 107 -114.

22. Shirling, E.B. and Gottlieb, D. (1966).Methods for characterization of Streptomyces species. Int J Syst Bacteriol., 16: 313 - 340.

23. Nonomura, H. (1974). Key for classification and identification of 458 species of the *Streptomycetes* included in ISP. J Ferment Technol., 52: 78 - 92.

24. Shirling, E.B. and Gottlieb, D. (1972). Cooperative description of type strains of Streptomyces. V. Additional descriptions. Int J Syst Bacteriol., 22: 265 - 394.

25. Kuster, E. and Williams, S. (1964). Selection of media for isolation of *streptomycetes*. Nature, 202: 928 - 929.

26. Lechevalier, M.P. and Lechevalier, H.A. (1970). Chemical composition as a criterion in the classification of aerobic *actinomycetes*. Int J Syst Bacteriol., 20: 435 - 443.

27. Wipat, A., Wellington, E. and Saunders, V. (1991). *Streptomyces* marker plasmids for

monitoring survival and spread of *Streptomycetes* in soil. Appl Environ Microbiol., 57: 3322 - 3330.

28. Pisano, M.A., Sommer, M.J. and Bracaccio, L. (1989). Isolation of bioactive actinomycetes from marine sediments using Rifampicin. Applied Microbiology Biotechnology, 31: 609 - 612.

29. Waksman, S.A. (1961). The actinomycetes, pp.327. Classification, Identification and Description of Genera and Species. Volume 2, Williams and Wilkins Company, Baltimore, USA.

30. Prauser, H. (1964). Aptness and application of colour for exact description of colours of *streptomyces*. Zeitsch Allgem Mikrobiol., 4: 95 – 98.

31. Gordon, R.E., Barnett, D.A., Handerhan, J.E. and Pang, C.H. (1974). Nocardia coeliaca, Nocardia autotrophica and the Nocardia strain. Int J Syst Bacteriol., 24: 54-63.

32. Hasegawa, T., Takizawa, M. and Takida, S. (1983). A rapid analysis for chemical grouping of aerobic actinomycetes. J Gen Appl Microbiol., 29: 319 - 322.

33. Becker, B., Lechevalier, M.P. and Lechevalier, H.A. (1965). Chemical composition of cell-wall preparation from strains of various form-genera of aerobic *actinomycetes*. Appl Microbiol., 13: 236 - 243.

34. Shirling, E.B. and Gottlieb, D. (1968). Cooperative description of type cultures of *Streptomyces* II.Species descriptions from first study. Int J Syst Bacteriol.,18:69-189

35. Waksman, S.A. and Curtis, R.E. (1916).The *Actinomyces* of the soil. Soil Sci., 1: 99- 134.

36. Williams, S.T., Goodfellow, M. and Alderson, G. (1989). Genus *Streptomyces,* pp. 2452 - 2492. In: Williams, S.T., Sharp, M.E. and Holt, J.G.(Eds), Bergey's Manual of Systematic Bacteriology, Vol 4, The Williams and Wilkins Co, Baltimore.

37. Shirling, E.B. and Gottlieb, D. (1968). Cooperative description of type cultures of *Streptomyces* III. Additional species descriptions from first and second studies. Int J Syst Bacteriol., 18: 279 - 392.

38. Hata, T., Yokoyama, Y., Higuchi, T., Sano, Y., and Sawachika, K., 1951. Physiology of Actinomycetes . J Antibiot., Set A 4: 31 - 39.

39. Shirling, E.B. and Gottlieb, D. (1969). Cooperative description of type cultures of Streptomyces. IV. Species descriptions from the second, third and fourth studies. Int J Syst Bacteriol., 19: 391 - 512.

Formulation of Controlled Release Levodopa and Carbidopa Matrix Tablets: Influence of Some Hydrophilic Polymers on the Release Rate and *In Vitro* Evaluation

Jagan Mohan. S[1,2], Kishan V[1], Madhusudan Rao Y[1] and Chalapathi Rao N.V[2]

[1]University College of Pharmaceutical Sciences, Kakatiya University, Warangal, Andhra Pradesh
[2] Danmed Pharma (Group of Medopharma), Phase III, Charlapally, Hyderabad, Andhra Pradesh
For Correspondence : yamsani123@gmail.com

Abstract

This work aims at investigating different types and levels of hydrophilic matrix agents, including Hydroxy Propyl Methyl Cellulose K15M (HPMC K15M), Hydroxy Propyl Methyl Cellulose K4M (HPMC K4M) and Carbopol 974P, in an attempt to formulate controlled release matrix tablets containing 200 mg of levodopa (LD) and 50 mg of carbidopa (CD). The tablets were prepared by direct compression. Majority of the matrix tablets that contained less than 7.5 % of the polymer disintegrated prematurely. Polymers, HPMC K15M and Carbopol 974P produced the desired drug release at 10 % concentration whereas HPMC K4M at 20 % concentration of the tablet weight. The prepared matrix tablets were evaluated for weight variation, hardness, friability, drug content and in vitro drug release studies. From the *in vitro* release studies of the prepared formulations, one formula was optimized from each polymer. HPMC K15M and Carbopol 974P based tablet formulations showed high release retarding efficiency. Matrix tablets produced with Carbopol 974P showed sticking and weight variation problems. All the formulations showed linear release profiles (r^2=0.96) and sustained the release of levodopa and carbidopa over 8–12 h. The release profiles of levodopa and carbidopa from the selected formulations are close to zero order and follow diffusion dependent release. The prepared matrix tablets produced from the optimized formulations were compared with standard commercial tablets (SYNDOPA). The similarity factor (*f2* value*)* was calculated for all these formulations and found to be above 50. Irrespective of the polymer type and its concentration, the prepared hydrophilic matrix tablets showed non-Fickian (anomalous) release, coupled diffusion and polymer matrix relaxation as the values of release exponent (n) are in between 0.5 and 0.89. Finally it was clear that it is possible to design a formulation with any of the above three polymers giving the desired drug release profile suggesting that HPMC K15M and HPMC K4M are good candidates for preparing controlled release matrix tablets of levodopa and carbidopa.

Keywords: levodopa, carbidopa, HPMC K15M, HPMC K4M, Carbopol 974P, controlled release tablets

1. Introduction

A typical controlled release system is designed to provide constant or nearly constant

drug levels in plasma with reduced dose, frequency of administration and fluctuations in plasma concentrations via slow release over an extended period of time (1). A matrix device consists of drug dispersed homogenously throughout a polymer matrix. Two major types of materials are used in the preparation of matrix devices (2), which include hydrophobic carriers like glyceryl tristearate, fatty alcohols, fatty acids, waxes; carnaubawax, methylmetha crylate, polyvinyl chloride, polyethylene, ethylcellulose and hydrophilic polymers like, sodium carboxymethylcellulose, hydroxypropy lmethylcellulose, sodium alginate, xanthan gum, polyethylene oxide and carbopols.

Matrix systems offer several advantages relative to other extended release dosage forms like easy to manufacture, versatile, effective, low cost and can be made to release high molecular weight compounds (3). Since the drug is dispersed in the matrix system, accidental leakage of the total drug component is less likely to occur, although occasionally, cracking of the matrix material can cause unwanted release.

Levodopa and Carbidopa are used to treat Parkinson's disease (4). Parkinson's disease is believed to be related to low levels of a chemical called dopamine in the brain. Levodopa is turned into dopamine in the body. If levodopa alone is administered, readily undergoes peripheral decarboxylation by DOPA decarboxylase, as a result it loses its lipophilicity and can not cross the blood brain barrier (5). If it is administered in combination with Carbidopa, Carbidopa prevents the peripheral decarboxylation of levodopa so it retains its lipophilicity.

The objective of investigation is to develop levodopa and carbidopa using hydrophilic matrices, HPMC K15M, HPMC K4M and Carbopol 974P. The developed formulations were evaluated for weight variation, hardness, friability and in vitro release studies.

2. Experimental
2.1. Materials

Levodopa and Carbidopa were obtained from Venkar labs, Hyderabad. Polymers HPMC K4M and HPMC K15M were obtained from Colorcon limited, U.K. Carbopol 974P was obtained from IPS chemical company, Mumbai. All other chemicals were of analytical grade and were used as such.

2.2. Methods
2.2.1. Drug excipient compatibility

The simple physical mixtures of Levodopa and Carbidopa drugs with all the polymers and other excipients used in the formulations were taken in glass vials and observed every week to make sure that there is no drug-excipient interaction.

2.2.2. Micromeritics

Static angle of repose, compressibility index, Hausner ratio, poured (or fluff) bulk and tapped bulk densities were determined according to the fixed funnel and freestanding cone method reported by Raghuram et al.(6).

2.2.3. Preparation of tablets:

Formulations DK15:1-4, DK: 1-5, DC: 1-4 were prepared using HPMC K15M, HPMC K4M and Carbopol 974P respectively by direct compression (7, 8). Microcrystalline cellulose was used as the filler. Magnesium stearate, talc and aerosil were used as lubricant and glidant respectively. All the ingredients were weighed and sifted through 40 mesh except the brilliant

blue colour which is passed through 100 mesh. Then all the ingredients were mixed in a poly bag for 10 min. Now the blend is compressed into tablets with 12mm flat circular shaped punches. The composition of the tablets prepared under various trials with HPMC K4M, HPMC K15M and Carbopol 974P were given in the table 1.

Formulated tablets weighed 400 mg and measured 1.20 cm in diameter. All the formulation ingredients, except the lubricant and glidant, were mixed in a plastic container and shaken by hand for about 10–15 min. The lubricant and glidant were added to the powder mixture and mixed for another 2–3 min by hand. The tablets were compressed on a rotary tablet machine (Cadmech) fitted with flat faced 1.20 cm punch and die sets and compressed.

2.2.4. Dissolution studies

All the tablets prepared were subjected to dissolution studies using Labindia Dissolution test apparatus (Modified USP type II) equipped with an auto sampler and fraction collector for collection and replenishment of samples and dissolution medium respectively. Dissolution medium used is pH 4.0 acetate buffer. Temperature and rpm are $37 \pm 0.5\,°$ C and 50 respectively. Samples were taken at intervals 1, 2, 4, 6 and 12 hrs and analysed for levodopa and carbidopa by HPLC at 280nm.

2.2.5. Chromatographic apparatus and conditions

Chromatographic separation of levodopa and carbidopa was performed on a Shimadzu HPLC System (Japan) equipped with UV-Visible detector using C8 column (Phenomenex 150 x 4.6mmm I.D., 5μ particle size). The mobile phase used was phosphate buffer pH 3.4. Standard solution and dissolution samples were analyzed at 280 nm using a UV detector. The mobile phase was pumped at a flow rate of 1.0 ml/min with an injector valve fitted to a 20 μl volume sample loop.

2.2.6. Release Kinetics (9).

Different kinetic equations (zero-order, first-order, and Higuchi's equation) were applied to interpret the release rate of the drug from matrix systems. The best fit with higher correlation ($r^2 > 0.98$) was found with Higuchi's equation for all the formulations. Two factors, however, diminish the applicability of Higuchi's equation to matrix systems. This model fails to allow for the influence of swelling of the matrix (upon hydration) and gradual erosion of the matrix.

Therefore, the dissolution data were also fitted according to the well-known exponential Korsmeyer-Peppas equation (10), which is often used to describe drug release behaviour from polymeric systems:

$$M_t / M_8 = kt^n$$

M_t / M_8 is the fraction of drug release at time t, and k is the kinetic constant; n is the release exponent (indicating the general operating release mechanism). n value between 0.43 and 0.5 indicates Fickian (case I) diffusion-mediated release. Non-Fickian (anomalous) release, coupled diffusion, and polymer matrix relaxation occurs if $0.5 < n < 0.89$, purely matrix relaxation or erosion-mediated release occurs for n = 1 (zero-order kinetics), and super case II type of release occurs for $n > 0.89$ (11).

2.2.7. The optimized formulations in triplicate were prepared and kept for stability studies at 2-8ºC, 25 ± 2^{0}C/$60\pm5\%$ RH, 40 ± 2^{0}C/$75\pm5\%$ RH and in photostability chambers. The drug content in the tablets was determined after 30 and 60 days.

3. Results and discussion

3.1. Drug excipient interaction study

The results of drug excipient interaction study clearly indicated that there is no drug excipient interaction at 25°C but at 40°C after 3 weeks levodopa developed slight brown colour in all the vials where it is present. So levodopa is found to be unstable at 40°C if it is kept for prolonged period. Therefore it is better to store the formulations containing levodopa at a temperature of about 25°C.

3.2. Micromeritics

The various micromeritic properties like Bulk Density, Tapped Density, Compressibility index (%), Angle of repose and Hausner Ratio were determined for both the drugs and are given in the table 2. The compressibility index, Hausner ratio and angle of repose indicated poor flow characteristics. So it was improved by inclusion of suitable amounts of lubricants and glidants.

3.3. Weight variation, hardness and friability

The prepared tablets were subjected to hardness, friability, weight variation, drug content and dissolution and the results are given in the table 3 and all these results were found to be in the permissible limits.

3.4. Dissolution studies

The release profiles of both the levodopa and carbidopa in all the formulations are very close to each other. The drugs were releasing for 12 hrs and follow near zero order release. The drug release rate from HPMC K15M, HPMC K4M and Carbopol 974P based matrix tablets decreased with the increase in the polymer level. This effect might be ascribed to an increase in the extent of gel formation in the diffusion layer (12).

The results of *in vitro* release from HPMC K15M matrix tablets were shown in figures 1 a-b. All the formulations except DK15-4 release less than 70% of drug with in12 hrs due to higher concentration of polymer. The formulation DK15-4 released more than 95% of the drug in 12 hrs. However at various time intervals the cumulative % drug release is very close to zero order. Hence the formulation DK15-4 was selected as optimized formulation.

The results of *in vitro* release from HPMC K4M matrix tablets were shown in figures 2 a-b. Formulations DK4-1 and DK4-2 released less than 85% of drug with in12 hrs due to higher concentration of polymer. The formulations DK4-4 and DK4-5 released more than 95% of the drug within 8 hrs due to lower concentration of polymer. The formulation DK4-3 exhibited a release profile close to first order with a drug release more than 95% within 12 hrs. Hence this DK4-3 was considered as the optimized formulation. According to figures 2a-b, HPMC K4M-based matrices exhibited significantly lower drug release-retarding efficiency than the HPMC K15M and Carbopol 974P. These results might be attributed to the relatively low swellability and rapid dilution and erosion of the diffusion gel layer (13).

The results of *in vitro* release from Carbopol 974P matrix tablets were shown in figures 3 a-b. All the formulations except DC-4 released less than 75% of drug within12 hrs due to higher concentration of polymer. The formulation DC-4 released more than 95% of the drug within 12 hrs. The formulation DC-4 showed a cumulative % drug release close to zero order. Hence the DC-4 formula was found to be optimized.

3.5. Determination of *in vitro* release of drug from marketed formulation.

Marketed LDCD CR formulations (SYNDOPA 200+50) are subjected to dissolution studies using Labindia dissolution test apparatus and cumulative % drug release was depicted in the figures 4 a-b. Because of the nature of measurement, f1 was described as difference factor, and f2 as similarity factor. A f2 value of 50 or greater (50-100) ensures sameness or equivalence of the two curves and, thus, the performance of the two products. *f1 & f2* values were calculated for all the optimized formulations and are given in the table 4.

3.6. Release kinetics

The values of release exponent (n) and correlation coefficients (R^2) of all the optimized formulations are given in the table 5. Upon comparison of correlation co-efficient values (R^2) of all the optimized formulations, it was indicated that the release profiles of Levodopa and Carbidopa are close to zero order in the case of HPMC K15M and Carbopol 974P where as first order in case of HPMC K4M. Irrespective of the polymer type and its concentration, the prepared hydrophilic matrix tablets showed non-Fickian (anomalous) release, coupled diffusion and polymer matrix relaxation as the values of release exponent (n) are in between 0.5 and 0.89.

3.7. Stability studies

The drug content remained same in the formulations stored at 2-8°C, 25 °C/60 RH but small difference in levodopa level was found in the formulations stored at 40°C/75 RH. Apart from this a small difference in carbidopa level was also found in the formulations stored in photostability chambers. These results might be attributed to the temperature sensitivity of the levodopa and photosensitivity of the carbidopa.

4. Conclusions:

The drug release from all matrix tablets showed a polymer concentration dependent retardation effect and a non-Fickian (anomalous) release. Though the dissolution profiles of all the optimized formulations were close to the zero order, DC-4 was not considered to be advantageous as the Carbopol 974 used in this formulation posed sticking and weight variation problems as it picks up water very quickly. DK15-4 and DK4-3 were found to be advantageous due to their method of formulation i.e. direct compression which was very easy, feasible, fast and economical. No significant difference in the drug content between initial and the formulations stored at 25 ° C but a small difference was found between initial and formulations stored at 40° C and in photostability chambers. Therefore it is recommended that these formulations should be stored at 25 ° C and protected from light.

References

1. Reza, M.S., Abdul Quadir, M., and Haider, S.S. (2003) Comparative evaluation of plastic, hydrophobic and hydrophilic polymers as matrices for controlled-release drug delivery. J Pharm Pharm Sci.6: 282Y291.

2. Bala Ramesh Chary, R., and Madhusudan Rao, Y. (2000) "Formulation and evaluation of methocel K15M bioadhesive matrix tablets." Drug Development and Industrial Pharmacy, 26(8).

3. Krishna Veni, Jayasagar, G. and Madhusudan Rao, Y. (2001) "Formulation

and evaluation of diclofenac sodium, using hydrophilic matrices." Drug Development and Industrial Pharmacy, 27(8): 161-168.

4. Chase, T.N., Juncos, J., Serrati, C., Fabbrini. G., and Bruno, G. (1987) Fluctuation in response to chronic Levodopa therapy: pathogenetic and therapeutic considerations. Adv Neurol, 45: 477-480.

5. Stocchi , F., Vacca, L., Ruggieri, S., Olanow, C.W. (2005) Intermittent vs continuous Levodopa administration in patients with advanced Parkinson disease: a clinical and pharmacokinetic study. Arch Neurol. 62: 905-910.

6. Raghuram, R.K., Srinivas, M., and Srinivas, R. (2003) Once-daily sustained-release matrix tablets of nicorandil: formulation and in vitro evaluation.AAPS PharmSciTech [serial online]. 4:E61.

7. Block, G., Liss, C., Reines, S., Irr, J., and Nibbelink, D. (1997) Comparison of immediate-release and controlled release Carbidopa/Levodopa in Parkinson's disease. A multicenter 5-year study. The CR First Study Group. Eur Neurol. 37: 23-27.

8. Klausner, E. A., Eyal, S., Lavy, E., Friedman, M. and Hoffman, A. (2003) Novel levodopa gastroretentive dosage form: *In vivo* evaluation in dogs. J. Control. Release 88:117–126.

9. Ritger, P.L., and Peppas, N.A. (1987) A simple equation for description of solute release, II: Fickian and anomalous release from swellable devices. J Control Release. 5:37Y42.

10. Korsmeyer, R.W., Gurny, R., Doelker, E., Buri, P., and Peppas, N.A. (1983) Mechanisms of solute release from porous hydrophilic polymers. Int J Pharm.15: 25Y35.

11. Peppas, N. A. (1985) Analysis of Fickian and Non-Fickian Drug Release from polymers. Pharm. Acta. Helv. 60, 110-111.

12. Alderman, D.A. (1984) A review of cellulose ethers in hydrophilic matrices for oral controlled release dosage forms. Int J Pharm Technol Prod Manuf. 5: 1Y9.

13. Erni, W., and Held, K. (1987) The hydrodynamically balanced system: a novel principle of controlled drug release. Eur Neurol. 27:21Y27.
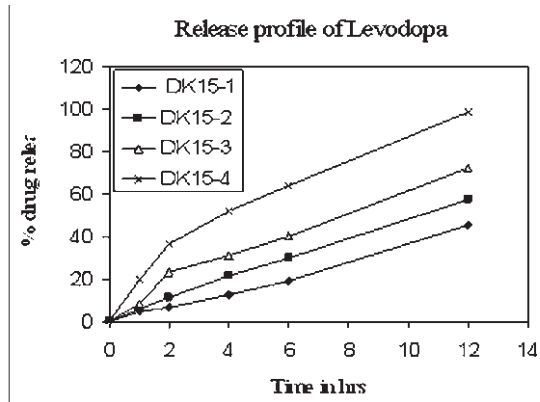
Fig.1 a Cumulative % drug release of Levodopa
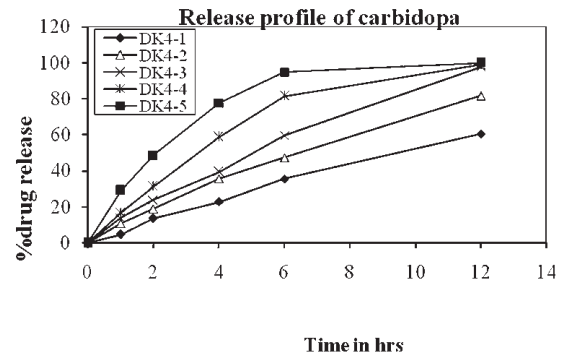
Fig.2b Cumulative % drug release of Carbidopa
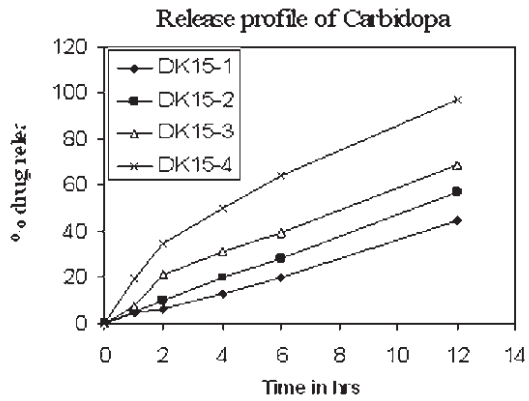
Fig.1b Cumulative % drug release of Carbidopa
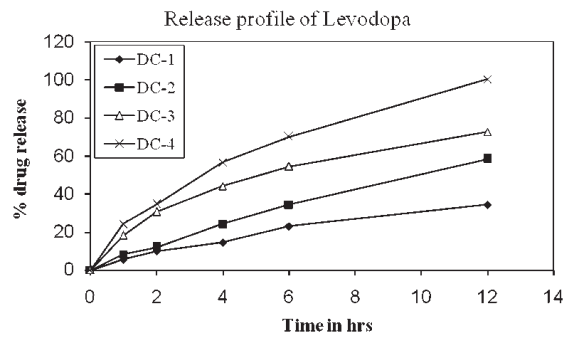
Fig. 3a Cumulative % drug release of Levodopa
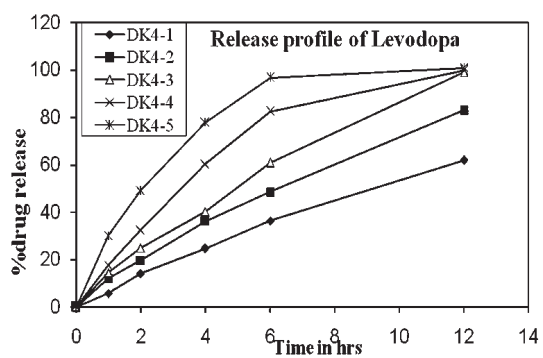
Fig.2a Cumulative % drug release of Levodopa
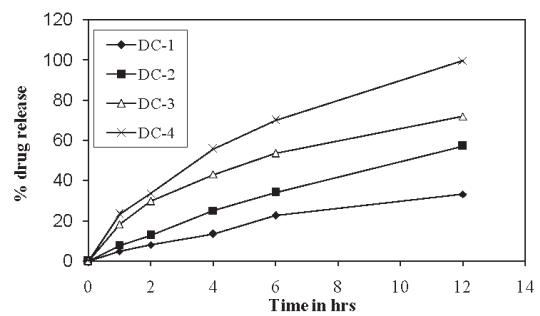
Fig. 3b Cumulative % drug release of Carbidopa

InVitro Evaluation

Table 1. Composition of levodopa and carbidopa (200mg+50mg) controlled release tablet formulations

COMPOSITIONS	FORMULATIONS												
	DK15-1	DK15-2	DK15-3	DK15-4	DK4-1	DK4-2	DK4-3	DK4-4	DK4-5	DC-1	DC-2	DC-3	DC-4
Levodopa	200.00	200.00	200.00	200.00	200.00	200.00	200.00	200.00	200.00	200.00	200.00	200.00	200.00
Carbidopa	50.00	50.00	50.00	50.00	50.00	50.00	50.00	50.00	50.00	50.00	50.00	50.00	50.00
HPMC K15M	60.00	50.00	40.00	30.00	-	-	-	-	-	-	-	-	-
HPMC K4M	-	-	-	-	120.00	100.00	80.00	60.00	50.00	-	-	-	-
Carbopol 974P	-	-	-	-	-	-	-	-	-	70.00	60.00	50.00	40.00
MCC	81.00	91.00	101.00	111.00	21.00	39.00	61.00	81.00	91.00	31.00	41.00	51.00	61.00

Each 400mg LDCD CR formulation contains 0.025% Brilliant blue, 0.1% Ascorbic acid, 0.625% Talc, 0.625% Aerosil. MCC: Microcrystalline cellulose, LDCD CR: Levodopa Carbidopa Controlled Release.

Table: 2   Micromeritic properties of drugs (levodopa and carbidopa)

S.No	Parameter	Levodopa	Carbidopa
1	Angle of repose	48^0	50^0
2	Bulk density (g/ml)	0.50	0.31
3	Tapped density (g/ml)	0.83	0.50
4	Compressibility index	21	22
5	Hausner ratio	1.60	1.62

Table: 3 Thickness, Hardness, Weight variation, Friability and Drug content of prepared   tablets.

Formula code	Thickness (mm)	Hardness (Kg/cm^2)	Weight variation (mg)	Friability (%)	Drug content (%)	
					Levodopa	Carbidopa
DK15-1	3.5±0.06	5± 0.5	402.05 ±5.54	<1	95.26	94.91
DK15-2	3.5±0.13	5± 0.5	403.40 ± 4.02	<1	98.96	97.91
DK15-3	3.5±0.08	5± 0.5	404.45 ± 3.35	<1	96.33	98.73
DK15-4	3.5±0.04	5± 0.5	401.00 ± 4.06	<1	97.32	97.01
DK4-1	3.5±0.10	5± 0.5	401.50 ± 2.74	<1	98.65	98.24
DK4-2	3.5±0.12	5± 0.5	400.05 ± 3.54	<1	96.54	95.54
DK4-3	3.5±0.09	5± 0.5	401.75 ± 4.32	<1	99.76	98.97
DK4-4	3.5±0.02	5± 0.5	402.75 ± 4.04	<1	98.21	98.23
DC-1	3.5±0.15	5± 0.5	400.50 ± 5.84	<1	95.91	96.02
DC-2	3.5±0.28	5± 0.5	403.40 ± 6.28	<1	98.79	98.65
DC-3	3.5±0.37	5± 0.5	404.50 ± 7.74	<1	97.41	97.14
DC-4	3.5±0.39	5± 0.5	403.25 ± 7.83	<1	96.24	99.76

Table: 4 f_1 and f_2 factors of the optimized formulations.

Formulation code	Levodopa		Carbidopa	
	f_1	f_2	f_1	f_2
DK15-4	8	65	6	69
DK4-3	5	75	5	73
DC-4	6	70	7	66

InVitro Evaluation

Table: 5 Release kinetics of different optimized formulations

Formulation Code	R^2 values								Release exponent (n)	
	Zero order		First order		Higuchi		Peppas			
	LD	CD	LD	CD	LD	CD	LD	CD	LD	CD
DK15-4	0.939	0.942	0.832	0.833	0.993	0.989	0.989	0.991	0.62	0.63
DK4-4	0.875	0.879	0.728	0.730	0.962	0.960	0.963	0.963	0.72	0.74
DC-4	0.922	0.925	0.853	0.851	0.994	0.993	0.996	0.995	0.58	0.59

Table 6. Stability results of the optimized formulations for Levodopa & Carbidopa (N=3)

Formulation code		Exposed conditions								
			2-8^{0}C		25±2^{0}C/60±5% RH		40±2^{0}C/75±5% RH		Photo stability study	
		Initial	30 days	60 days	30 days	60 days	30 days	60 days	30 days	60 days
Levodopa	DK15-4	98.24	98.20	98.00	30 days	97.81	95.55	94.85	97.28	97.11
	DK4-3	97.98	97.9	97.85	97.01	97.28	94.74	94.16	96.39	96.15
	DC –4	97.41	97.32	97.19	98.03	96.96	94.47	94.13	96.82	96.46
Carbidopa	DK15-4	97.32	97.12	97.01	97.12	97.03	95.24	94.14	94.12	93.94
	DK4-3	99.76	98.97	98.36	97.28	97.18	96.75	96.24	94.27	94.03
	DC-4	99.56	98.95	98.89	97.74	97.67	95.44	95.11	92.87	92.14

Homology modeling of family 39 glycoside hydrolase from *Clostridium thermocellum*

Shadab Ahmed, Tushar Saraf and Arun Goyal*
Department of Biotechnology, Indian Institute of Technology Guwahati
Guwahati-781039, Assam, India
*For correspondence - arungoyl@iitg.ernet.in

Abstract

The homology based 3-Dimensioanl structure prediction of family 39 glycoside hydrolase (*Ct*GH39) from *Clostridium thermocellum* was carried out using bioinformatics tools. The *Ctgh39* gene from *Clostridium thermocellum* is 1170 base pair sequence. The *Ct*GH39 sequence on PSI-BLAST analysis for homology search revealed 54 hits and out which a few had significant E score (E <0.005) and better sequence similarity. The phylogenetic tree showed that *Ct*GH39 evolved from dockerin type cellulosome enzyme from *Clostridium thermocellum* ATCC 27405 and its closest neighbour is a hypothetical protein from *Thermotoga petrophila*. Multiple sequence alignment analysis of *Ct*GH39 using MultAlin and HHpred showed above 90% similarities with protein sequences of *Thermotoga petriphila (Hypothetical protein), Geobacillus stereothermophilus* (1w91; 99.5%; E score=1.2 E-11), *Thermoanaerobacterium saccharolyticum* (1uhv; 99.4%; E score=2.9 E-11) and *Bacillus stereothermophilus* (1qw9; 98.5%; E score=4.9 E-6) from the PDB database. The secondary structure of *Ct*GH39 using PSIPRED VIEW revealed many helices, strands and coils in the protein structure. The tertiary structure prediction of *Ct*GH39 by MODELLER 8v2 showed a (ß/á)$_8$ fold. The program VERIFY 3D assessed the quality of the predicted structure of *Ct*GH39 with acceptable scores. Ramachandran plot revealed that the structure of *Ct*GH39 contains many segments of helix and further showed a tight grouping of phi (ϕ), psi (ψ) angles around -50, -50. There were 22 residues in 3_{10} helical regions and 188 residues in beta sheets. The number of residues in alpha helix is 156 which are close to $\phi \sim -50$ and $\psi \sim -50$ and these residues are clustered together. The Ramachandran plot for *Ct*GH39 using RAMPAGE software showed that among 390 residues, 352 (90.7%) were in favoured region, 26 (6.7%) were in allowed region and 10 (2.6%) were in disallowed region elucidating the acceptability of the predicted model. All the results converged to the fact that the predicted 3-Dimensional structure of *Ct*GH39 is of good quality with acceptable scores.

Introduction

Clostridium thremocellum is an anaerobic, thermophilic and cellulolytic, Gram-positive bacterium capable of degrading crystalline cellulose (1). *C. thermocellum* live in anaerobic, thermophilic environments and will most likely interact with living systems that have cellulose such as plants. Also, because of *C. thermocellum* ability to degrade cellulose into fermentative products, it affects the environment by

contributing to the carbon cycle and the natural decomposition of biomass. Biodegradation and carbon cycle impact the environment because nutrients and more usable compounds are available for other organisms to feed on. This bacterium degrades the cellulosic materials by a large multi-enzymes system called the "cellulosome". The cellulosome is a complicated protein complex consisting of nearly 20 different catalytic subunits or glycoside hydrolases ranging in size from about 40 to 180 kDa with a total molecular weight in millions. The database for glycoside hydrolases is available at website (http://www.cazy.org/fam/acc_GH.html) (2), that contains classification of glycoside hydrolases in the families based on amino acid sequence similarities: i) reflects the structural features of these enzymes ii) helps to reveal the evolutionary relationships between these enzymes iii) provides a convenient tool to derive mechanistic information. According to the glycoside hydrolase classification system, several families GH3, GH39 and GH43 exhibit â-xylosidase activity (3,4,5,6,7). The IUBMB enzyme nomenclature of glycoside hydrolases is based on their substrate specificity and occasionally on their molecular mechanism; such a classification does not reflect the structural features of these enzymes. Family 39 glycoside hydrolases (EC:3.2.1.—) are group of enzymes that hydrolyze the glycosidic bond between two or more carbohydrates, or between a carbohydrate and a non-carbohydrate moiety. The known activities of GH39 are: i) á-L-iduronidase (EC:3.2.1.76) and ii) â-xylosidase (EC:3.2.1.37). In most cases, the hydrolysis of the glycosidic bond is performed by two catalytic residues of the enzyme *vis-a-vis* a general acid residue (proton donor) and a basic residue. Depending on the spatial position of these catalytic residues, hydrolysis occurs via overall retention of the anomeric configuration (8).

MODELLER is used for homology and comparative modelling of protein three-dimensional structures (9,10). MODELLER implements comparative protein structure modelling by satisfaction of spatial restraints (11,12). It can perform many additional tasks, including *de novo* modelling of loops in protein structures, optimization of various models of protein structure with respect to a flexibly defined objective function, multiple alignments of protein sequences and/or structures, clustering, searching of sequence databases, comparison of protein structures. G.N. Ramachandran used computer models of small polypeptides to systematically vary phi and ψ with the objective of finding stable conformations (13). For each conformation, the structure was examined for close contacts between atoms. Atoms were treated as hard spheres with dimensions corresponding to their van der Waals radii. Therefore, ϕ and ø angles which cause spheres to collide correspond to sterically disallowed conformations of the polypeptide backbone. In a Ramachandran plot (13), the core or allowed regions are the areas in the plot show the preferred regions for psi/phi angle pairs for residues in a protein (14). Presumably, if the determination of protein structure is reliable, most pairs will be in the favoured regions of the plot and only a few will be in "disallowed" regions. (14,15). Extensive scientific work on *C. thermocellum* has been done on the genes that control cellulose degradation. Over 100 genes are involved in encoding proteins involved in cellulose degradation. This research is essential for future development of conversion of biomass into energy that can be achieved by understanding the genes encoding the cellulose degrading proteins and how their expressions are regulated. Cellulose degrading ability of *C. thermocellum* can be manipulated and amplified as a mass energy source. In the present study the sequence analysis and homology based 3-dimensioanl structure prediction of family 39 glycoside hydrolase (*Ct*GH39) from *Clostridium thermocellum* using above bioinformatics tools

was carried out. The predicted structure contains a fold $(\hat{a}/\acute{a})_8$ shape at the core. The secondary structure tells about the possible alpha helices, beta sheets and coiled regions in the *CtGH39*. The Ramachandran plot tells about the residues which have favourable conformation for psi and phi angles which will further help in understanding the mechanism of cellulolysis.

Materials and Methods

The amino acid sequence of *Ct*GH39 (UniProt id A3DHB2) was first subjected to analysis by HHpred with 8 iterations of PSI-BLAST (16) for homology, it could also build a phylogenetic tree based on alignment scores so that evolutionary relationship among closely matching sequences can be understood. Thereafter, very closely resembling sequences with better E score <0.005 and higher % similarity were used for finding conserved regions of *Ct*GH39 with similar proteins from other species using Multiple sequence alignment (MSA; http://www.ebi.ac.uk/Tools/clustalw2/index.html). The MSA was done using HHpred and Multalin (17,18). The secondary structure was predicted using the software PSIPRED VIEW (19). It provides information regarding the various turns, coils and helices possible at particular position in a protein.

The 3-dimensional structure prediction was carried out by alignment of target sequences with template structures using MODELLER 8v2 (Max-Planck Institute, Department of Developmental Biology; bioinformatics toolkit link (20) and further, the model was assessed by VARIFY 3D (21,22). Out of the few predicted iterative models, the best model having lowest value of MODELLER objective function was reported. The selected model was visualized using RasMol v2.5 (23) and the image was imported.

In a Ramachandran plot, the core or allowed regions are the areas in the plot show the preferred regions for psi/phi angle pairs for residues in a protein. The Ramachandran plot using RAMPAGE (24,25) software, shows various residues falling under allowed, favoured and in disallowed regions. In Ramachandran plot rotation about the N-$C^{\acute{a}}$ bond of the peptide is denoted by torsional angle (ϕ), rotation about $C^{\acute{a}}$-C' bond by (ψ) and about the peptide bond (C'-N) by ù. Variations in á-helix in which the chain is either more tightly or more loosely coiled, with hydrogen bonds to residues $i + 1$ and $i + 5$ ($C^{\acute{a}}$-H), are designated as 3_{10} – helix and the ð-helix, respectively. The packing of the backbone atoms is somewhat too tight in the 3_{10} – helix and the hydrogen bonds are nonlinear. The name of this helix refers to the occurrence of 3 residues per turn and the 10 atoms between the hydrogen-bond donor and acceptor (26).

Results and Discussion

The sequence analysis and homology based 3-dimensional structure prediction of family 39 glycoside hydrolase (*Ct*GH39) from *Clostridium thermocellum* using bioinformatics tools was carried out. *Ctgh39* gene from *C. thermocellum* is 1170 base pair sequence. The *Ct*GH39 on analysis by HHpred with 8 iterations of PSI-BLAST for homology search revealed 54 hits out of which a few had significant E score (E <0.005) and better sequence similarity (>40%). A phylogenetic tree, also called an evolutionary tree, is a tree showing the inter-relationships among various species or other entities that are believed to have a common ancestor. The phylogenetic tree showed that *Ct*GH39 evolved from dockerin type cellulosome enzyme from *Clostridium thermocellum* ATCC 27405 and its closest neighbour is a hypothetical protein from *Thermotoga petrophila* (Fig. 1).

Multiple sequence alignment analysis of *Ct*GH39 using HHpred and MultAlin (17,18) showed above 90% similarities with matching sequences *viz.* proteins from *Thermotoga petrophila (Hypothetical protein)*, *Geobacillus*
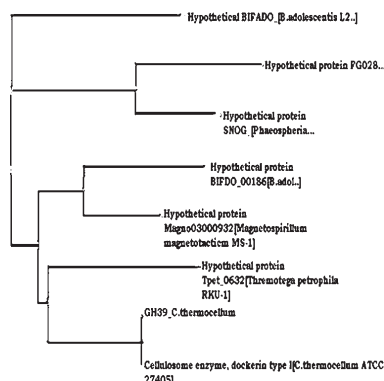
Fig. 1. Phylogenetic tree generated (showing distance) using BLASTp shows that *Ct*GH39 comes from dockerin type cellulosome enzyme complex from *Clostridium thermocellum* ATCC 27405 and a hypothetical protein from *Thermotoga petrophila* must be its closest neighbour.

stereothermophilus (1w91), *Thermoanaero bacterium saccharolyticum* (1uhv) and *Bacillus stereothermophilus* (1qw9) (Fig. 2). High consensus portions shown in red are identical amino acids in all 5 sequences (Fig. 2). Those regions represented in blue are the conserved amino acids at least 4 out of 5 sequences and the neutral portions are shown in black (Fig. 2). Multiple sequence alignment (MSA) is often used to assess sequence conservation of protein domains, tertiary and secondary structures and even individual amino acids or nucleotides (17). The MSA results of *Ct*GH39 using HHpred and MultAlin (17,18) showed the conserved regions that are present among the closely matching sequences and these sequences helped in further model building or structure prediction (Fig. 2).
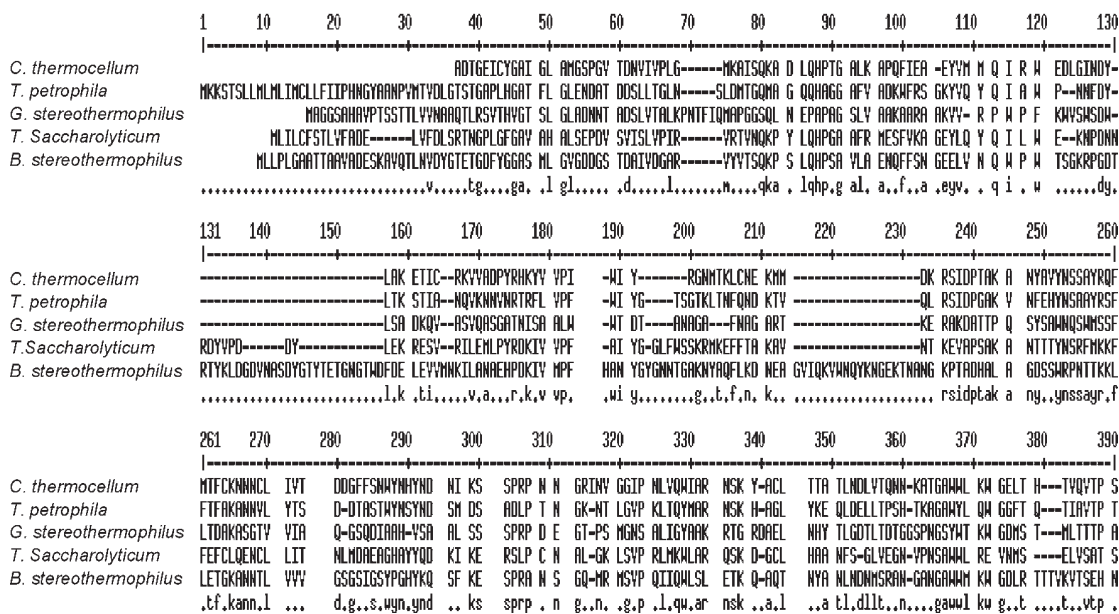
Fig. 2. Multiple sequence alignment analysis of *Ct*GH39 using ClustalX. Multiple sequence alignment analysis of *Ct*GH39 using MultAlin and HHpred showed above 90% similarities with protein sequences of *Thermotoga petriphila (Hypothetical protein)*, *Geobacillus stereothermophilus* (1w91), *Thermoanaerobacterium saccharolyticum* (1uhv) and *Bacillus stereothermophilus* (1qw9) from the PDB database. High consensus portions shown in red (>90%) are identical amino acids in all 5 sequences. Blue regions (>50%) are the conserved amino acids in at least 4 out of 5 sequences and the neutral portions are shown in black.

Conf: ⊐⊐⊐⊐⊐⊐⊐⊃⊃⊃⊃⊃⊐⊐⊐⊃⊐⊐⊐⊐⊐⊐⊃⊃⊃⊃⊃⊃⊐⊐⊐⊐⊐⊃⊃⊃⊃⊃⊐⊔
Pred:
Pred: CCCCCCCCCCEEEEECCCCCCCCCHHEECCCCCCCCCCCC
AA: ADTGEICYGAIGGLYAMGSPGVPTDNVIVPLGMKAISQKA
              10   20   30   40

Conf: ⊐⊐⊐⊐⊐⊃⊃⊐⊐⊃⊃⊃⊐⊐⊐⊃⊃⊃⊐⊐⊐⊐⊐⊐⊐⊃⊃⊃⊐⊐⊐⊐⊐⊐⊐⊐⊐⊔
Pred:
Pred: CCCCCCCCCCCCCHHHHHCCCCCEECCCCCCCCCCCCCCC
AA: PDGLQHPTGDALKVAPQFIEAGEYVMIMMQDIYRNWPYED
              50   60   70   80

Conf: ⊐⊐⊐⊐⊐⊐⊐⊐⊐⊐⊐⊐⊐⊐⊐⊐⊃⊃⊃⊃⊃⊐⊐⊐⊐⊐⊃⊃⊐⊐⊐⊐⊃⊃⊐⊐⊐⊔
Pred:
Pred: CCHHHHHHHHHHHHCCCCCCCCCEEEEEEECCCCCCCCCC
AA: LGINDYLAKIETICRKVVADPYRHKYVYVPINEPEWIWYR
              90   100   110   120

Conf: ⊐⊐⊐⊐⊐⊐⊐⊐⊐⊐⊐⊐⊐⊐⊐⊐⊐⊐⊃⊃⊃⊃⊃⊐⊐⊐⊐⊐⊐⊐⊃⊃⊐⊐⊐⊐⊔
Pred:
Pred: CCHHHHHHHHHHHHHHHHHCCCCEEEECCEECCCCHHHHH
AA: GNMTKLCNEWKMMYDKIRSIDPTAKIAGPNYAVYNSSAYR
              130   140   150   160

Conf: ⊐⊐⊐⊐⊐⊐⊐⊐⊐⊐⊐⊐⊐⊐⊐⊐⊐⊃⊃⊐⊐⊐⊐⊐⊐⊐⊐⊐⊐⊐⊐⊐⊐⊐⊐⊐⊔
Pred:
Pred: HHHHHHHCCCCCEEEEECCCCCCCHHHHHHHHHHHH
AA: QFMTFCKNNNCLPDIVTWHELDDGPFSNWYNHYNDYRNIE
              170   180   190   200

Conf: ⊐⊐⊐⊃⊃⊐⊐⊐⊐⊐⊐⊐⊐⊃⊃⊐⊐⊐⊐⊐⊐⊐⊃⊃⊃⊃⊔
Pred:
Pred: HHCCCCCEEEECCCCCCCCCCCCHHHHHHHHHCCCH
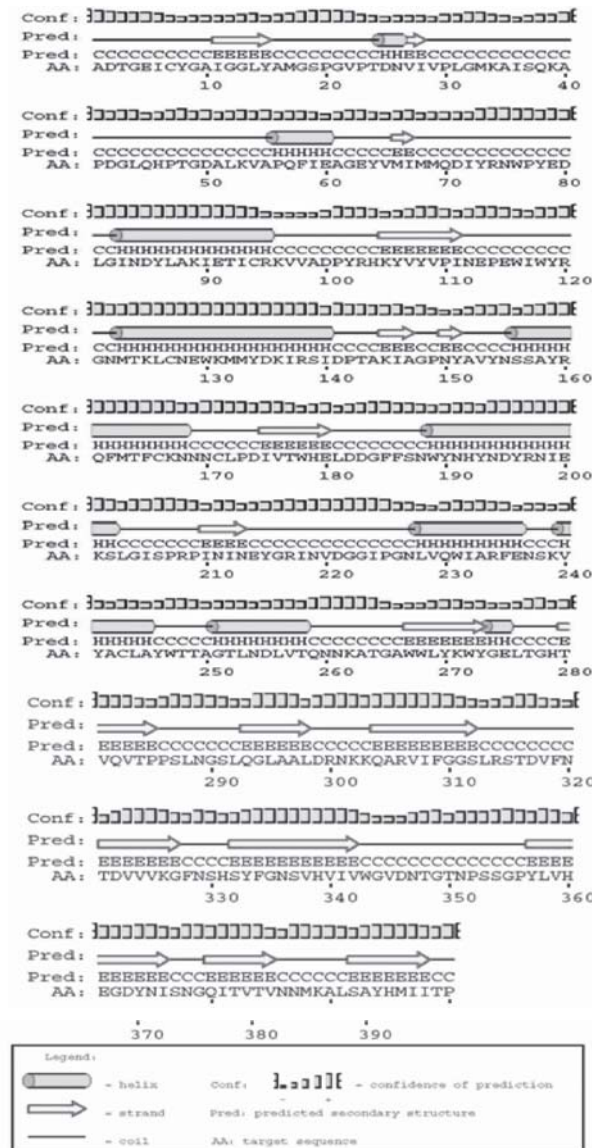AA: KSLGISPRPININEYGRINVDGGIPGNLVQWIARFENSKV
              210   220   230   240

Conf: ⊐⊐⊃⊃⊐⊐⊐⊐⊐⊐⊐⊐⊐⊐⊐⊐⊐⊐⊐⊐⊐⊃⊃⊃⊃⊃⊐⊐⊔
Pred:
Pred: HHHHHCCCCHHHHHHHCCCCCCCCEEEEEEEEHHCCCCE
AA: YACLAYWTTAGTLNDLVTQNNKATGAWWLYKWYGELTGHT
              250   260   270   280

Conf: ⊐⊐⊐⊐⊃⊃⊐⊐⊐⊐⊃⊃⊃⊐⊐⊐⊐⊐⊐⊐⊐⊐⊐⊐⊐⊐⊐⊃⊃⊃⊐⊐⊐⊔
Pred:
Pred: EEEEECCCCCCEEEEEECCCCCEEEEEEEEECCCCCCCC
AA: VQVTPPSLNGSLQGLAALDRNKKQARVIFGGSLRSTDVFN
              290   300   310   320

Conf: ⊐⊐⊐⊐⊐⊃⊃⊐⊐⊐⊐⊐⊐⊐⊐⊐⊐⊐⊐⊐⊐⊃⊃⊃⊐⊐⊐⊐⊃⊃⊐⊐⊔
Pred:
Pred: EEEEEECCCCEEEEEEEEEEECCCCCCCCCCCCCCCEEEE
AA: TDVVVKGFNSHSYFGNSVHVIVWGVDNTGTNPSSGPYLVH
              330   340   350   360

Conf: ⊐⊐⊐⊐⊐⊐⊃⊐⊐⊐⊐⊃⊃⊐⊐⊐⊐⊐⊐⊐⊐⊐⊐⊔
Pred:
Pred: EEEEECCCEEEEEECCCCCCEEEEEEECC
AA: EGDYNISNGQITVTVNNMKALSAYHMIITP
              370   380   390

Legend:
⬭ - helix   Conf: ⊔▪⊐⊐⊏ - confidence of prediction
⇨ - strand   Pred: predicted secondary structure
— - coil   AA: target sequence

Fig. 3. Secondary structure of *Ct*GH39 predicted using PSIPRED VIEW software (18) showing helix (shown as cylinders) and beta strands (shown as arrow region) and coils (as continuous line) with confidence level of prediction.
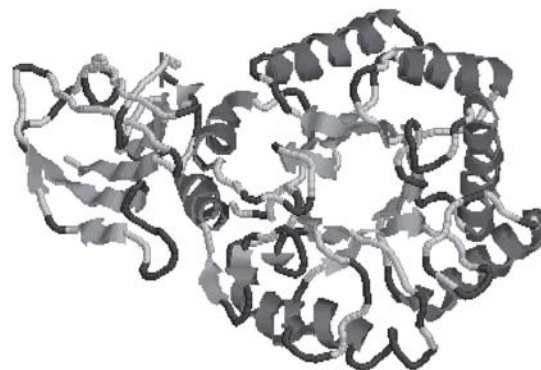
Fig. 4. Three dimensional structure of *Ct*GH39 developed utilizing MODELLER 8v2 and visualized using RASWIN (RASMOL) software showing the characteristic $(\beta/\alpha)_8$ fold (alpha helix in red ribbons and beta sheets in yellow arrows)

The secondary structures of proteins are the regularly repeating local structures stabilized by hydrogen bonds. The most common examples are the alpha-helix and beta-sheet. Because secondary structures are local, many regions of different secondary structure can be present in the same protein molecule. Protein secondary structure prediction of *Ct*GH39 from its sequence using PSIPRED VIEW is shown in (Fig. 3). It revealed many helices, strands and coils present at various positions in the protein structure along with their confidence level for such occurrence.

Tertiary structure is generally stabilized by non-local interactions, most commonly the formation of a hydrophobic core, but also through salt bridges, hydrogen bonds, disulfide bonds and even post-translational modifications. The term "tertiary structure" is often used as synonymous with the term fold. The tertiary structure prediction of *Ct*GH39 using the structures from PDB (27,28,29) as template was done (Fig. 4) by utilizing MODELLER 8v2 (9,10,11,12) a web service provided by Max-Planck Institute (20). The characteristic feature of *Ct*GH39 showing a $(\beta/\alpha)_8$ fold was easily identified from the predicted 3-dimensional structure of *Ct*GH39 as it also belonged to Clan 'A' according to the CAZy

classification (4,5). The predicted structure was analyzed using VERIFY 3D (21,22) which assessed and confirmed the quality of the predicted structure of *Ct*GH39 with acceptable scores. The scores (from -1 to +1) were added and plotted for individual residues. The residues falling in the area where the blue line crosses 0.1 have low prediction accuracy and less stable conformation whereas most of the residues fall above 0.2-0.4 and so we can say that the model is of good quality (Fig. 5).
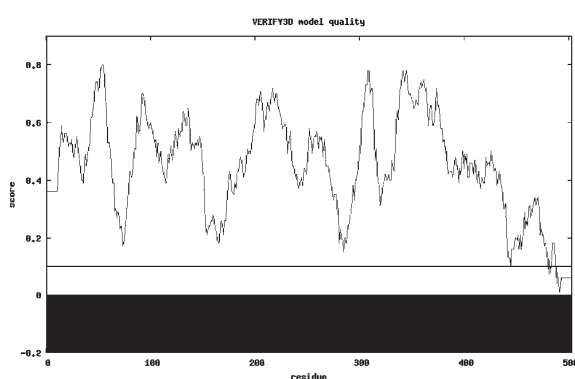

Fig. 5. Three dimensional model testing for assessing the quality of predicted 3-D model by VARIFY 3D software (very few residues cross the red line having negative value implying predicted model is good).

Ramachandran plot (24) reveals that the repeating values of phi and psi angles along the polypeptide chain results in regular structure, such as repeating values of phi ~-57 and psi ~-47 give a right-handed helix (the á-helix). The structure of *Ct*GH39 showed many segments of helix and the Ramachandran plot showed a tight grouping or clustering of (ϕ), (ψ) angles around -50, -50 (Fig. 6). The total number of residues in alpha helix is 156 which have (ϕ)~ -50 and (ψ)~ -50, these alpha helix residues are more clustered than spread like clouds i.e. these structures are more rigid than beta sheets and thus have less allowed conformations. Similarly, repetitive values in the region (Fig. 6) of ϕ = -110 to -140 and ψ = +110 to +135 gave extended chains with conformations
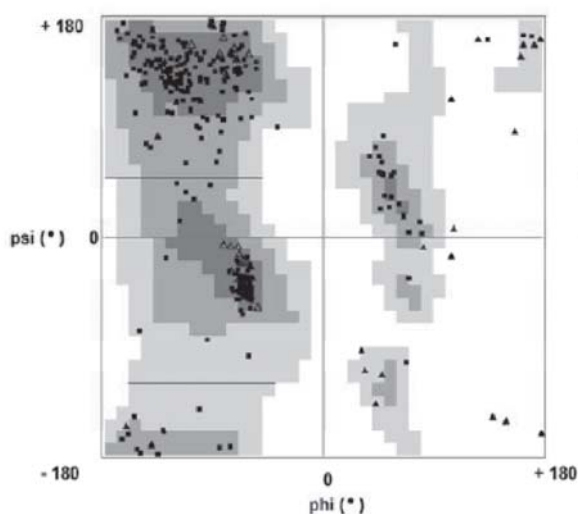

Fig. 6. Ramachandran plot for *Ct*GH39 from *Clostridium thermocellum* using RC plot online server available from IISc Bangalore (13). It shows the left-handed as well as right-handed helices, beta sheets and disallowed and allowed areas. Black areas are allowed only for Gly residues.

that allow interactions between closely folded parallel segments (â-sheet structures). The structure of *Ct*GH39 is composed mostly of â-sheets and the Ramachandran plot showed a broad range of values in the -110, +130 regions (Fig. 6). Repeating ϕ, ø angles always lead to a regular structure provided it is sterically allowed. There are total 22 residues in 3_{10} helical regions, which are present in first quadrant of conformational map (Fig. 6). The total number of residues in beta sheet is 188, which covers almost all the region of second quadrant and extremities of the 3rd quadrant (Fig. 6). The Ramachandran plot for *Ct*GH39 using RAMPAGE software (24), revealed that among the 390 residues, 352 (90.7%) were in favoured region, 26 (6.7%) were in allowed region and 10 (2.6%) were in disallowed region proving again that the predicted model is acceptable (Fig. 7). Ramachandran plot for general, glycine, pre-proline and proline was also done and it showed the glycine, pre-Pro and proline of *Ct*GH39 falling under allowed regions and also

those glycine residues falling in disallowed region (Fig. 8). The overall results provided the evidences that the predicted 3-Dimensional structure of *Ct*GH39 is acceptable and of good quality.

Acknowledgments

Number of residues in favoured region (~98.0% expected) : 352 (90.7%)
Number of residues in allowed region (~2.0% expected) : 26 (6.7%)
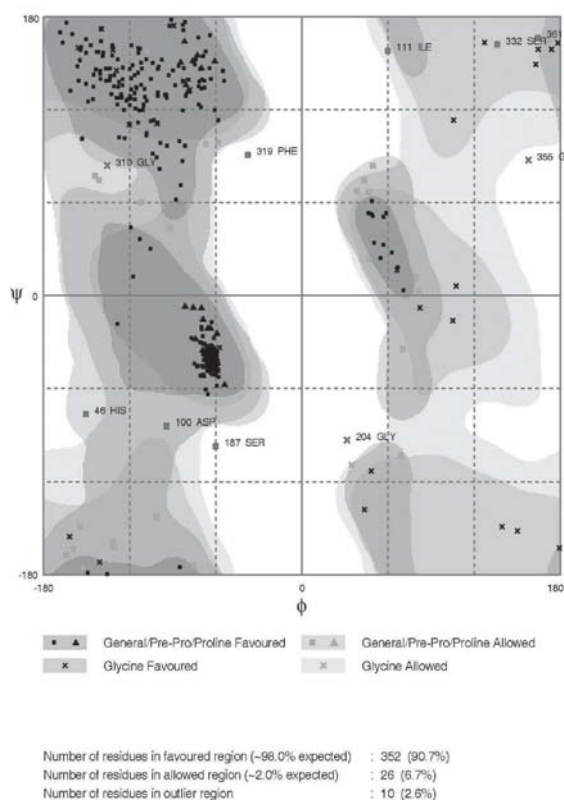Number of residues in outlier region : 10 (2.6%)

Fig. 7. Ramachandran plot analysis of *Ct*GH39 using RAMPAGE software(24,25). It shows the various residues falling in favoured allowed and disallowed region and the Glycine residues (352 residues are in favoured region, 22 in allowed region and 10 in disallowed region) so > 90% residues have allowed conformations.

References

1. Johnson, E.A., Sakajoh, M., Halliwell, G., Madia, A. and Demain, A.L. (1982). Saccharification of complex cellulosic substrates by cellulase system from *Clostridium thermocellum*. Appl. Environ. Microbiol. 43, 1125–1132.

2. Carbohydrate active enzymes (CAZY) link (http://www.cazy.org/fam/acc_GH.html).

3. Henrissat, B. (1991). A classification of glycosyl hydrolases based on amino-acid sequence similarities. Biochem. J., 280, 309-316.

4. Davies, G. and Henrissat, B. (1995). Structures and mechanisms of glycosyl hydrolases. Structure, 3, 853-857.

5. Henrissat, B. and Bairoch, A. (1993). New families in the classification of glycosyl hydrolases based on amino-acid sequence similarities. Biochem. J., 293, 781-788.

6. Lairson, L.L., Henrissat, B., Davies, G.J. and Withers, S.G. (2008). Glycosyl-transferases: Structures, Functions and Mechanisms. Ann. Rev. Biochem., 77, 521-555.

7. Henrissat B. and Bairoch A. (1996). Updating the sequence-based classification of glycosyl hydrolases. Biochem. J., 316, 695-696.

8. Lynd, L.R, Weimer, P.J., van Zyl, W.H. and Pretorious, I.S. (2002). Microbial cellulose utilization: fundamentals and biotechnology. Microbiol. Mol. Biol. Rev., 66, 506-577.

9. Sánchez, R. and Sali, A. (2000). Comparative protein structure modeling: Introduction and practical examples with MODELLER. In: Protein Structure Prediction: Methods and Protocols. Ed: D. M. Webster. Humana Press, Totowa, NJ, 97-129.
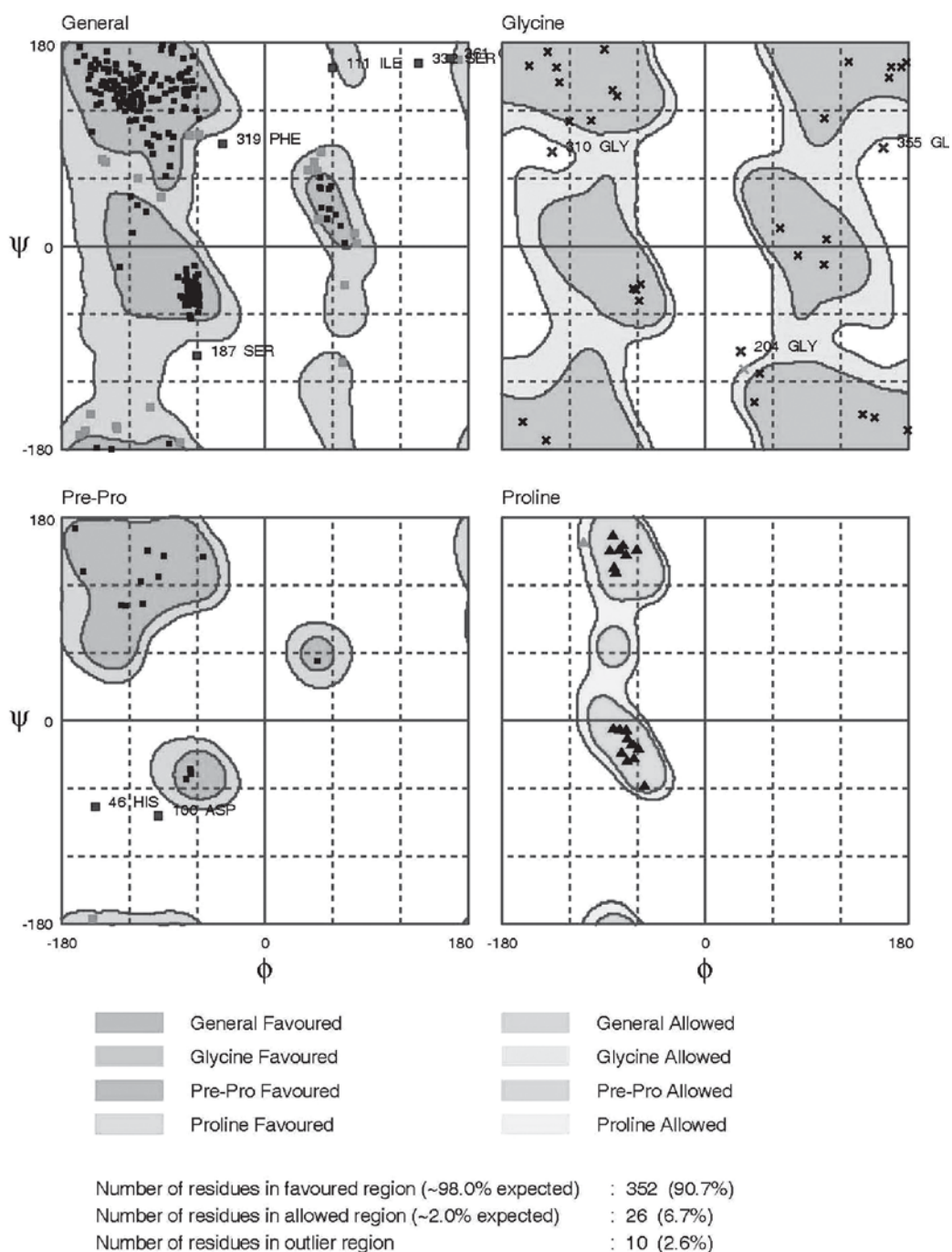
Fig. 8. Ramachandran plot analysis of *Ct*GH39 for general, gly, Pre-Pro, Pro using RAMPAGE (24,25). The conformations and location of each of the above is shown in individual plots having heading as general, Glycine, pre-Pro and Pro.

Ahmed *et al*

10. Marti-Renom, M.A., Stuart, A., Fiser, A., Sánchez, R., Melo, F. and Sali, A. (2000). Comparative protein structure modeling of genes and genomes. Ann. Rev. Biophys. Biomol. Struct., 29, 291-325.

11. Sali, A. and Blundell, T.L. (1993). Comparative protein modelling by satisfaction of spatial restraints. J. Mol. Biol., 234, 779-815.

12. Fiser, A., Do, R.K. and Sali, A. (2000). Modeling of loops in protein structures. Prot. Sci., 9, 1753-1773.

13. Server link for Ramachandran plot (http://dicsoft1.physics.iisc.ernet.in/rp).

14. Ramachandran, G.N., Ramakrishnan, C. and Sasisekharan, V. (1963). Stereochemistry of polypeptide chain configurations. J. Mol. Biol., 7, 95-99.

15. Ramachandran, G.N. and Sasisekharan, V. (1968). Conformation of polypeptides and proteins. Adv. Prot. Chem., 23, 283-437.

16. Altschul, Madden S.F., Schaffer, T.L., Zhang, A.A., and Miller, W. and Lipman, D.J. (1997). Gapped BLAST and PSI-BLAST: A new generation of protein database search programs. Nucl. Acid Res., 25, 3389-33402.

17. Söding, J, Biegert, A., Lupas A, N. (2005). The HHpred interactive server for protein homology detection and structure prediction. Nucl. Ac. Res. 33 (Web Server Issue): W244-W248.

18. MultAlin link (http://bioinfo.genotoul.fr/multalin/multalin.html).

19. PSIPRED VIEW link (http://bioinf2.cs.ucl.ac.uk/psiout/a43f2d904ff1ff82.psi.pdf).

20. Max Planck server link (http:/toolkit.tuebingen.mpg.de/modeller/).

21. Luethy, R., Bowie, J. and Eisenberg, D. (1992). Assessment of protein models with three-dimensional profiles. Nature 356, 83-85.

22. The VERIFY 3D link is (http://toolkit.tuebingen.mpg.de/modeller/verify3d/).

23. Rasmol link (rasmol@ggr.co.uk).

24. RAMPAGE Link (www.cryst.bioc.cam.ac.uk/rampage).

25. Ramachandran, G.N., Sasisekharan, V. and Ramakrishnan, C. (1966). Molecular structure of polyglycine II. Biochim. Biophys. Acta, 112, 168-170.

26. Lovell, S.C., Davis, I.W., Arendal, W.B., deBaker, P.I.W., Word, J.M., Prisant, J.S. and Richardson, D.C. (2002). Structure validation by C$\acute{a}$ geometry: $\ddot{o}/\phi$ and C$\hat{a}$ deviation. Proteins: Struct. Funct. & Genomics, 50, 437-450.

27. Bernstein, F.C., Koetzle, T.F., Williams, G.J.B., Meyer Jr, E.F., Brice, M.D., Rodgers, J.R., Kennard, Shimanouchi, O. and Tasumi, T.M. (1977). The Protein Data Bank: A computer-based archival file for macromolecular structures. J. Mol. Biol., 112, 535-542.

28. Berman, H.M., Westbrook, J., Feng, Z., Gilliland, G., Bhat, T.N., Weissig, H., Shindyalov, I.N. and Bourne, P.E. (2000). The Protein Data Bank. Nucl. Acid Res., 28, 235-242.

29. Berman, H.M., Henrick, K., Nakamura, H., Markley, J., Bourne, P.E. and Westbrook, J., (2007) Realism about PDB. Nature Biotech. 25, 845 - 846.

Hepatoprotective effect of leaves of *Balanites roxburghii* against carbon tetrachloride-induced hepatic damage in rats

K. Thirupathi, D.R. Krishna, B. Ravi Kumar, A.V.N. Apparao and G. Krishna Mohan[*]

Department of Pharmacognosy and Centre for Ethnopharmacology, University College of Pharmaceutical Sciences, Kakatiya University, Warangal 506009, India

* For Correspondence - drgkrishnamohan@yahoo.co.in

Abstract

The methanolic extract of leaves of *Balanites roxburghii* (BLR) was evaluated for its hepatoprotective activity against carbon tetrachloride (CCl_4)-induced hepatic damage in rats. It was evaluated by measuring levels of serum marker enzymes like serum glutamate oxaloacetate transaminase (SGOT), serum glutamate pyruvate transaminase (SGPT), alkaline phosphatase (ALP) and total bilirubin (TBR). The histological studies were also carried out to support the above parameters. Administration of BLR (200 and 400 mg/kg, p.o.) markedly prevented CCl_4-induced elevation of levels of serum GPT, GOT, ALP and TBR. A comparative histopathological study of liver exhibited near to normal architecture, as compared to CCl_4-treated group.

Keywords: Carbon tetrachloride; *Balanites*; Marker enzymes; Hepatoprotective activity.

1. Introduction

Balanites roxburghii is a medicinal herb, found in Bengal, drier parts of India and Myanmar. In Ayurvedic, the fruit has a bitter sharp taste, digestible, alterative, anthelmintic, analgesic and in Unani system of medicine for treatment of skin diseases (1), in Sudanese folk medicine for treatment of jaundice (2), In Egyptian folk medicine, the fruits of *Balanites* (after removal of the apocarps) are commonly used as an oral antidiabetic drug, in tropical Africa as fish poison (3).

It was reported to possess immune modulating properties (4), hypocholesterolemic action (5), anti-inflammatory, antinociceptive and antioxidant activities (6). An aqueous extract of the mesocarp of the fruits of Balanites was reported to exhibit a prominent antidiabetic activity in streptozotocin (STZ) induced diabetic mice (7).

Phytochemical investigations have revealed the presence of saponin glycosides, flavonoids, tannins, alkaloids, phenols from different parts of this plant (8).Chemically, Six flavonoid glycosides: quercetin 3-glucoside, quercetin-3-rutinoside; 3-glucoside, 3-rutinoside, 3-7-diglucoside and 3-rhamnogalactoside of isorhamnetin were extracted and identified from the leaves and branches (9). Saponins (10) have also been identified from the plant

The local people (Warangal) use the leaves as a traditional medicine for the treatment of jaundice. For this purpose, the leaves are crushed, made five small doughs and taken orally once. Hepatoprotective activity of the bark as well as fruit pulp of *B. roxburghhi* has been reported. (11, 12). Therefore, in view of these reasons, we selected to study the Hepatoprotective activity of leaves of the plant.

2. Materials and Methods

2.1. Animals

Wistar rats of either sex, weighing 100–150 g, were used. They were procured from the animal house of Mahaveera Enterprises (Reg. No.146/1999/CPCSEA), Ranga Reddy District, AP, India. They were housed in well-ventilated room at 27^0 C (±2) and photoperiod of 12-h light/dark cycle and fed with standard rodent pellet diet with tap water ad libitum. All procedures described were reviewed and approved by the Institutional animal ethical committee (Regn.No.169/1999/CPCSEA).

2.2. Preparation of leaf extract

The plant (*B.roxburghii*) growing in Karimnager Dist, Andhra pradesh, India was authenticated by Prof. Raju S. Vastavaya, Taxonamist, Department of Botany, Kakatiya University, Warangal. Fresh leaves (Voucher number: LBR-055, deposited in: Herbarium, director: Prof. Raju S.V.) from the plant were collected in the morning, the month of July 2008. Collected leaves were dried and powdered. The methanolic extract was prepared by maceration of leaves powder (1000g) with methanol (3L) for 7 days with intermittent stirring. After extraction, the solvent was filtered and concentrated under reduced pressure. The extract (yield: 27%) obtained was stored at -20ºC until being used.

2.3. Chemicals

Silymarin was supplied as a gift sample by Micro Labs, Hosur, India. The solvents used were purchased from Merck India Ltd. (Mumbai). SGOT, SGPT, ALP and TBR estimation kits were purchased from Span diagnostics, Surat, India.

2.4. Acute toxicity test

The methanolic extract was administered orally only once in doses of 100, 300, 1000 and 2000 mg/kg to groups of mice (n = 6, age 35 days, weight 18-22 g) and percentage mortality was noted beginning with 24 h up to a period of 7 days (13).

2.5. Hepatoprotective activity

Hepatic injury was induced in rats by subcutaneous administration of a single dose of 0.3 ml/kg CCl_4 mixed with equal volume of olive oil on the 7th day, 2 h after the last treatment of the drug (14). Animals were grouped as follows:

GroupI: Control group, treated with 2%w/v acacia in water at the dose of 2.0 ml, p.o (vehicle) daily for 7 days, followed by olive oil treatment (0.3 ml, s.c.) on day 7.

Group II: Treated with vehicle (2.0 ml, p.o.) daily for 7 days followed by CCl_4 on day 7. Group III: Treated with silymarin (100 mg p.o.) daily for 7 days followed by CCl_4 on day 7.

Groups IV and V: Treated with methanolic extract of BLR suspended in 5% gum acacia in water at doses of 200 and 400mg/kg daily for 7 days followed by CCl_4 on day 7, respectively.

2.6. Estimation of Biochemical Parameters

The rats were sacrificed 24 h after the administration of last dose under anaesthesia using thiopentone sodium (35 g/kg b.w.i.p). The blood was collected and allowed to stand for 30 min at room temperature and then centrifuged to separate the serum.The separated serum was estimated for various biochemical parameters like serum glutamate oxaloacetate transaminase (SGOT), serum glutamate pyruvate transaminase (SGPT) (15), Serum Alkaline Phosphatase (ALP) (16) and Total Bilirubin (17).

2.7. Statistical analysis

All values are expressed as means ± S.D. The data were subjected to one-way ANOVA

followed by Newman-Keuls multiple comparison test and $P<0.05$ were considered significant.

2.8. Histopathological Studies

Liver was rapidly excised immediately after sacrifice. Liver was washed with normal saline (0.9%) and fixed in formalin (10%), serially sectioned and microscopically examined after staining with hematoxylin and eosin (18).

3. Results

In mice, oral administration of the methanolic extract of leaves at a dose of 100–2000 mg/kg did not produce any overt changes in behavior or symptoms of toxicity. The extract was found to be safe up to a dose 2000 mg/kg in mice.

In rats, hepatic damage induced by CCl_4 caused significant rise in marker enzymes SGOT, SGPT, ALP and Total serum bilirubin (Table 1). Oral administration of BLR 400 mg/kg was observed to lower significantly ($P < 0.001$) the levels of marker enzymes namely SGOT, SGPT and TBR. It also lowered ALP ($P < 0.05$). While, BLR 200 mg/kg was observed to lower

significantly the levels of SGOT ($P < 0.01$), SGPT ($P < 0.05$) and TBR ($P < 0.01$) but not lowered ALP. The effect of BLR seemed dose dependent. However, the protection offered by Silymarin seemed relatively greater. Fig. 1 exhibits the histological section of liver of rats treated with BLR. The normalcy of hepatic cells and central vein can be easily observed.

4. Discussion and Conclusion

Hepatotoxicity is due to the consequence of CCl4 activation by cytochrome P-450 to trichloromethyl free radical ($CCl_3^{\bullet}$) (19) and which in turn disrupts the structure and function of lipid and protein macromolecule in the membrane of the cell organelles (20). The leaves of *B.roxburghii* were reported to posses flavonoids. It was suggested that the plants containing flavonoids to posses hepatoprotective activity (21).

The increased level of SGOT, SGPT, ALP and TBR is sensitive indicator of liver injury (22). In the present study, also it was seen that administration of CCl_4 elevates the levels of serum marker enzymes SGOT, SGPT, ALP and TBR.

Table 1. Effect of BLR treatment on different biochemical parameters in the serum of rats

Parameter	Treatment				
	Control	CCl_4	Silymarin (100mg/kg, orally) + CCl_4	BLR (200mg/kg, orally) + CCl_4	BLR (400mg/kg, orally)+CCl_4-
SGOT (U/ml)	48.63±7.30	116.38±9.28[*]	58.30±8.73[†]	98.39±9.23[§§]	69.82±10.25[†]
SGPT (U/ml)	37.22±6.02	131.93±8.11[*]	43.48±6.71[†]	120.59±7.66[§]	95.93±7.72[†]
ALP (KA unit)	11.85±2.61	29.06±3.71[*]	16.13±2.50[†]	27.77±2.11	24.20±2.12[§]
Bilirubin (mg/dl) Total	0.53±0.07	1.39±0.06[*]	0.60±0.04[†]	1.26±0.08[§§]	0.93±0.06[†]

Values are expressed as mean ±S.D. of six animals in each group.
*$P < 0.001$ as compared with group 1.
§ $P < 0.05$, §§ $P < 0.01$, † $P < 0.001$ as compared with group 2.

a

b

c

d

e
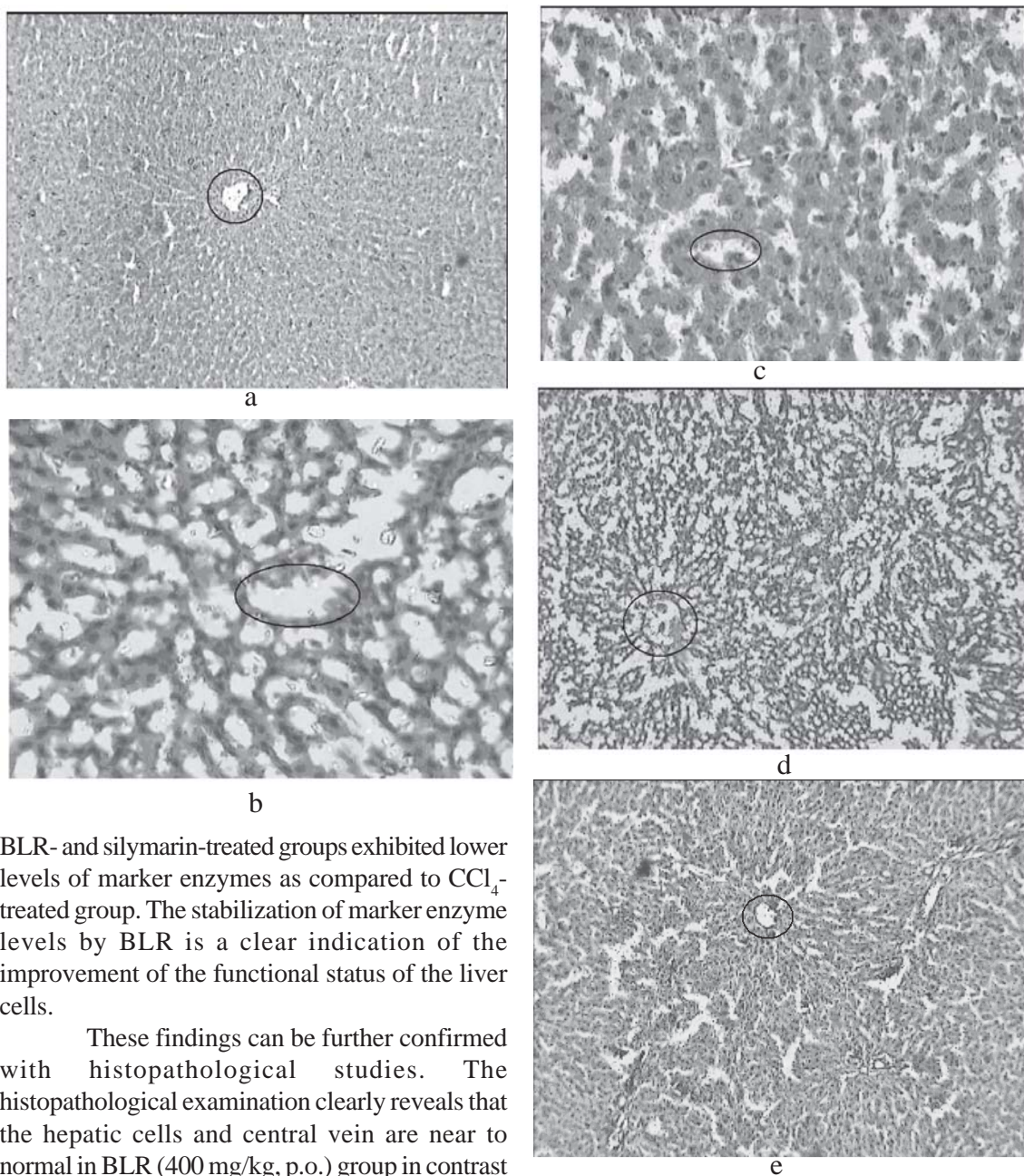
BLR- and silymarin-treated groups exhibited lower levels of marker enzymes as compared to CCl_4-treated group. The stabilization of marker enzyme levels by BLR is a clear indication of the improvement of the functional status of the liver cells.

These findings can be further confirmed with histopathological studies. The histopathological examination clearly reveals that the hepatic cells and central vein are near to normal in BLR (400 mg/kg, p.o.) group in contrast to group which received CCl_4. Thus, BLR can be considered to be an effective hepatoprotective drug as it brings near to normalcy the damage caused by CCl_4 to hepatic function. Hence this drug can be used in polyherbal formulations to provide a synergistic effect with other hepatoprotective drugs and there by preventing

Fig.1. (a). Section through the liver of normal rats showing central vein and hepatocytes. (b). Section through the liver of CCl_4-treated rats showing central vein and hepatocytes. Note the necrosis of hepatic cells and formation of vacuoles. (c,d, e). Section through the liver of BLR-treated (100 mg/kg, 400 mg/kg and Standard respectively) rats showing the central vein (round marking) and hepatocytes.

the process of initiation and progress of hepatocellular diseases (23).

References

1. Kirtikar, B.D. and Basu, B.D. (1933) Indian medicinal plants, International Book Distributors, Deheradun, Vol. III, pp:1823-1824.

2. Mohamed, A.H., Eltahir, K.E.H., Ali, M.B., Galal, M., Ayeed, I.A., Adam, S.I. and Hamid, O.A. (1999) Some pharmacological and toxicological studies on *Balanites aegyptiaca* bark. Phytotherapy Research; 13 (5), 439 – 41.

3. Neuwinger, H.D. (2004): Plants used for poison fishing in tropical Africa. Toxican., 44 (4): 417-430.

4. Koko, W.S., Ahmed Mesaik, M., Yousaf, S., Galal M. and Iqbal Choudhary, M. (2008). In vitro immunomodulating properties of selected Sudanese medicinal plants. Journal of Ethnopharmacology. 118(1): 26-34.

5. Speroni, E., Cervellati, R., Innocenti, G., Costa, S., Guerra, M.C., Dall Acquac, S., Govonid, P. (2005). Anti-inflammatory, anti-nociceptive and antioxidant activitiesof *Balanites aegyptiaca*. Journal of Ethnopharmacology., 98:117–125.

6. Abdel-Rahim, E.A., El-Saadany, S.S. and Wasif, M.M. (1986). Biochemical dynamics of hypocholesterolemic action of *Balanites aegyptiaca* fruit. Food Chemistry., 20(1): 69-78.

7. Kamel, M.S., Ohtani, K., Kurokawa, T., Assaf, M.H., El-Shanawany, M.A., Ali, A.A., Kasal, R., Ishibashi, S. and Tanaka, O. (1991). Studies on Balanites Aegyptiaca, fruits, an antidiabetic Egyptian folk medicine. Chem Pharm Bull., 39: 1229–1233.

8. Parvati, A. and L. L. Narayana. (1978) Systematic position of Balanites Delile. Current Science; 47, 968—970.

9. Salwa A. Maksoud. and Hadidi, M. N. E. (1988) The flavonoids of*Balanites aegyptiaca* (*Balanitaceae*) from Egypt. Plant Systematics and Evolution., 160,(3-4), 153-158.

10. Dan Staerk., Bishnu, P., Hapagain., Therese Lindin., Zeev Wiesman. and Jerzy W, Jaroszewski. (2006). Structural analysys of complex saponins of *Balanites Aegyptiaca* by 800 MHz ^{1}H NMR spectroscopy. Magnetic resonance in chemistry., 44: 923-928.

11. Jaiprakash, B., Aland,R., Karadi, R.V., Savadi, R.V. and Hukkeri, V.L. (2003). Hepatoprotective activity of bark of Balanites aegyptiaca Linn. Journal of natural remedies., 3(2): 205-207.

12. Hatapakki, B.C., Hukkeri, VI., Gopalkrishna, B., Patil D.N. and Kandale J.B. (2006). Hepatoprotective Activity of Fruit Pulp of Balanites Roxburghii. Indian Drugs –Bombay., 43(7): 583-585.

13. Thakur. V/D., Mengi, S.A. (2005). Neuropharmacological profile of *Eclipta alba* (Linn.) Hassk. Journal of Ethnopharmacology., 102: 23–31.

14. Saraswat, B., Visen, P.K.S., Patnaik, G.K., Dhawan, B.N. (1993). Indian J Exp Biol, 31: 316

15. Reitman, S., Frankel, S. (1957). A colorimetric method for the determination

of serum glutamic oxaloacetic acid and glutamic pyruvic transaminases, American Journal of Clin Path., 28:56-63.

16. Kind, P.R.N. and King, E.J.J. (1954). Estimation of plasma phosphatase by determination of hydrolyzed phenol with aminopyrines. J Clinic Path., 7: 332.

17. Jendrassik, L. and Grof, P. (1938). Simplified photometric methods for the determination of the blood bilirubin. Biochem Z., 297: 81-89.

18. Valeer, J. D. (2003). Liver tissue examination, Journal of Hepatology. 39: S43-S49.

19. Tappel, A.C. (1973). Lipid peroxidation damage to cell components. Federal Proceedings., 32: 1870-1874.

20. Mujumdar, A.M., Upadhye, A.S., Pradhan, A.M. (1998). Effect of *Azadirachta indica* leaf extract on CCl_4 induced hepatic damage in albino rats, Indian Journal of Pharmaceutical Sciences., 60: 363–367.

21. Giulia, Di Carlo., Nicola, mascolo., Angelo, A.Izzo. and Fracesco capasso. (1999). Flavonoids: old and new aspects of a class of natural therapeutic drugs. Life sciences., 65(4):337-353.

22. Molander, D.W., Wroblewski, F. and La Due J.S. (1955). Transaminase compared with cholinesterase and alkaline phosphatase an index of hepatocellular integrity. Clinical Research Proceedings., 3: 20-24.

23. Wilkinson, J.H. (1962). An introduction to diagnostic enzymology, In: Arnold. E. (Ed.),Academic Press, London, 1-277.

THIRD ANNUAL CONVENTION OF ASSOCIATION OF BIOTECHNOLOGY AND PHARMACY

Third Annual Convention of Association of Biotechnology and Pharmacy and the International Symposium on "Emerging Trends in Biomedical and Nanobiotechnology: Relevance to Human Health" is being organized jointly by Centre for Biotechnology and Department of Nanotechnology at Acharya Nagarjuna University

during 19-21 December, 2009.

For further details contact

Prof. K.R.S. Sambasiva Rao
Director of the Symposium &
Coordinator, Centre for Biotechnology
Acharya Nagarjuna University
Nagarjunanagar – 522 510, Guntur , A.P., India
Email – krssrao@yahoo.com

Association of Biotechnology and Pharmacy

(Regn. No. 28OF 2007)

Executive Council

Hon. President
Prof. B. Suresh
President, Pharmacy Council of India, New Delhi

President Elect
Prof. K. Chinnaswamy
Chairman, IPA Education Division and EC Member, Pharmacy Council of India

Vice-Presidents
Prof. M. Vijayalakshmi, Guntur   **Prof. T. K. Ravi, Coimbatore**

General Secretary
Prof. K. R. S. Sambasiva Rao, Guntur

Regional Secretary
Prof. T. V. Narayana, Bangalore
Southern Region

Treasurer
J.Ramesh Babu, Guntur

Advisory Board

Prof. C. K. Kokate, Belgaum   **Prof. M. D. Karwekar, Bangalore**

Prof. B. K. Gupta, Kolkata   **Prof. K. P. R.Chowdary, Vizag**

Prof. Y. Madhusudhana Rao, Warangal   **Dr. V. S.V. Rao Vadlamudi, Hyderabad**

Executive Members

Prof. V. Ravichandran, Chennai   Prof. T. Somasekhar, Bangalore
Prof. Gabhe, Mumbai   Prof. S. Vidyadhara,Guntur
Prof. Unnikrishna Phanicker, Trivandrum   Prof. K. S. R. G. Prasad,Tirupathi
Prof. R. Nagaraju, Tirupathi   Prof. G. Devala Rao, Vijayawada
Prof. S. Jaipal Reddy, Hyderabad   Prof. B. Jayakar, Salem
Prof. C. S. V. Ramachandra Rao, Vijayawada Prof. S. C. Marihal, Goa
Dr. C. Gopala Krishna, Guntur   M. B. R. Prasad, Vijayawada
Dr. K. Ammani, Guntur   Dr. M. Subba Rao, Nuzividu
Dr. P. Sudhakar, Guntur   Prof. Y. Rajendra Prasad, Vizag
Prof. G. Vidyasagar, Kutch   Prof. P. M.Gaikwad, Ahamednagar